U.S.NRC
United States Nuclear Regulatory Commission
Protecting People and the Environment

NUREG/CR-7134

The Estimation of Very-Low Probability Hurricane Storm Surges for Design and Licensing of Nuclear Power Plants in Coastal Areas

Office of Nuclear Regulatory Research

AVAILABILITY OF REFERENCE MATERIALS IN NRC PUBLICATIONS

NRC Reference Material

As of November 1999, you may electronically access NUREG-series publications and other NRC records at NRC's Public Electronic Reading Room at http://www.nrc.gov/reading-rm.html. Publicly released records include, to name a few, NUREG-series publications; *Federal Register* notices; applicant, licensee, and vendor documents and correspondence; NRC correspondence and internal memoranda; bulletins and information notices; inspection and investigative reports; licensee event reports; and Commission papers and their attachments.

NRC publications in the NUREG series, NRC regulations, and Title 10, "Energy," in the *Code of Federal Regulations* may also be purchased from one of these two sources.

1. The Superintendent of Documents
   U.S. Government Printing Office Mail Stop SSOP
   Washington, DC 20402–0001
   Internet: bookstore.gpo.gov
   Telephone: 202-512-1800
   Fax: 202-512-2250
2. The National Technical Information Service
   Springfield, VA 22161–0002
   www.ntis.gov
   1–800–553–6847 or, locally, 703–605–6000

A single copy of each NRC draft report for comment is available free, to the extent of supply, upon written request as follows:

Address: U.S. Nuclear Regulatory Commission
Office of Administration
Publications Branch
Washington, DC 20555-0001
E-mail: DISTRIBUTION.RESOURCE@NRC.GOV
Facsimile: 301–415–2289

Some publications in the NUREG series that are posted at NRC's Web site address http://www.nrc.gov/reading-rm/doc-collections/nuregs are updated periodically and may differ from the last printed version. Although references to material found on a Web site bear the date the material was accessed, the material available on the date cited may subsequently be removed from the site.

Non-NRC Reference Material

Documents available from public and special technical libraries include all open literature items, such as books, journal articles, transactions, *Federal Register* notices, Federal and State legislation, and congressional reports. Such documents as theses, dissertations, foreign reports and translations, and non-NRC conference proceedings may be purchased from their sponsoring organization.

Copies of industry codes and standards used in a substantive manner in the NRC regulatory process are maintained at—

The NRC Technical Library
Two White Flint North
11545 Rockville Pike
Rockville, MD 20852–2738

These standards are available in the library for reference use by the public. Codes and standards are usually copyrighted and may be purchased from the originating organization or, if they are American National Standards, from—

American National Standards Institute
11 West 42nd Street
New York, NY 10036–8002
www.ansi.org
212–642–4900

Legally binding regulatory requirements are stated only in laws; NRC regulations; licenses, including technical specifications; or orders, not in NUREG-series publications. The views expressed in contractor-prepared publications in this series are not necessarily those of the NRC.

The NUREG series comprises (1) technical and administrative reports and books prepared by the staff (NUREG–XXXX) or agency contractors (NUREG/CR–XXXX), (2) proceedings of conferences (NUREG/CP–XXXX), (3) reports resulting from international agreements (NUREG/IA–XXXX), (4) brochures (NUREG/BR–XXXX), and (5) compilations of legal decisions and orders of the Commission and Atomic and Safety Licensing Boards and of Directors' decisions under Section 2.206 of NRC's regulations (NUREG–0750).

U.S.NRC
United States Nuclear Regulatory Commission
Protecting People and the Environment

NUREG/CR-7134

The Estimation of Very-Low Probability Hurricane Storm Surges for Design and Licensing of Nuclear Power Plants in Coastal Areas

Manuscript Completed: May 2012
Date Published: October 2012

Prepared by
Donald T. Resio, Ty V. Wamsley, Mary A. Cialone,
and T. Christopher Massey

U.S. Army Engineer Research and Development Center
Coastal and Hydraulics Laboratory
3909 Halls Ferry Road
Vicksburg, MS 39180

John Randall, NRC Project Manager

NRC Job Code N6676

Office of Nuclear Regulatory Research

Abstract

Design criteria for nuclear power plants require, in part, that structures, systems, and components important to safety be designed to withstand the effects of natural phenomena, including floods, without loss of capability to perform their safety functions. The objective of this project is to provide the NRC with a technical basis for estimating probable maximum water levels due to storm surge from extreme events along the southern coast of the U.S. A review of the existing guidance was conducted and limitations in the technical basis for estimating storm surge identified. Required updates based on the most recent data available and state-of-the-practice analysis methods, tools, and models are recommended for NRC consideration. A deterministic-probabilistic approach for estimating very-low probability hurricane storm surges for design and licensing of nuclear power plants in coastal areas is developed. The proposed approach determines which factors affecting hurricane surges can be shown to have asymptotic upper limits and which factors should be treated within a context that allows for natural uncertainty in estimating an upper limit for surges at a specified site. The proposed approach is demonstrated through application at three nuclear plant sites. A screening method is also developed to determine if a prospective site is at risk of flooding from coastal storm surge. The proposed screening method includes criteria for proceeding or not proceeding to more detailed definitions of design-basis storm surges and explicitly considers local conditions and bathymetry that may affect water level estimates.

FOREWORD

This report documents work sponsored by the U.S. Nuclear Regulatory Commission (NRC) as part of the research project "Research to Develop Guidance on Probable Maximum Storm Surge Flood Estimates along the U.S. Southern Coast". The objective of the project was to provide the NRC with modern, state-of-the-practice methods for hurricane storm-surge estimation. The methods described in this report represent significant advances that have been made in hurricane storm surge estimation since the relevant NRC guidance on design-basis flood estimation (Regulatory Guide 1.59, "Design Basis Floods for Nuclear Power Plants," Revision 2) was last updated in 1978. The work and recommendations presented in this report will be considered by the NRC as it updates Regulatory Guide 1.59.

This report provides example calculations to illustrate use of the state-of-the-practice technical basis for deriving low-probability storm surge estimates. The example calculations are performed for three locations near existing nuclear power plants. However, the report does not make detailed, site-specific comparisons between surge estimates used for licensing of the existing power plants at these locations and the example surge estimates derived using the proposed methods. It would not be appropriate to draw conclusions about the adequacy of flood protection for existing plants based on the example calculations in this report. It should be noted that, as part of the its overall response to the March 2011 Fukushima accident, the NRC has issued a request for information to all power reactor licensees and holders of construction permits under 10 CFR Part 50 on March 12, 2012. The March 12, 2012 50.54(f) letter includes a request that respondents reevaluate flooding hazards at nuclear power plant sites using updated information and present-day regulatory guidance and methodologies.

Richard Correia, Director
Division of Risk Analysis
Office of Nuclear Regulatory Research

TABLE OF CONTENTS

LIST OF FIGURES

LIST OF FIGURES
(continued)

LIST OF FIGURES
(continued)

LIST OF TABLES

ABBREVIATIONS AND ACRONYMS

B	Holland B parameter
c_d	coefficient of drag
G	acceleration due to gravity; and
h	water depth on the shelf
L	shelf width
N'	effective number of years used to estimate the distribution parameters
N	number of samples used to estimate the distribution parameters
P_n	non-encounter probability of exceedance of the design value in n years
p	seal level pressure at distance r from the storm center
p_0	minimum pressure at the center of the hurricane
p_w	pressure at the storm periphery
R	radius to maximum winds
R_{max}	distance from storm eye to maximum winds
r	distance from the center of the storm
T	return period
V	wind speed
V_{max}	maximum wind speed
V_{10}	wind speed 10 m above the mean water surface
x	along coast spatial coordinate
v_f	forward velocity of the storm
x_0	along coast location of landfall
Z	ratio of spatial area covered to the spatial extent of a hurricane surge
Δp	peripheral pressure minus central pressure
ε	deviation in storm due to potential errors in estimate
ρ	density of air
ρ_w	density of water
Φ_i	multiplicative functions of surge that depend on the specific bathymetric/topographic setting of the specific point being investigated
σ_T	rms error at return period
σ	distribution standard deviation
σ_T'	rms error at return period, $T' = T / \hat{T}$
$\hat{T}$	average years between hurricanes
η	water surface elevation
θ_f	angle of storm heading

ADCIRC	ADvanced CIRCulation model
FEMA	Federal Emergency Management Agency
GEV	Generalized Extreme Value
HURDAT	HURricane DATabase
HWM	High Water Mark
IPET	Interagency Performance Evaluation Team
JPM	Joint Probability Method
JPM-OS	Joint Probability Method with Optimal Sampling
LaCPR	Louisiana Coastal Protection and Restoration
MPI	Maximum Possible Intensity
MsCIP	Mississippi Coastal Improvements Program

ABBREVIATIONS AND ACRONYMS
(continued)

NOAA	National Oceanic and Atmospheric Administration
NRC	Nuclear Regulatory Commission
NWS	National Weather Service
PBL	Planetary Boundary Layer
PMS	Probable Maximum Surge
PMSS	Probable Maximum Storm Surge
PMH	Probable Maximum Hurricane
SPH	Standard Project Hurricane
SPMSS	Screening Probable Maximum Storm Surge
SST	Sea Surface Temperature
STWAVE	STeady state WAVE model
USACE	U.S. Army Corps of Engineers
WAM	WAve Model

1.0 INTRODUCTION

Design criteria for nuclear power plants require, in part, that structures, systems, and components important to safety be designed to withstand the effects of natural phenomena, including floods, without loss of capability to perform their safety functions. These structures, systems and components must be designed such that appropriate consideration is given to the most severe of the natural phenomena that have been historically reported for the site and surrounding region, with sufficient margin for the limited accuracy and quantity of the historical data and the period of time in which the data have been collected. Design guidance specifically requires that the probable maximum flood be estimated. Applicants for nuclear reactor operating licenses must therefore demonstrate the ability of the proposed facilities to withstand the probable maximum flood, among other hazards. The demonstration is scrutinized by the Nuclear Regulatory Commission (NRC) internally and through a public review process.

The NRC staff is in need of a review of relevant data collected and used since the 1977 publication of its Regulatory Guide 1.59, "Design Basis Floods for Nuclear Power Plants," to estimate the probable maximum flood for appropriate locations. The NRC also needs to be able to specify acceptable methods for estimating design-basis floods that reflect changes in the state of the art flood estimation since 1977, especially for regions susceptible to severe storm events. The objective of this project is to provide the NRC with a technical basis for estimating probable maximum water levels due to storm surge from extreme storm events along the southern coast of the U.S. for consideration in evaluating flood protection for nuclear power plants.

For decades, the U.S. Army Corps of Engineers (USACE) has conducted storm surge and wave studies to support the design of flood control systems. The hurricanes of 2005 produced unparalleled wave and storm surge conditions that affected the entire southern coast of the U.S. from the panhandle of Florida to Texas, causing direct destruction to the immediate coast and its population centers. In response to this disaster, the USACE created the Interagency Performance Evaluation Task Force (IPET), a distinguished group of government, academic, and private sector scientists and engineers. USACE Coastal and Hydraulics Laboratory (CHL) team members conducted much of the technical work for IPET. IPET applied some of the most sophisticated capabilities available in civil engineering to understand what happened during Hurricane Katrina and why. The IPET purpose was not just to acquire new knowledge, but also to improve engineering practice and policies. Peer reviews have been conducted by the distinguished External Review Panel of the American Society of Civil Engineers, and the National Academy of Sciences. In addition, the Congress of the United States authorized the USACE to initiate two important and comprehensive planning efforts to address the impacts caused by the 2005 storms and to plan actions that would make the region more resilient and less susceptible to future risk from such disasters. The Louisiana Coastal Protection and Restoration (LaCPR) and Mississippi Coastal Improvements Program (MsCIP) efforts applied and further developed the technical approach and tools for estimating storm surge flood levels and waves established under IPET. These USACE studies, tools, and approaches were also extensively reviewed.

The USACE interagency team of engineers and scientists, which also included members from academia and the private sector, developed an integrated modeling system to estimate storm surge inundation along the Gulf Coast. Through the work of IPET, the following requirements for accurate simulations were recognized: inclusion of numerically simulated wave set-up, use of detailed grids to capture high-resolution bathymetric effects, and the application of improved

near-coast meteorological models for hurricane evolution and wind-field behavior. The modeling system can be applied to establish the coastal surge flood limits associated with statistical return periods.

One of the clear lessons from the Gulf of Mexico storms of 2005 was the need to develop a new method for estimating hurricane inundation probabilities. Previous methodologies suffered from a paucity of historical data; and an interagency research team led by USACE developed a modified Joint Probability Method (JPM), termed the JPM-OS (JPM with Optimal Sampling), since the underlying concept of this methodology is to provide a good estimate of the surges in as small a number of dimensions as possible. The approach attempts to minimize the issues related to the lack of quantity and quality historical hurricane data and the number of model simulations required by a typical JPM by improving methods used for interpolating between combinations of variables in different simulations. Previous methodologies for estimating flood levels also did not include many of the modeling advances that are now regarded as necessary for accurate simulations. The Federal Emergency Management Agency (FEMA) has adopted the modeling system and methodology and applied it in under USACE leadership in Louisiana, and is currently applying the methodology in Texas, North Carolina, the Great Lakes, and in the Chesapeake Bay area.

Section 2 documents a review of the existing guidance and identifies limitations in the technical basis for estimating storm surge. It provides recommendations for updating the technical basis based on the most recent data available and state-of-the-practice analysis methods, tools, and models. Section 3 presents a proposed deterministic-probabilistic approach for estimating very-low probability hurricane storm surges. The proposed approach determines which factors affecting hurricane surges can be shown to have asymptotic upper limits and which factors should be treated within a context that allows for natural uncertainty in estimating an upper limit for surges at a specified site. Section 4 documents the application of the proposed approach at three nuclear plant sites. The Matagorda Bay site served as a platform for developing the initial concepts for very low probability surges. Analyses of the upper limit for storm surges at two other sites in Florida were also examined. Section 5 introduces a screening method developed to determine if a prospective site is at risk of flooding from coastal storm surge. The proposed screening method includes criteria for proceeding or not proceeding to more detailed definitions of design-basis storm surges and explicitly considers local conditions and bathymetry that may affect water level estimates. Section 6 summarizes the procedures recommended, for NRC consideration, for estimating the probable maximum storm surge at a site. It should be noted that the approach presented herein is a methodology for estimating the flood hazard from coastal storm surges and wave setup only on the U.S. southern coast. River flows can also be included in the modeling of a system but other contributors to flooding such as precipitation and runoff from the watershed are not considered.

2.0 REVIEW OF EXISTING GUIDANCE

The purpose of this Section is to document a review of the National Oceanic and Atmospheric Administration (NOAA) Technical Report NWS 23, "Meteorological Criteria for Standard Project Hurricane and Probable Maximum Hurricane Windfields, Gulf and East Coasts of the United States" and the NRC Regulatory Guide 1.59, "Design Basis Floods for Nuclear Power Plants". Both NWS Report 23 and Regulatory Guide 1.59 require updating. Based on the review of NWS Report 23, procedures for supplementing and or modifying the report are recommended that reflect data and analysis methods that have been developed since its publication in 1979. The review of Regulatory Guide 1.59 and its supporting documents focused on the storm surge section of the report "Probable Maximum Flood and Hurricane Surge Estimates," which is cited in Regulatory Guide 1.59 and Appendix A of Regulatory Guide 1.59, "Determining Design-Basis Flooding at Power Reactor Sites". The technical basis for estimating storm surge was reviewed and required updates recommended for NRC consideration.

2.1 Probable Maximum Hurricane Surge Estimate

Regulatory Guide 1.59 and its supporting documents provide a methodology for estimating the probable maximum surge (PMS) for open coast locations of the Atlantic and Gulf of Mexico. The PMS estimates are determined by use of the probable maximum hurricane (PMH) parameters applied as input to the Bathystrophic Storm Surge model developed in the early 1970s (Bodine 1971; Pararas-Carayannis 1975). The PMH is a hypothetical hurricane having a combination of characteristics that give the highest sustained wind speed that can probably occur at a specified location. A review of the guidance on developing PMH characteristics and recommendations for modifying the guidance are presented in a subsequent section.

The Bathystrophic Storm Surge model applied in NRC guidance was originally developed by Bodine (1971). The model estimates the sea surface rise along the open ocean coast as a response to surface winds and pressures, as well as the Coriolis forces. Pararas-Carayannis (1975) describes the model as a quasi-two-dimensional numerical scheme, which is a steady-state integration of the wind stresses of the hurricane winds on the surface of the water from the edge of the continental shelf to the shore. The storm surge is computed along a single "traverse line" at a time over the continental shelf for a straight open-ocean coast by numerically integrating the two-dimensional hydrodynamic equations of motion and neglecting the continuity equation. Surge propagation along most coasts is heavily influenced by the surrounding bathymetry/topography. The one-dimensional nature of the Bathystrophic model does not allow the simulation of these effects. In addition, the "traverse line" is a straight line that must be oriented perpendicular to the sea bed contours. This orientation restriction is a problem for most realistic shorelines which have complex bed contours and it creates problems when placing a "traverse line" in relation to a storm that moves over the shelf with a large crossing angle. In some locations, storms with large crossing angles may produce the maximum surge values and this cannot be simulated with the Bathystrophic model. An important point is that this model is intended solely for use on open coasts and not for use on protected bays, estuaries, and inlets. Additional analysis must be performed to simulate the propagation of the surge into these areas, which are common along both the Atlantic and Gulf coasts. Existing technology now allows for the simulation of surge propagation in these areas as well as along the open coast in the same simulation.

The Bathystrophic model is limited by a number of initial conditions and assumptions. The assumptions made that have some of the greatest impact on the physics being modeled are:

(1) there is no volume transport normal to the shore, (2) the onshore wind setup responds instantaneously to the onshore wind stress, (3) advection of momentum is negligible, and (4) the alongshore sea surface height and velocity is uniform. In addition, the barometric and astronomical tide effects are not accounted for directly within the discrete equations and the model is best suited for slow moving storms and not for fast moving storms where inertial effects become important. Because there is no volume transport normal to the shore, no inundation is allowed during the simulation. Instead a boundary condition is imposed at the coastline that basically represents an impermeable vertical wall. This is a physically unrealistic assumption that impacts the accuracy of the surge level and the velocity solutions.

In terms of the initial conditions, the model assumes a constant value for the initial water rise, or "forerunner" of the hurricane. The initial water level is an important contribution to the overall storm surge value and can be over 6 ft (Kennedy *et al.* 2011). This initial water level can be captured in modern simulations without specifying it as a constant. Another limiting factor is that wind and bottom frictional stresses are coupled in the Bathystrophic model and it does not allow for each to have an individual resolution.

In summary, the Bathystrophic Storm Surge model is extremely limited by restrictions and simplifications made in order to make the problem computationally tractable given the computer resources available in the early to mid 1970's. The model assumptions and simplifications reduce the applicability and accuracy of the model. Because the surge is not allowed to propagate onshore, but instead piles up at the coastline, it does not allow for accurate representation of the inundation. The treatment of the surface and bottom frictional stresses are combined and do not allow for accurate spatially varying values. The model can only be applied on open-ocean coasts and does not allow for predictions at protected bays, inlets, and estuaries. Most alarming, yet not surprising, is the fact that the accuracy of the model can vary wildly. To this end, Pararas-Carayannis (1975) states that while the model can produce reasonable estimates of surge, there are times the surge estimate can be in error by a factor of two or more. Such a large potential error is not acceptable by today's standards.

Many regions along the Atlantic and Gulf of Mexico coasts are extremely complex, characterized by bays, inlets, barrier islands, and wetlands. Modeling coastal surge in complex regions requires an accurate definition of the physical system and inclusion of all significant flow processes. Processes that affect storm surge inundation include atmospheric pressure, winds, air-sea momentum transfer, waves, river flows, tides, and friction. Numerical models now exist that can properly define the physical system and include an appropriate non-linear coupling of the relevant processes. A coupled system of wind, wave, and coastal circulation models has been developed and implemented for regions in both the Gulf of Mexico and the Atlantic. The system combines the TC96 Planetary Boundary Layer (PBL) model (Thompson and Cardone 1996), the WAM offshore (Komen et al 1994) and STWAVE nearshore (Smith et al 2001, Smith 2007) wave models, and the ADCIRC (Westerink *et al.* 2008; Bunya *et al.* 2009) basin to channel scale unstructured grid circulation model.

There are several advantages of this modern modeling system. First, because ADCIRC is based on an unstructured finite element formulation, it allows for accurate representation of the coastline and surrounding features. ADCIRC also solves the full depth-averaged set of equations that describe storm surge and includes the ability to inundate dry land, thereby better capturing the actual dynamics of the surge, not just the surge height. ADCIRC can therefore estimate the influence of surrounding bathymetry/topography on storm surge across the coastline, unlike the Bathystrophic Storm Surge model. ADCIRC also allows for separate spatially and temporarily varying treatments of surface and bottom stress. Furthermore, there

are no restrictions on the orientation of the grid/mesh with respect to the coastline, the bed contours, or the storms track. Storms with large crossing angles across complex bathymetries are readily simulated. The ADCIRC model can also be coupled with wave models to include the impact of wave set up. The wave model outputs include estimates of hurricane generated wave heights and periods, which may be important in understanding the flood threat in some areas.

To illustrate the capability of existing modeling technology, six hypothetical storms with high surge potential and landfall points along the Mississippi coast were simulated. These six large surge potential storms made landfall at various points along the coast as shown in Figure 2-1. The storms were defined at their most intense point as having a minimum central pressure of 880 mb, radius to maximum winds of 36 nm, and a forward speed of 11 kt. Peak water level envelopes from each of the six storm simulations were computed. The peak water level envelope is the maximum water level estimated at each node during the entire simulation. The six peak water level envelopes were then combined to compute the "peak of peaks", which is considered the inundation limit along the entire Mississippi coastline (Figure 2-2).

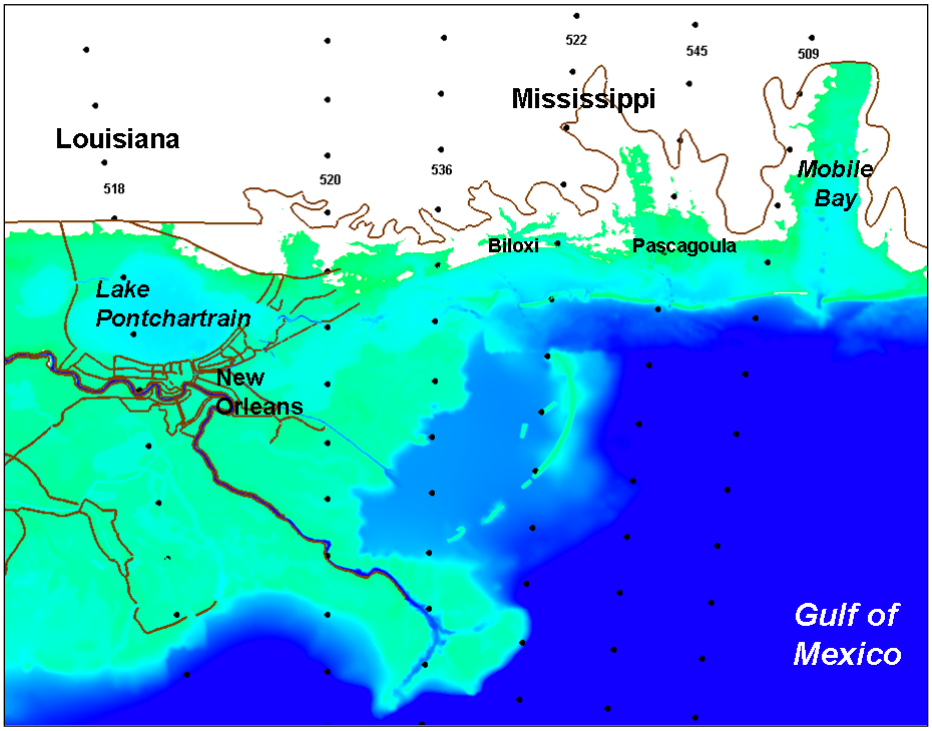

Figure 2-1. Storm tracks for maximum possible intensity storms. Brown lines are ADCIRC sub-grid features or grid extents.

Figure 2-2 illustrates the spatial variability in the surge both along and across the coastline. Coastal features such as barrier islands, inlets, bays, and wetlands can significantly influence surge propagation as seen in Figure 2-2. The ADCIRC modeling system is able to capture the influence of these features, unlike the Bathystrophic model. The current guidance provided by Regulatory Guide 1.59 allows for interpolation along the coast between locations with computed PMS values. Figure 2-2 illustrates how this is unrealistic as there is significant variability in peak surge values due to the complex nature of surge propagation in many coastal regions.

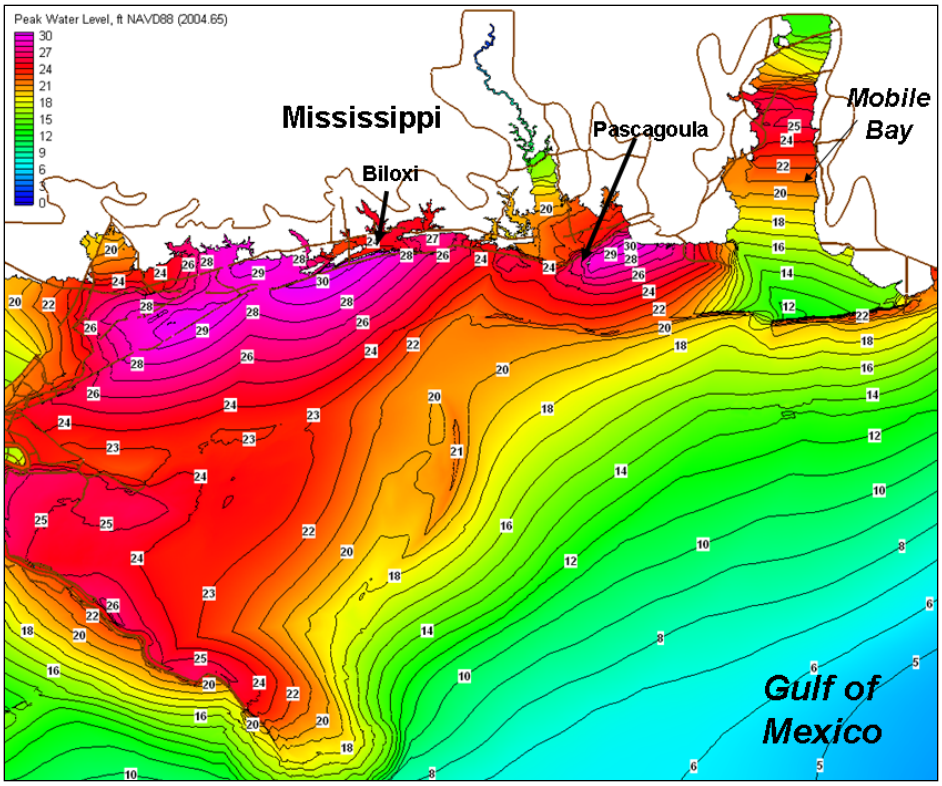

Figure 2-2. Envelope of maximum water level for all six storms.

2.2 Meteorological Criteria for a Probable Maximum Hurricane

In 1959, the USACE contracted the National Weather Service (NWS) to develop a hypothetical hurricane that could be used to design hurricane protection projects along the Gulf and Atlantic coasts of the United States. At that time the NWS, as part of its National Hurricane Research Project, set out to define "the most severe storm that is considered reasonably characteristic of a region." A storm with such characteristics was termed the Standard Project Hurricane (SPH). This effort is described in U.S. Weather Bureau Report No. 33 (Graham and Nunn, 1959).

In 1979, the NWS (NWS Technical Report 23 authored by Schwerdt *et al.* in 1979, hereafter termed NWS 23) redefined the SPH as "a steady state hurricane having a severe combination of values of meteorological parameters that will give high sustained wind speeds reasonably characteristic of a given region," removing the idea that the SPH pertained to the "most severe storm" for a particular area from the definition of the SPH. Since most of USACE projects are examined on an economic basis over a fixed interval of time, this re-definition of the SPH offered improved quantitative guidance for the relative costs and benefits of projects (given that the probability of an SPH is properly estimated) over the use of an absolute maximum value. In fact, NWS goes on to say that this revised "concept of the SPH has been developed for Gulf and Atlantic coasts as a bench mark against which to judge the hazards for a particular community".

Also in NWS 23, the concept of a Probable Maximum Hurricane (PMH) was introduced as "a hypothetical steady-state hurricane having a combination of values of meteorological

parameters that will give the highest sustained wind speed that can probably occur at a specified coastal location." It is clear from this definition that the PMH was intended to be an event that was much rarer than the SPH; but it is not clear that an objective definition can be gleaned from what is written in NWS 23. For example, it is not clear exactly what is meant by the words "the highest wind speed that can probably occur." In its executive summary, NWS 23 states that the central pressure of the PMH "is simply the lowest sea-level pressure at the hurricane center." It does not state the specific geographic area for this determination around U.S. coasts. Figure 2-3, taken from NWS 23, shows the estimated values of the central pressure for the PMH within the Gulf of Mexico, with values varying between about 887 mb at Port Isabel, Texas to about 891 in the vicinity of Apalachicola, Florida and then diminishing to about 885 at Ft Myers, Florida. All of these are values that are substantially lower than the lowest central pressure in the observations within the Gulf of Mexico available at that time, so it is hard to interpret the meaning of these values in an objective context. It is more likely that a considerable dose of "expert judgment" was utilized in estimating the central pressure for the PMH.

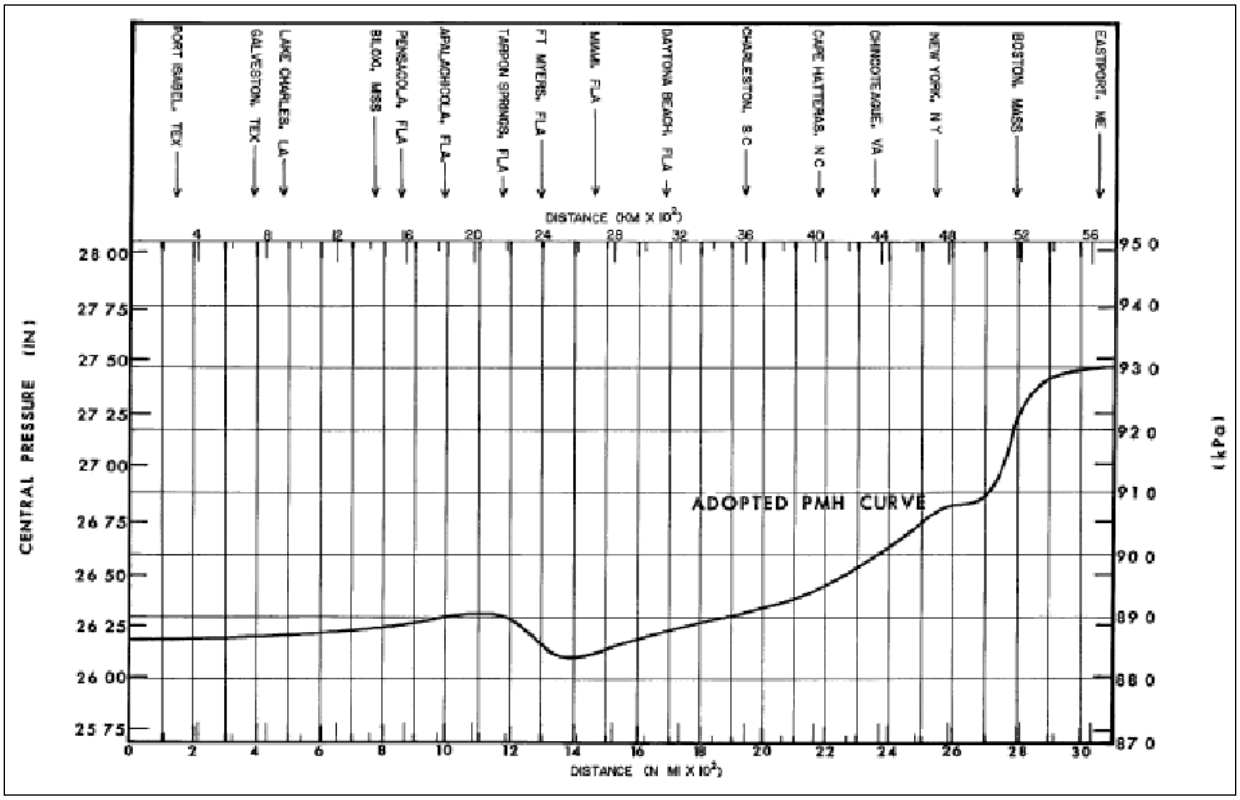

Figure 2-3. Alongshore variation in PMH central pressure from NWS 23.

The meteorological criteria for the Probable Maximum Hurricane (PMH) wind fields are developed in a general sense in NOAA Technical Report NWS 23. This is an excellent treatment of hurricanes, given the time frame in which that study was conducted; however, additional information from the many sources which were unavailable at the time of that study, along with data from many well-documented storms since the report was published in 1979, have shown some potentially important inconsistencies between the PMH derived in that study and our present understanding of the characteristics of intense hurricanes. In addition to the general guidelines for the PMH that appeared in NWS 23, which in many cases only specified

acceptable ranges for parameters, there were some specific values of parameters that were selected for application to specific coastal sites in the Probable Maximum Surge (PMS) studies as a part of the U.S. Nuclear Regulatory Commission's Regulatory Guide produced by its Office of Standards Development. Information from both the NWS 23 and Office of Standards Development sources are considered in this review.

The state of the art in 1979 was such that hurricane wind fields were estimated parametrically from a "vortex model" which was a function of 5 primary parameters: storm intensity (central pressure), storm size (radius to maximum winds), forward translation speed of the storm, direction of heading of the storm, and location of landfall. Holland (1980) showed that an additional factor (now termed the Holland "B" factor) was needed to properly specify winds and pressures within a hurricane. The radial pressure profile formula adopted in NWS 23 is given by

$$\frac{p - p_0}{p_w - p_0} = \exp\left(\frac{-R}{r}\right), \qquad \text{Equation 2-1}$$

where

- p is the seal level pressure at distance r from the storm center;
- p_0 is the minimum pressure at the center of the hurricane;
- p_w is the pressure at the storm periphery;
- R is the radius to maximum winds; and
- r is the distance from the center of the storm.

In the Holland *B* model of hurricane pressure field, this pressure profile is written as

$$p = p_0 + (p_w - p_0)\exp\left(\frac{-A}{r^B}\right), \qquad \text{Equation 2-2}$$

where A and B are scaling parameters such that $A=R^B$ has units of meters. It can be shown that the form given in Equation 2-2 will be equivalent to that shown in Equation 2-1 only if B is equal to 1. Existing data shows that this is not the case. Instead, characteristic values of B vary from basin to basin, typically over a range of values from 0.8 to 2.5 (IPET 2009). The form for the maximum gradient wind based on Equation 2-1 is given as:

$$V_g = \left(\frac{1}{\rho e}\right)^{1/2}(p_w - p_0)^{1/2} - \frac{rf}{2}, \qquad \text{Equation 2-3}$$

where

- ρ is the density of air;
- e is ~2.71828; and
- f is the Coriolis parameter.

The form for the maximum gradient wind based on Equation 2-2 is given by:

$$V_g = \left[\frac{AB(p_w - p_0)\exp\left(\frac{-A}{r^B}\right)}{\rho r^B} + \frac{r^2 f^2}{4}\right]^{1/2} - \frac{rf}{2}. \qquad \text{Equation 2-4}$$

For values of *B* greater than 1, the maximum wind speeds predicted by Equation 2-4 can be substantially higher than those predicted by Equation 2-3, which can lead to a potential under-conservative estimate in the PMH winds.

In modern surge prediction, the reduction of wind speeds from the gradient level to a fixed 10-meter reference level is typically handled within a planetary boundary layer model or from empirical factors based on large sets of data. Such models, although in existence at the time that NWS 23 was written, were not widely used and data sets were very limited in the 1970s; consequently, the reduction factor used in NWS 23 is a simple empirical relationship given by

$$V_{10} = 0.95 V_g, \qquad \text{Equation 2-5}$$

where V_{10} is the wind speed 10 m above the mean water surface. The value of the empirical constant in Equation 2-5 can be shown to vary substantially depending on a number of dynamical factors; however, the 0.95 value in Equation 2-5 represents an upper limit for the range of values determined in planetary boundary model studies.

For a number of years now, the theoretical concept of a PMH has been replaced by a concept of the "Maximum Possible Intensity" (MPI) since this latter concept has theoretical underpinning to support the empirical data. Figures 2-4 and 2-5 are from papers by Tonkin *et al.* (2000) and Schade (2000) and plot the relationship between storm intensity and sea surface temperatures (SST). These figures indicate that the probable lowest central pressure is approximately 880 mb and possibly even a bit lower if SSTs within the Gulf of Mexico rise due to climate change. The dashed vertical line corresponds to the record high average August to September SST, which occurred in 1962. Since the lowest central pressure in the Gulf of Mexico according to NWS 23 is 885 mb, it is possible that the central pressures used in the PMH do not represent the reasonably expected worst storm case.

The radius to maximum winds specified in NWS 23 covers a relatively wide range (typically from about 5 nm to slightly over 20 nm in the Gulf of Mexico); however, the NRC publication on the PMS applies a specific value in its calculations. The values listed in that publication are in all cases somewhat higher than the limits described in NWS 23. As a typical example, the specified value for the PMS calculations at Biloxi is 30 nm, whereas the upper limit for the PMH in that area is about 23 nm. For hurricanes still offshore, this might be a relatively conservative value; however, Katrina at landfall in Mississippi had an estimated value of 33 nm for the radius to maximum winds (IPET 2007). Thus, the 30 nautical mile value does not appear to represent a realistic upper limit to the storm sizes in this area.

An important point raised in the last paragraph concerns the behavior of hurricanes as they approach the coast. In the 1970's it was believed that hurricanes retained their strength until after making landfall and then began to substantially modify and weaken. Recent studies (e.g. IPET 2009) have shown that in the Gulf of Mexico the overall storm strength and the structure of the wind fields change significantly during the approach to the coast (IPET 2009). It is difficult to gage the impact of this difference on storm surges, since both storm intensity and storm structure affect the surge levels.

The range of values for storm translation speed and storm heading given in NWS 23 are consistent with values obtained in more recent studies. Also, since storm locations are distributed in the PMS calculations according to some idea of maximum surges, this aspect of NWS 23 does not present any problems in its applications.

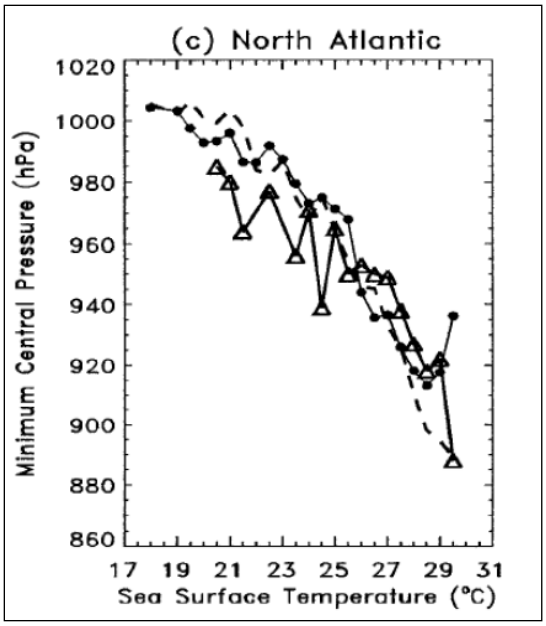

Figure 2-4. Minimum central pressure as a function of SST from Tonkin *et al.* (2000); Emanuel Model (black dots joined by a solid line), Holland's model (dashed line), and observed intensities (open triangles joined by a solid line).

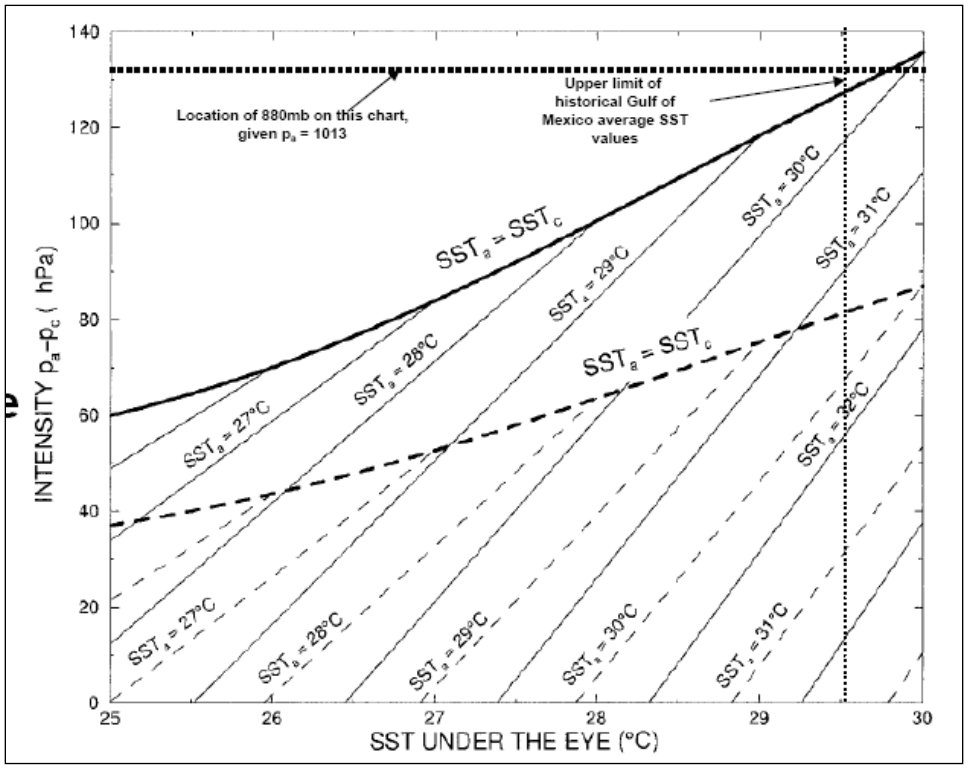

Figure 2-5. Storm intensity as a function of SST under the eye with feedback due to relative humidity considered, from Schade (2000). Subscript *a* is ambient and subscript *c* is center of storm.

Besides nagging issues with the objectivity of the PMH definition, other problems with the earlier work have arisen. For example, the use of "sustained wind speed" as the parameter of primary basis for the evaluation of the PMH characteristics has been superseded by the adoption of the Probable Maximum Storm Surge (PMSS) (U.S. Nuclear Regulatory Commission, 2007) as a project design basis. The degree of severity implicit within the PMH was also clarified somewhat in this report; however, the report mixes the PMH and the PMSS when it states that the "PMSS is the surge that results from a combination of meteorological parameters of a probable maximum hurricane (PMH)…. and has virtually no probability of being exceeded in the region involved." It is not clear how the PMH can be used in this context, unless the definition is altered from its purely sustained wind speed basis, since Irish *et al.* (2008) and Irish and Resio (2010) have clearly shown that storm size, in addition to maximum wind speed, is extremely important to the magnitude of the storm surges generated. Based on this evidence, it is logical to retain the term PMSS and to drop usage of the term PMH in future discussions of very extreme surges used for determining potential locations for critical infrastructure such as nuclear power plants.

2.3 Uncertainty

The range of uncertainty that is inherent in the storm wind fields and the resulting modeling representation of these wind fields must be considered. A considerable amount of uncertainty exists for the predictive models and the limiting estimates of the meteorological inputs to the predictive models. There are three main types of uncertainty with respect to understanding hurricane hazards along coasts. First, there is uncertainty that the actual sample of storms is representative of the "true" climatology today. Second, there is uncertainty in the events within future intervals of time, even if the "true" climatology is known exactly. And, third, there is uncertainty that some non-stationary process (sea level rise, subsidence, climate change, new development patterns, man-made alterations to the coasts, marsh degradation, etc.) will affect future hazards. The approach proposed in this report attempts to determine which factors affecting hurricane surges can be shown to have asymptotic upper limits and which factors must be treated within a context that allows for this natural uncertainty in estimating an upper limit for surges at a specified site.

2.4 Recommendations for NRC Consideration

The Bathystrophic Storm Surge model is extremely limited by restrictions and simplifications made in order to make the problem computationally tractable given the computer resources available in the early to mid 1970's. The model assumptions and simplifications reduce the applicability and accuracy of the model. It is recommended that a modern coupled system of wind, wave, and coastal circulation models that properly define the physical system and include an appropriate non-linear coupling of the relevant processes be adopted. The USACE hurricane modeling system combines the TC96 PBL model for winds, the WAM offshore and STWAVE nearshore wave models, and the ADCIRC basin to channel scale unstructured grid circulation model. The modeling system is well validated and, in addition to being applied for USACE projects, has also been adopted by several Federal FEMA regional offices for flood mapping.

There are several assumptions in the PMH described in NWS 23 that are now known to be invalid. It is recommended that the PMH concept be updated in accordance with new theoretical concepts and data. Two particular changes should be to:

- Allow the MPI to attain a somewhat lower central pressure than the older values; and
- Estimate storm size as a conditional probability function of storm intensity in simulations.

Also, the term PMSS should be retained and the usage of the term PMH dropped in future discussions of very extreme surges used for determining potential site locations for critical infrastructure such as nuclear power plants. Finally, it should be noted that it is also important to consider the range of uncertainty that is inherent in the storm wind fields, and the resulting modeling representation of these wind fields and surges.

3.0 DETERMINISTIC-PROBABLISTIC APPROACH FOR DERIVING LOW-PROBABILITY HURRICANE STORM SURGES

Two fundamentally different methods for estimating design surge levels have been utilized in past studies: deterministic-based methods and probability-based methods. Deterministic methods typically use the estimated maximum surge value from either a single storm or a small set of storms as its design level and do not consider the probability of that surge level. Probabilistic methods consider surges from a range of events along with the probabilities of those events and attempt to develop a relationship between surge levels and return period. A simple example of the deterministic method would be to define a single PMH and to simulate surges from that storm, which would yield a single deterministic surge value at a site of interest. An example of a probabilistic method would be to simulate the appropriate population of historical storms, rank the resulting surge values at a point of interest, and fit the cumulative distribution function based on these ranked results with some extremal distribution. There are deficiencies with both of these approaches for estimating very-low probability hurricane surges. The purpose of this Section is to develop a hybrid approach that considers a natural upper limit for hurricane generated surges and allows for natural uncertainty in estimating this upper limit.

3.1 Problems with a Strictly Deterministic Approach

The deterministic (single design storm) approach is clearly suitable for estimating a very-low-probability surge level in a rigorous sense if 1) the selected design event is known to be the event which creates the maximum possible surge at the site of interest or 2) the probability of the surge created by the design event is known and accepted as an adequate design criterion. In the latter case, subjective words, such as “reasonably be expected” must be replaced by definitive, objective values such as “with a probability of exceedance less than z”, where z would be a fixed number. Thus, a strictly deterministic approach to the problem of very-low-probability design events would imply 1) that we know the precise set of forcing conditions that can create the maximum (or at least a given fixed very-low probability) surge at a given location and 2) that there was no uncertainty in either the predictive models utilized or the limiting estimates of the inputs to the predictive model. Unfortunately, since neither of these conditions is met, a strictly deterministic approach may not represent the actual maximum condition (or very-low-probability event) expected at a given location. For this reason, it is difficult, and perhaps impossible, to generalize a strictly deterministic approach for application in a wide range of coastal environments.

3.2 Problems with a Strictly Probabilistic Approach

If the peak surge level at a point only depended on a single scalar variable, such as wind speed, the maximum value of that variable could clearly be associated with the maximum surge value. However, hurricane surge response at a specific site depends on several storm factors and not just a single, scalar variable (e.g. wind speed). Therefore, the maximum surge produced by a storm of a given size (as defined by the radius to maximum winds) and wind speed might still be exceeded by a storm with a larger radius to maximum winds and precisely the same wind speed. Figure 3-1 shows the scatter of storm surge versus a scale based on wind speed (Saffir-Simpson Scale), and Figure 3-2 shows the scatter of the storm surge versus a scale based on storm size (Powell and Reinhold, 2007). Figure 3-3 shows the scale developed by Irish and Resio (2010) based on simplified hydrodynamics. Although the Irish-Resio scale certainly improves upon previous scales, the omission of wave set-up contributions, storm forward

speed, and angle of intersection of the storm track with the coast still leave very large scatter in the data and confirms that dependence on a single variable is not possible.

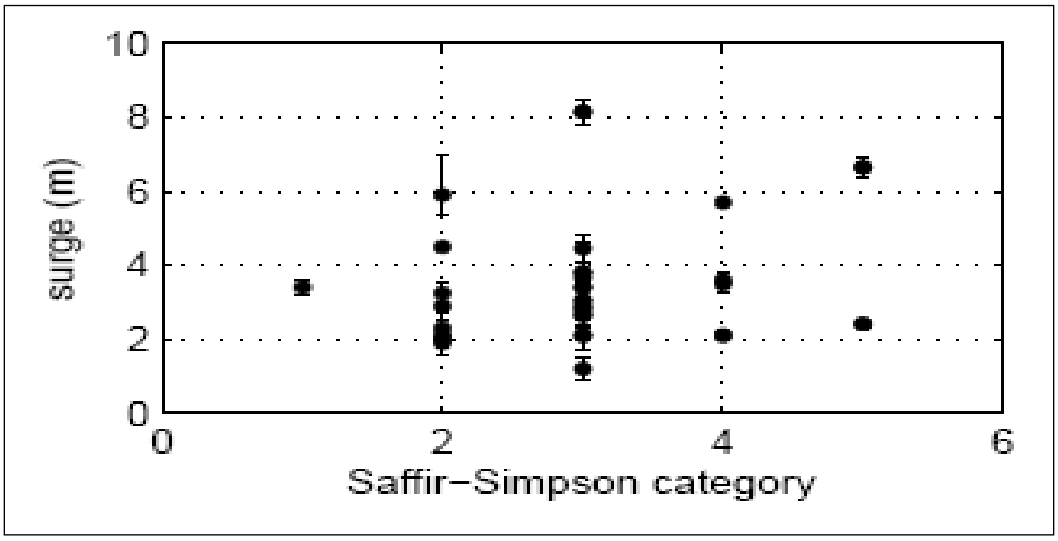

Figure 3-1. Comparison of Saffir-Simpson scale to actual measured maximum surge values at coast for historical storms (from Irish and Resio, 2010).

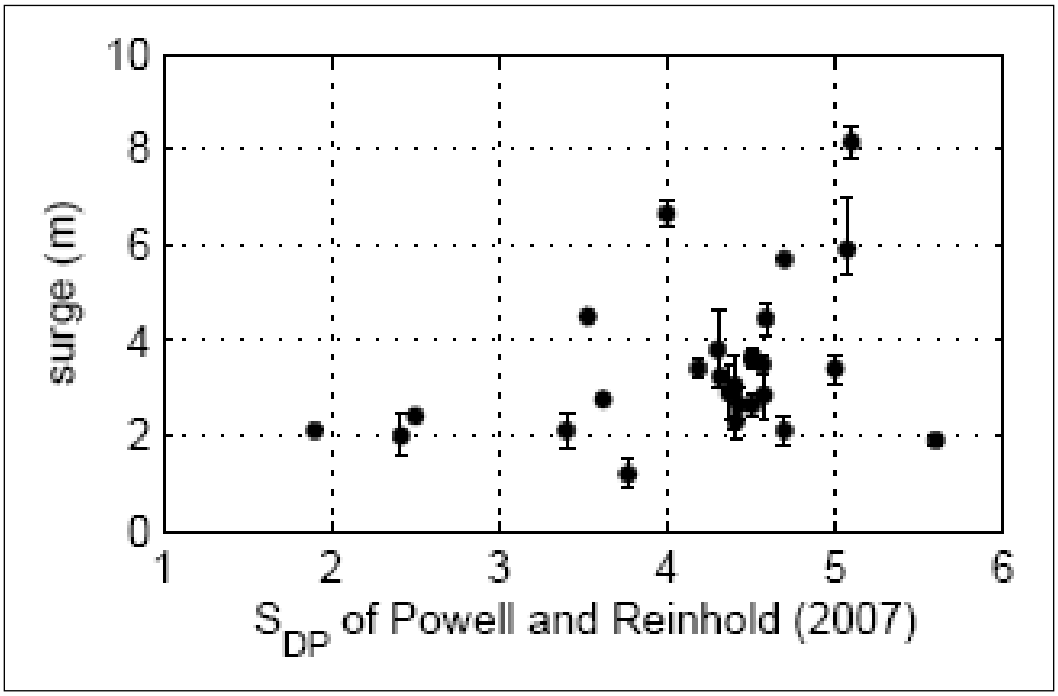

Figure 3-2. Comparison of Powell-Reinhold scale to actual measured maximum surge values at coast for historical storms (from Irish and Resio, 2010).

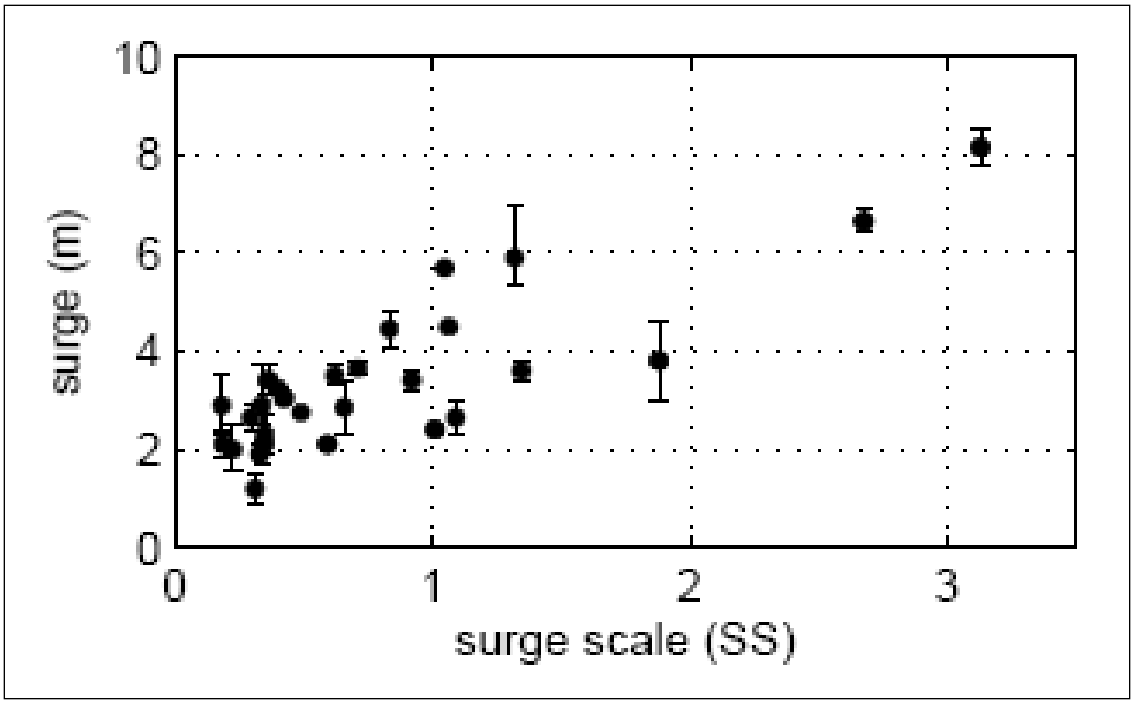

Figure 3-3. Comparison of simplified hydrodynamics based scale to actual measured maximum surge values at coast for historical storms (from Irish and Resio, 2010).

Several recent studies (IPET, 2009; Resio *et al.*, 2008; Irish *et al.*, 2008; Irish and Resio, 2010) have shown that the maximum surge can be estimated as a function of several storm parameters:

$$\eta_{\max}(x,y) = \eta_{\max}(x,y,\Delta p,R_{\max},v_f,\theta_f,B,x_0) + \varepsilon \qquad \text{Equation 3-1}$$

where

x	along coast spatial coordinate
y	cross coast spatial coordinate
Δp	peripheral pressure minus central pressure
R_{max}	distance from storm eye to maximum winds
v_f	forward velocity of the storm
θ_f	angle of storm heading
B	Holland B parameter
x_0	along coast location of landfall
ε	deviation in storm due to potential errors in estimate.

The last term in this equation, in essence, represents the sum of a wide range of omissions and errors in our predictive state of the art for surges. Some examples of this are 1) the difference between actual (very complex) space-time varying winds in a real hurricane and the parametric representation of these winds in a model driven by a small set of parameters; 2) numerical surge models are still imperfect and produce errors related to these imperfections (in both the physics and numerical approximations utilized within the models); and 3) the coast is always in

a state of change, so the use of present-day topographic/bathymetric representations in simulations of a future storm may not be precise.

Before proceeding, it is important to note that the verified accuracy of a numerical model for its application to a particular situation/area is absolutely essential to ensuring that any of the results are usable for critical applications. As discussed in Resio and Westerink (2008), this absolutely requires 1) the application of a model with sufficient resolution to represent important bathymetric/topographic features accurately and 2) that all terms contributing to the surge are represented in the proper physical context. For modern applications, this latter stipulation has shown that a coupled surge-wave model must be applied and the computational domain must be sufficiently large to negate the need for empirical factors along an offshore grid boundary. In turn, this means that run time requirements for such models tend to be considerably higher than for simpler models.

Given the general form of Equation 3-1, Joint Probability Methods (JPM's) can be used to estimate the expected probability density functions and cumulative density functions from sets of many numerical simulations with an appropriate numerical model (IPET, 2009; Resio *et al.*, 2008; Irish *et al*., 2008; Toro *et al*., 2010a and 2010b; Niedoroda *et al*., 2010). However, present JPM methods are focused on providing estimates of surges for a range of return periods in the neighborhood of 50 to 1000 years. Although it has been clearly established that estimates from the JPM are more stable than estimates based only on historical hurricanes, the confidence limits in estimated values using either of these methods is expected to become very large for very low probability surge values.

If the population of hurricanes were known exactly (i.e. the multivariate probability density function of all possible combinations of hurricane parameters was known exactly), "boot-strap" methods could be used to re-sample from that population to determine *N* sets of *M*-year samples, where *M* is often regarded as the "design life" of the decision/design being made. This could be used to estimate the range of surge conditions that might be expected in a particular *M*-year period in the future. However, error bands determined in this way do not differentiate between initial samples based on a small number of years versus initial samples based on many years of data, nor will it allow a simple estimate of the effects of non-stationarity (i.e. climate variability) on future samples.

Three main types of uncertainty with respect to the estimation of extremes are relevant to understanding hurricane hazards along coasts. First, there is uncertainty that the actual sample of storms is representative of the "true" climatology today. Second, there is uncertainty in the events that will actually occur within future intervals of time, even if the "true" climatology is known exactly. And, third, there is uncertainty that some non-stationary process (sea level rise, subsidence, climate change, new development patterns, man-made alterations to the coasts, marsh degradation, etc.) will affect future hazards. The first of these has traditionally been addressed via sampling theory. The second can be addressed via re-sampling or "boot strap" methods. And, the third must be estimated from ancillary information, often not contained within the initial hazard estimates themselves.

The first type of uncertainty listed above pertains to what was termed confidence bands (or control curves) for estimates of extremes. It cannot be estimated with re-sampling techniques, since these techniques use the initial sample as the basis for their re-sampling and implicitly assume that the initial sample represents the actual population characteristics. Thus, some parametric method must be applied to obtain this information. The data can be fit with many classes of distributions. Since we are only using the parametric fits to estimate uncertainty and

not to replace the non-parametric estimates obtained from the JPM, we are somewhat free to use any distribution for which the sampling uncertainty is known. Gringorten (1962, 1963) has shown that the expected root-mean-square (rms) error of an estimated return period (T) in a two-parameter Fisher-Tippett Type I (Gumbel, 1959) distribution is given by

$$\sigma_T = \sigma\sqrt{\frac{1.1000y^2 + 1.1396y + 1}{N}} \qquad \text{Equation 3-2}$$

where

σ_T	is the rms error at return period, T;
σ	is the distribution standard deviation;
N	is the number of samples used to estimate the distribution parameters;
y	is the reduced Gumbel variate given by $y=(\eta-a_0)/a_1$;
η	is the variate of interest (surge level in this case); and
a_0 and a_1	are parameters of the Gumbel distribution.

The reduced variate and return period are related by:

$$y = -\ln\left[\ln\left(\frac{T}{T-1}\right)\right] \qquad \text{Equation 3-3}$$

which for $T>7$ approaches an exponential form given by:

$$\left(T - \frac{1}{2}\right) \rightarrow e^y \qquad \text{Equation 3-4}$$

Equation 3-2 shows that the rms error at a fixed return period is related to the distribution standard deviation and the square root of a non-dimensional factor involving the ratio of different powers of y to the number of samples used to define the parameters. By the method of moments, the Gumbel parameters can be shown to be given by:

$$a_0 = \gamma a_1 - \mu \qquad a_1 = \frac{\sqrt{6}}{\pi}\sigma \qquad \text{Equation 3-5}$$

where γ is Euler's constant (=0.57721…) and μ is the distribution mean. Thus, the distribution standard deviation is related to the slope of the line represented by Equation 3-5 and can be used for estimating the expected width of the confidence limits for a specified return period.

Although Equation 3-2 was initially derived for applications to annual maxima, it can be adapted to any time interval for data sampling in a straightforward manner. For the case of hurricanes, the average interval between storms (the inverse of the Poisson frequency used in the compound Gumbel-Poisson distribution) can be used to transform Equation 3-2 into the form:

$$\sigma'_T = \sigma\sqrt{\frac{1.1000y'^2 + 1.1396y' + 1}{N'}} \qquad \text{Equation 3-6}$$

where

σ_T' is the rms error at return period, $T' = T/\hat{T}$
where $\hat{T}$ is the average years between hurricanes; and

N' is the effective number of years used to estimate the distribution parameters.

As an example of how this might be applied, let us examine some actual data from the interval 1941 to 2005 for hurricanes in the Gulf of Mexico. Since the form of Equation 3-4 is logarithmic, the slope is not affected by a multiplicative factor, and thus, the distribution standard deviation remains the same. *N'* in Equation 3-6 can be estimated from the equivalent total number of years in the sample divided by $\hat{T}$. The total number of years for this case is 65 (1941 to 2005, inclusive) times a factor, *Z*, which relates the spatial area covered by the sample to the spatial extent of a hurricane surge.

For relatively intense storms capable of producing surges that are exceeded only every 100 years or more, the along-coast extent of very high surges at least 60% of the peak value is about 60 nm for a storm with a 20-nm radius to maximum winds (IPET 2009). In that study, the "local" values used to estimate the distribution parameters were drawn from an alongshore section covering ±3.5 degrees longitude along 29.5 degrees north latitude. The value of *Z* is given by:

$$Z = \frac{\text{Distance along coast}}{\text{Width of a single sample}} \qquad \text{Equation 3-7}$$

which in this case is 365.5 nm divided by 60 nm, or approximately 6.1. Thus, the effective number of years is 396.

Combining Equations 3-4 and 3-6 shows that the asymptotic behavior of the error estimate for large return periods will have the functional form:

$$\sigma'_T = \frac{\sigma \ln(T)}{\sqrt{N'}} \qquad \text{Equation 3-8}$$

Since the distribution standard deviation (σ) and the effective number of years are independent of the return period, it is apparent that the spread in width of the control band will continue to increase in proportion to the logarithm of the return period. Thus, a typical 90% error of 2.5 to 3.0 ft in the estimates of the 100-year surge value along the northern Gulf of Mexico coast will increase by a factor of three in an estimate of the 10^6 return period, making the equivalent 90% error band in the range of 7.5 – 9.0 ft for such an event. And, if a 99% error limit were used as the tolerable error threshold, the error band would increase to approximately 11.3 to 13.5 ft. Another problem with this approach that is more of an operational nature, is that it would require somewhere around 100 to 200 storm surge simulations for a single nuclear power facility site in order to cover the range of storm parameter combinations in a JPM approach required for very-low-probability storms. This is due to the fact that the JPM approach covers a much larger range in probabilities rather than just focusing on the very high end of the storm surges.

The issue of non-stationarity related to changing coastal landscapes, sea level rise, and climate variability cannot easily be included within this estimate, since the theoretical foundation for these errors is based upon a single, homogeneous population. In areas undergoing rapid land loss, such as much of coastal Louisiana, it is particularly important that any simulations used as the basis for decision-making consider both the existing coastal landscape and the potential future coastal landscape at the end of the expected design life of any critical infrastructure. Even in areas where the coastal landscape is not expected to change radically, the issue of

continuing and/or accelerating sea level rise must be dealt with in a quantitatively defensible fashion.

The previous discussion shows that there are two substantial problems in the estimation of the very-low-probability events using a strictly probabilistic approach: 1) the large error associated with extrapolations based on a relatively small number of years to very large return periods and 2) problems with including non-stationarity into the error bands. Another problem is the lack of a strong probabilistic basis for selecting a level of risk appropriate for a surge to exceed a design level. This depends strongly on the number of years in the assumed lifetime of the structure being designed. It can be shown that for very long return periods, such as the 10^6 return period referenced above, the expected total encounter probability (not the annual encounter probability) rises linearly with the number of years in the assumed lifetime, i.e.:

$$P_n = 1 - \left(1 - \frac{1}{T}\right)^n \approx 1 - \left(1 - \frac{n}{T}\right) \qquad \text{Equation 3-9}$$

where P_n is the non-encounter probability of exceedance of the design value in n years. This can be expressed in somewhat simpler manner by recognizing that the non-encounter return period after n years is related to the initial return period by $T_n \sim T/n$ for very long return periods such as the example here. Thus, a one million year (10^6) return period for an occurrence in one year would be expected once every 20,000 50-year increments. Risk communication to the public should convey this total risk over an expected lifetime as well as the annual risk.

3.3 Development of a Combined Deterministic-Probabilistic Approach

Since both the probabilistic-only and the deterministic-only approaches to the estimation of very-low-probability hurricane surges have some deficiencies, it is logical to investigate joining the two approaches into a hybrid approach. Such a combination might provide some advantages over either approach implemented independently. Thus, instead of using either a probabilistic-only or a deterministic-only approach to the estimation of very-low-probability, the approach here attempts to determine which factors affecting hurricane surges can be shown to have asymptotic upper limits and which factors still have to be treated within a context that allows for natural uncertainty in estimating an upper limit for surges at a specified site. Resio *et al*. (2008), Irish *et al*. (2008) and Irish and Resio (2010), show that the response of surge levels can be addressed as a function of several variables, as shown specifically for the variation of surge levels along the coast in Figure 3-4. In this approach, the maximum surge level can be approximated as:

$$\eta_{\max} = \Phi_1(\Delta p)\Phi_2(R_{\max})\Phi_3(x - x_0)\Phi_4(v_f)\Phi_5(\theta_f) \qquad \text{Equation 3-10}$$

where the multiplicative functions Φ_i should be understood to depend on the specific bathymetric/topographic setting of the specific point being investigated, and x-x_0 denotes the alongshore position of the point of interest relative to the landfall position. As noted by Irish and Resio (2010), when the storm size becomes as large as the region of primary surge generation, additional increases in storm size do not produce substantial increases in storm surge. If we take L_* as the width of the primary surge generation region, it can be shown that Φ_2 will take a form such that

$$\Phi_2(R_{max}) \approx \frac{R_{max}}{L_*} \quad \text{for } R_{max} \le L_*$$
$$= 1 \qquad \text{otherwise.}$$

Equation 3-11

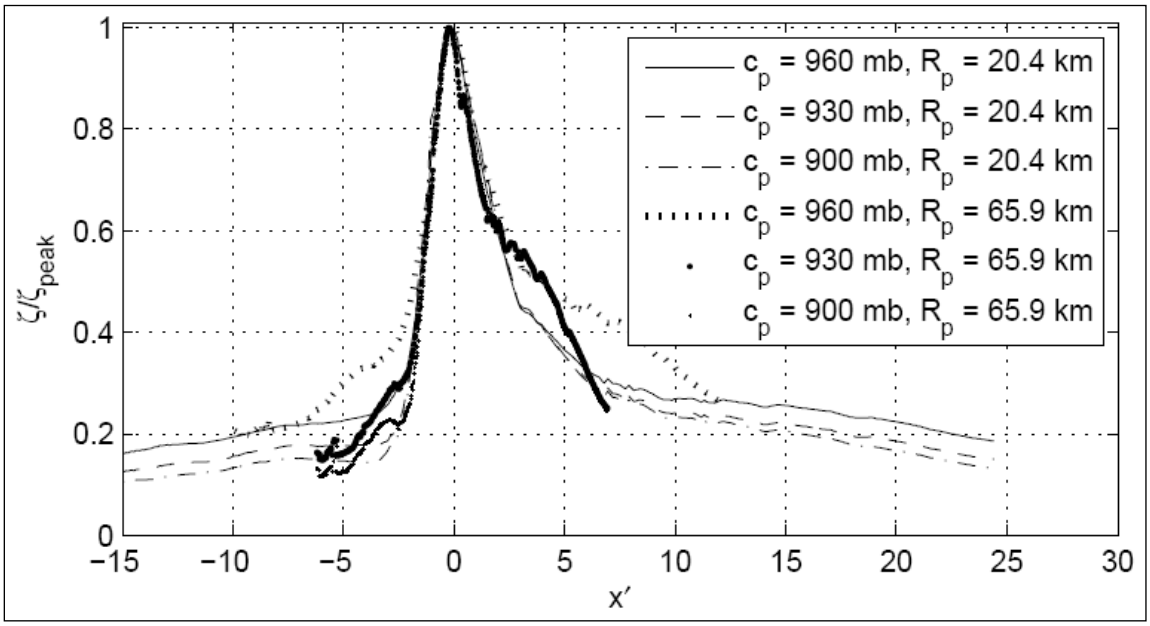

Figure 3-4. Numerically simulated (using ADCIRC) dimensionless alongshore surge (ζ/ζ_{peak}) distribution. Demonstrates the similarity in surge scaling for hurricanes of different sizes (R_p is an input value to the TC96 model that is equivalent to R_{max} for practical purposes) and intensities (c_p is storm central pressure), where *x*' is the deviation between a site and the landfall location divided by the radius to maximum winds (from Irish *et al.* 2008).

This is a natural limit related to what might be termed the fetch over which the wind can act to generate a significant slope in the water surface and hence forms an upper limit to the effect of increasing storm size on maximum surge levels in a storm. Hurricane Ike represents a good example of a storm for which the effect of storm size on peak surge levels was mitigated by the effective shelf width in the area of landfall and graphical support for this on a simple coast can be seen in Figure 3-5.

Irish and Resio (2010) have shown that three of the other four functions in Equation 3-10 have asymptotic limits. In extensive tests along the Texas coast and elsewhere, the relative position of the point of interest to the landfall location (Φ_3) has been shown to behave as seen in Figure 3-4. As expected the maximum surge occurs near the location where the maximum winds come ashore with surge levels decreasing monotonically to either side of this maximum. Φ_4 is an interesting function in that it reflects two physical mechanisms which tend to have opposite effects on surge levels. On one hand, as the storm speeds up, wind speeds inside a hurricane increase due to the contribution of these background winds. On the other hand, as the storm speeds up the time winds blow over the surge generation area is decreased. As might be expected in such a situation, the result of combining these two effects is that the surges typically increase to a maximum value at some intermediate forward speed and decrease monotonically to either side of this maximum value. The last function with a natural limiting behavior is Φ_5 (angle of approach). Changes in track angle increase peak surge by no more than 10% with respect to a shore normal approach. Figure 3-6 shows the general behavior of this function.

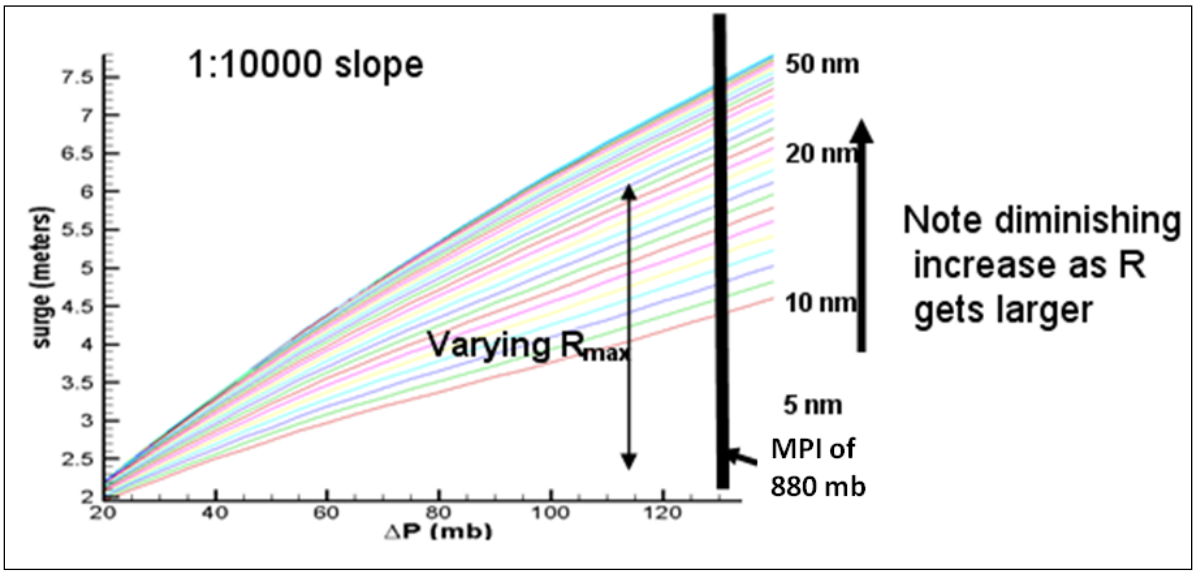

Figure 3-5. Results from numerical ADCIRC simulations showing maximum surge values as a function of storm size and storm intensity. The bold vertical line corresponds to a pressure differential of 133 mb.

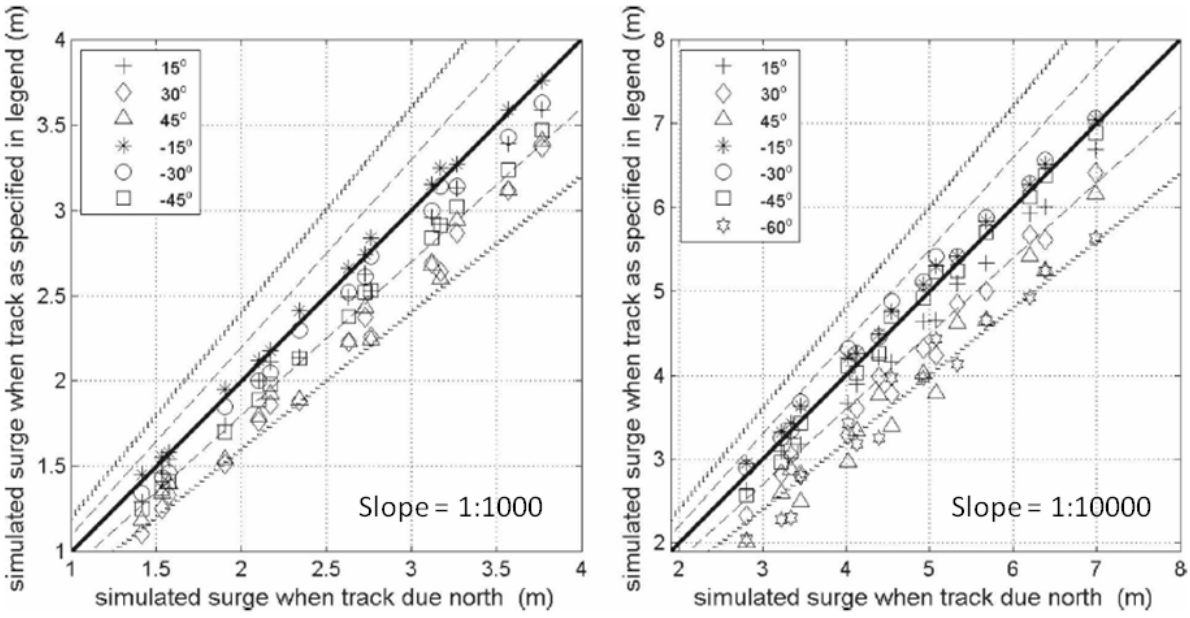

Figure 3-6. Simulated peak surge as a function of hurricane track angle, measured counterclockwise from a due north approach. Plus or minus 10%, and 20% increases or decreases in value are marked by the dashed and dotted lines, respectively (from Irish *et al.*, 2008).

The one function that does not have a clear upper limit in the potential maximum surge formulation is the pressure differential term, $\Phi_1(\Delta p)$. To examine the effect of the pressure differential on maximum surge, let us examine the simple case of a steady state wind over a

shelf of constant width and depth. In this case, a simple linear approximation for the surge at the coast yields:

$$\eta = \frac{\rho_a}{\rho_w}\frac{c_d V^2 L}{gh}$$ Equation 3-12

where

ρ_a, ρ_w are the densities of air and water, respectively;
c_d is the coefficient of drag;
V is the wind speed;
L is the shelf width;
g is the acceleration due to gravity; and
h is the water depth on the shelf.

This simple form can also be shown to be appropriate for more complex wind fields with a specified geometric similarity, such as found in hurricanes, and more complex offshore configurations. For a constant (no wind speed dependence) coefficient of drag, and noting that the pressure differential will be linearly proportional to V^2, it is expected that the maximum surge in hurricanes will depend linearly on the pressure differential. This result was confirmed numerically in a wide range of simulation along the Mississippi coast using simulations computed by the SLOSH code (Figure 3-7) (Niedoroda *et al.*, 2010).

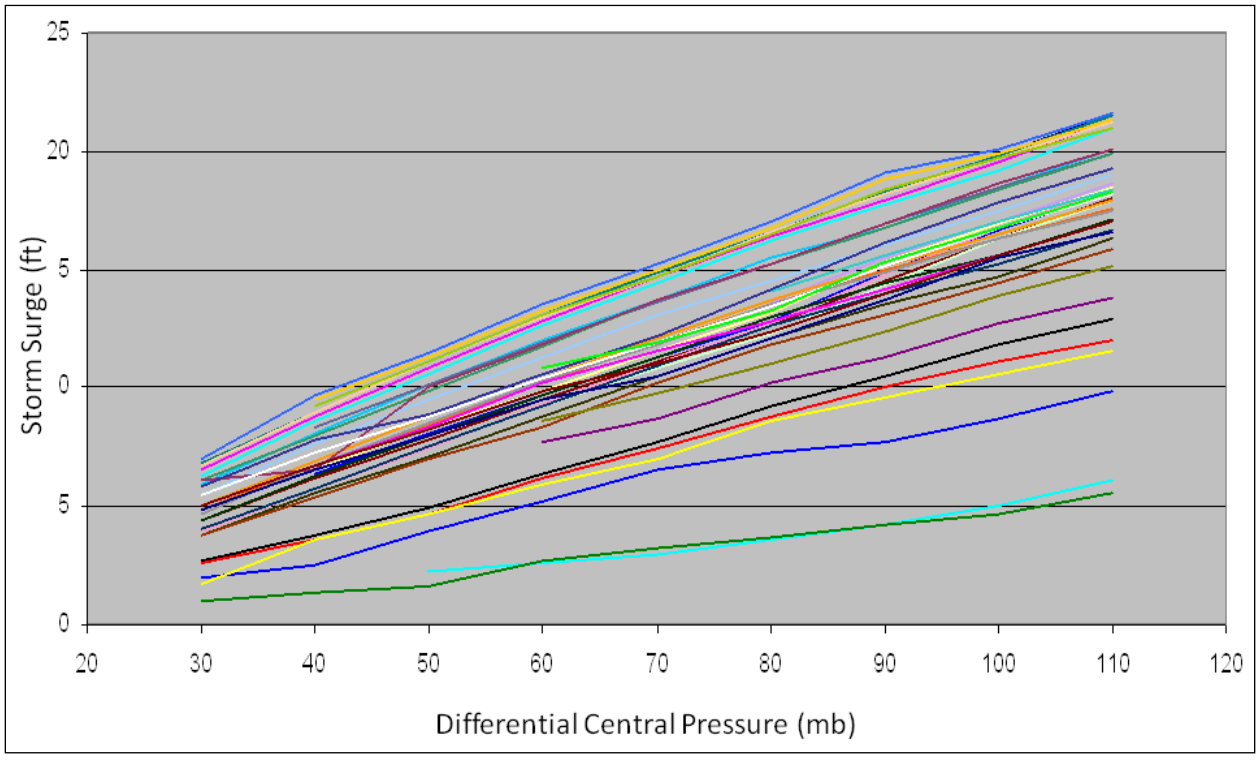

Figure 3-7. SLOSH results for a set of 44 points along the coast of Mississippi for storms of different central pressures.

However, wind speed profile data recently collected in real hurricanes (e.g. Powell *et al.* 2003, and Powell 2006) indicate that wind drag coefficients are not constant but rather increase until wind speeds of approximately 30-40 m/sec are reached and then the drag coefficient is reduced

for increasing wind speeds above this range of values. Capping or reducing the wind drag coefficient results in a nonlinear surge response to further increase in pressure differential. The complex relationship between storm size and maximum wind speeds should also be noted. In a natural system such as a hurricane with high winds moving circularly around a pressure minimum, the wind and pressure distribution will tend toward a cyclostrophic balance in which the outward centripetal acceleration is balanced by the pressure gradient. In this situation, as can be verified by hurricane wind vortex models (numerical simulations of the planetary boundary layer in hurricanes), the maximum wind speed tends to scale linearly with the square root of the pressure differential. If we assume a purely cyclostrophic flow exists, the force balance depends on only two terms, the centripetal force directed outward away from the center of the storm and the pressure gradient force directed inward toward the center of the storm; consequently, in the vicinity of the maximum wind speed, the governing equation for the motions is of the form:

$$\frac{V_{\max}^2}{R_{\max}} = \frac{\Delta p}{R_{\max}}$$; where V_{max} is the maximum wind speed Equation 3-13

which is consistent with a linear relationship between velocity squared and the pressure differential, independent of storm size. However, as the size of a hurricane becomes larger and larger, the geostrophic terms in the force-balance equation become the same order as the cyclostrophic terms and this equation changes form to:

$$\frac{V_{\max}^2}{R_{\max}} + fV_{\max} = \frac{\Delta p}{R_{\max}}$$; where fV_{max} is the coriolis acceleration Equation 3-14

In this situation, an increase in the storm size parameter will cause a decrease in the maximum wind speed and can have a larger effect on the total storm surge than the increase in size. In areas with smaller shelf widths, this effect can lead to a situation in which smaller storms can produce larger surges than a larger storm with the same intensity.

Finally, the discussion in Section 2 and data represented in Figures 2-4 and 2-5 indicate that the lowest central pressure possible is approximately 880 mb given recent SST. This value could be lower if SST within the Gulf of Mexico were to rise due to climate change. However, given a likely range of SST, data suggests there is a natural limit to storm intensity. This natural limit, and the relationships between storm size and wind drag coefficient to wind speed, as previously discussed, all suggest the existence of an asymptotic relationship between storm surge and the pressure differential term. The uncertainty in estimating this natural limit, however, must be considered. A full discussion of the natural limit (MPI) on hurricane central pressure and estimating the uncertainty in estimating this limit is provided in Section 4.2.

3.4 Upper Limit Storm Surge Estimation Procedure

The discussion in Section 3.3 suggests the existence of an upper limit for hurricane generated surges in natural environments. The following procedure is recommended for estimating maximum surge at a site of interest:

1. A high resolution state-of-the-art coupled wave-surge model with accurate bathymetric-

topographic data should be developed and the modeling system validated at the site of interest. The reliance on models in this approach requires that these models contain the best possible representation of the physics, that they properly resolve all critical scales of motion and topographic/bathymetric effects, and that they are calibrated and validated with historical data in the area of interest.

2. Develop a suite of synthetic storms. The storm suite should include a range of hurricane parameters and combinations of those parameters. For the southern U.S. coast, guidance for selecting the parameters to be simulated are:

    a. Central Pressure: Storms with an MPI of 880 mb (consistent with Schade (2000)) and a central pressure that is 10 mb lower than the MPI.
    b. Radius to Maximum Winds: Storms with an offshore R_{max} of 30 nm and 45 nm. These values are larger than any storms in the Gulf of Mexico with intensities greater than approximately 930 mb. In addition, as shown in Figure 3-5, on a 1 to 10,000 slope for an 880 mb storm, there is little or no variation of surge height with a change in storm size above an R_{max} of approximately 40 nm.
    c. Forward Speed: Three storm forward speeds should be simulated, a slow, medium, and fast, from approximately 5 to 22 knots. This range is based on the joint distribution storm speeds and central pressures in the Gulf of Mexico as shown in IPET (2009).
    d. Holland B: The Holland B should be set to 1.27 which is the mean value for the Gulf of Mexico (IPET 2009).
    e. Track: The track should be set to maximize storm surge potential. Irish *et al.* 2008 and Irish and Resio 2010 show that the peak is close to one R_{max} from the landfall location. The position and orientation of the tracks should be based on an analysis of historical high surge potential storm tracks in the area of interest and have minimal land interference as they approach the coast.

    The central pressure, radius to maximum winds, and Holland B all vary systematically during the storm's approach to land. Systematic variation in these parameters is identical to that used in the IPET (2009) and was adopted for the Gulf of Mexico FEMA and USACE studies. For details on the variation in these parameters see Appendix 8 of IPET (2009). It should be noted that these values are for the southern U.S. Gulf of Mexico coast only and are not applicable for other regions.

3. Applying the validated modeling system, simulate the surges that would be produced by these storms at the location of interest and determine the largest predicted surge. The modeling system can be applied with the existing mean sea level as the initial water level condition or include an estimate of eustatic sea level rise over the project life and an adjustment to reflect high tide. If these adjustments are not made to the initial water level condition, they must be added later. In areas with a large tidal range and/or high rates of sea level rise are estimated, it is recommended that the high water level is included in the modeling system.

4. Estimate the uncertainty in the estimate and add to the maximum calculated surge (guidance on estimating the uncertainty is provided in Section 4). If the tidal and sea level rise adjustments are not included in the simulated water level, they must also be added.

Effectively, the approach is deterministic in defining the storm suite. Each of the parameters has a range which is assumed to represent, or encompass, the value for that parameter that will generate the maximum possible surge. The probabilistic component is to define a 1% threshold based on estimated standard deviations in all relevant forcing mechanisms for surge, which allows for estimating the uncertainty in all the deterministic estimates.

The above procedure provides an estimate of the still water PMSS. Consideration must also be given to flooding potential from wave runup. A detailed analysis of wave runup requires very high resolution bathymetric/topographic data at the site location and application of a Boussinesq wave model or an approach such as that described by Melby (2012). Wave runup at a site is dependent upon the design of the nuclear plant and its protection features and its calculation is beyond the scope of this report.

3.5 Summary

Two fundamentally different methods for estimating design surge levels have been utilized in past studies. Deterministic methods typically use the estimated maximum surge value from either a single storm or a small set of storms as its design level and do not consider the probability of that surge level. Probabilistic methods consider surges from a range of events along with the probabilities of those events and attempt to develop a relationship between surge levels and return period. Both the deterministic-based and probability-based approaches to the estimation of very-low-probability hurricane surges have deficiencies and it is recommended to combine the two methods. The hybrid approach determines which factors affecting hurricane surges can be shown to have asymptotic upper limits and which factors still have to be treated within a context that allows for natural uncertainty in estimating an upper limit for surges at a specified site. The discussion in this Section supports the existence of an upper limit for hurricane generated surges in natural environments and a procedure for estimating maximum surge at a site of interest is recommended for NRC consideration.

4.0 APPLICATION OF APPROACH

The Matagorda Bay site served as a platform for developing the initial concepts for very low probability surges and is the primary site examined in Sections 4.1 and 4.2. Analyses of the upper limit for storm surges at two other sites in Florida are examined in Section 4.3. Section 4.4 develops a framework for quantifying exceedance probabilities of surges, including quantification of the effects of uncertainty on these estimates, and examines the relative magnitudes of surges obtained via the asymptotic upper limit method to estimated surge levels associated with the 10^{-6} annual frequency at the Florida sites.

4.1 Modeling System and Execution

The discussion in Section 3 lends support to the possible existence of an upper limit for hurricane-generated surges in natural environments; however, it is necessary to validate this concept with some actual detailed simulations. The test site selected is in the Matagorda, Texas area (Figure 4-1). Two types of tracks span the range of physically realistic major storms approaching this site, storms that form in the Bay of Campeche to the south of the site and storms that enter into the Gulf of Mexico between Cuba and Yucatan. The details of these tracks are not too critical, so they are represented as straight lines for the purpose of these tests (Figure 4-2). A suite of 20 storms (Table 4-1) was developed and simulated with a coupled system of wind, wave, and coastal circulation models. A schematic diagram of the modeling system is shown in Figure 4-3. All site and flood elevations are reported relative to the NAVD88 datum.

Figure 4-1. Project test site.

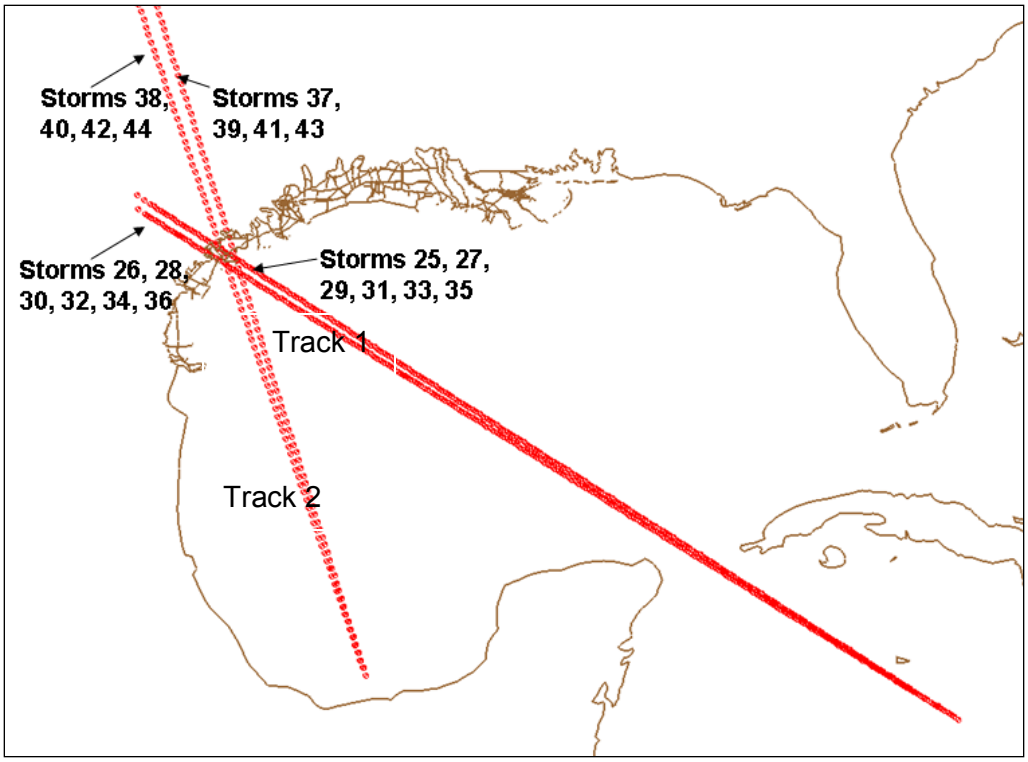

Figure 4-2. Storm tracks developed with the maximum wind speeds over the point of interest.

Table 4-1. Storm parameter values used in Matagorda Bay simulations.

Storm	Wind m/sec	Pres mb	W-Indf m/sec	P-Indf m/sec	Rp nm	Holland B	Vf kt
025	59.6	880	46.5	904	30-42	1.35-0.9	5.5
026	58	880	42.4	918.6	45-63	1.35-0.9	5.5
027	61.1	870	48.4	893.8	30-42	1.35-0.9	5.5
028	59.4	870	44.4	908.6	45-63	1.35-0.9	5.5
029	61.4	880	47.5	905.8	30-42	1.35-0.9	11
030	59.2	880	44.5	918.6	45-63	1.35-0.9	11
031	62.8	870	49.3	895.8	30-42	1.35-0.9	11
032	60.6	870	46.4	908.6	45-63	1.35-0.9	11
033	64.3	880	54.6	901.9	30-42	1.35-0.9	22
034	61.8	880	50.9	912.3	45-63	1.35-0.9	22
035	65.6	870	55.9	891.9	30-42	1.35-0.9	22
036	63	870	52.7	902.3	45-63	1.35-0.9	22
037	62.3	880	50	902.8	30-42	1.35-0.9	11
038	60	880	44.4	919.6	45-63	1.35-0.9	11
039	63.7	870	51.9	892.8	30-42	1.35-0.9	11
040	61.4	870	46.3	909.8	45-63	1.35-0.9	11
041	65.1	880	55.1	902.8	30-42	1.35-0.9	22
042	62.2	880	48.8	919.6	45-63	1.35-0.9	22
043	66.4	870	56.5	892.8	30-42	1.35-0.9	22
044	63.5	870	50.5	909.6	45-63	1.35-0.9	22

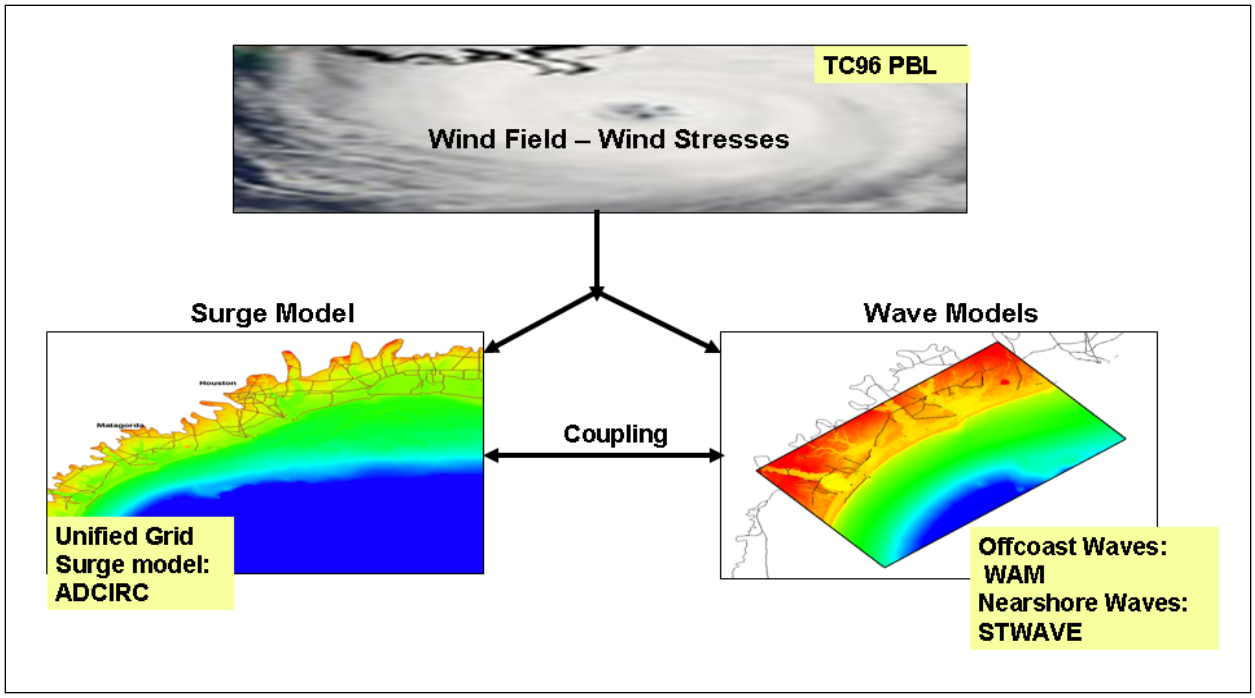

Figure 4-3. Schematic of hurricane modeling system.

For each storm, defined by a track and time-varying wind field parameters, the TC96 Planetary Boundary Layer (PBL) model (Thompson and Cardone 1996) is applied to construct snapshots of wind and atmospheric pressure fields every 15 minutes for driving surge and wave models. TC96 generates wind and pressure fields with a highly refined meso-scale moving vortex formulation developed originally by Chow (1971) and modified by Cardone *et al*. (1992). The model is based on the equation of horizontal motion, vertically averaged through the depth of the planetary boundary layer.

The depth-integrated circulation model ADCIRC (Luettich *et al*. 1992, Westerink *et al*. 1994, Luettich and Westerink 2004) is then run to compute the pressure- and wind-driven surge component. Imposing the wind and atmospheric pressure fields, the ADCIRC model can replicate tide induced and storm-surge water levels and currents. As noted previously in this report, the ADCIRC model solves the defined governing equations over complicated bathymetry encompassed by irregular seashore boundaries using an unstructured finite-element method. This algorithm allows for flexible spatial discretizations over the entire computational domain. The advantage of this flexibility in developing a computational grid is that larger elements can be used in open-ocean regions where less resolution is needed, whereas smaller elements can be applied in the nearshore and estuary areas where finer resolution is required to resolve hydrodynamic details and more accurately simulate storm surge propagation onto a complex coastal landscape.

In parallel with the initial ADCIRC runs, the large-domain, discrete, time-dependent spectral wave model WAM (Komen *et al.* 1994) is run to calculate directional wave spectra that serve as boundary conditions for the local-domain, near-coast wave model STWAVE (Smith *et al*. 2001, Smith 2007). WAM generates the offshore wave field and directional wave spectra. The model solves the action balance equation for the spatial and temporal variation of wave action in frequency and direction over a fixed longitude-latitude geospatial grid. The numerical model

STWAVE simulates nearshore wave transformation and generation. STWAVE numerically solves the steady-state conservation of spectral action balance along backward-traced wave rays. The source terms include wind input, nonlinear wave-wave interactions, dissipation within the wave field, and surf-zone breaking. STWAVE is a finite-difference model and calculates wave spectra on a rectangular grid. The model includes spatially variable wind and surge input fields. STWAVE generates the fields of energy-based, zero-moment wave height, peak spectral wave period, and mean direction; wave spectra at selected locations; and fields of radiation stress gradients. Using initial water levels from ADCIRC, winds that include the effects of sheltering due to land boundaries and reduction due to land roughness, and spectral boundary conditions from the large-domain wave model, STWAVE is run to produce wave fields and estimated radiation stress fields. The radiation stress fields are added to the estimated wind stresses, and applied as forcing in the ADCIRC model.

Model accuracy is directly related to how well the model represents the physical system (Westerink *et al.* 2008; Bunya *et al.* 2009). Many coastal landscapes are characterized by complex bathymetry and topography. Natural features such as barrier islands, bays, inlets, marshes, lakes and rivers as well as man-made features such as levees, roadways, railways, navigation channels, gates, and seawalls all influence surge and wave propagation. The surge and waves are not only influenced by the elevation of the landscape features, but also by the land cover, such as vegetation or buildings. The ADCIRC modeling system is able to capture the influence of these features across the coastal landscape (Wamsley *et al.*; 2009a, b).

Development of the ADCIRC grid utilized for this study was started in the 1990s (Westerink, Luettich and Muccino 1994). Considerable advancements were made for the IPET (2007) study and high-resolution wave model grids were developed. The IPET grids were then expanded and refined even further to create regional models that spanned the entire Louisiana and Mississippi coastal zone. The grid has been expanded further to include the Texas coastal zone and the mesh applied in this study has a reduced number of nodes in Louisiana and Mississippi for efficiency. The ADCIRC, TC96 PBL, and WAM model domains are shown in Figure 4-4. Note that the ADCIRC offshore boundary is in the deep Atlantic. Such a boundary allows for the model to accurately capture basin-to-basin and shelf-to-basin physics, which is important in estimating high water levels that often occur well in advance of a hurricane's landfall. The ADCIRC mesh contains over 2.3 million nodes. Grid resolution in the deep water is about 25 km. Figure 4-5 details the high level of resolution in the project area, with nodal spacing reaching as low as approximately 100 m in the most highly refined areas. Increased resolution across the coastal floodplain allows features such as inlets, rivers, navigation channels, levee systems and local topography/ bathymetry to be properly represented (Westerink *et al.* 1994). Levees and roadways are barriers to flood propagation that are generally below the defined grid scale. ADCIRC defines these structures as sub-grid scale parameterized weirs with a specified height (Westerink *et al.* 2001) within the domain. The sub-grid features such as levees and road systems are also shown in Figure 4-5. Figure 4-6 shows the STWAVE grid domain, a structured grid with 200 m resolution. Wave breaking zones must be resolved to ensure that the grid scales of the surge and nearshore wave models are consistent. The nearshore wave forcing function is properly incorporated by adding resolution where significant gradients in the wave radiation stresses exist (IPET 2007; Bunya *et al.* 2009).

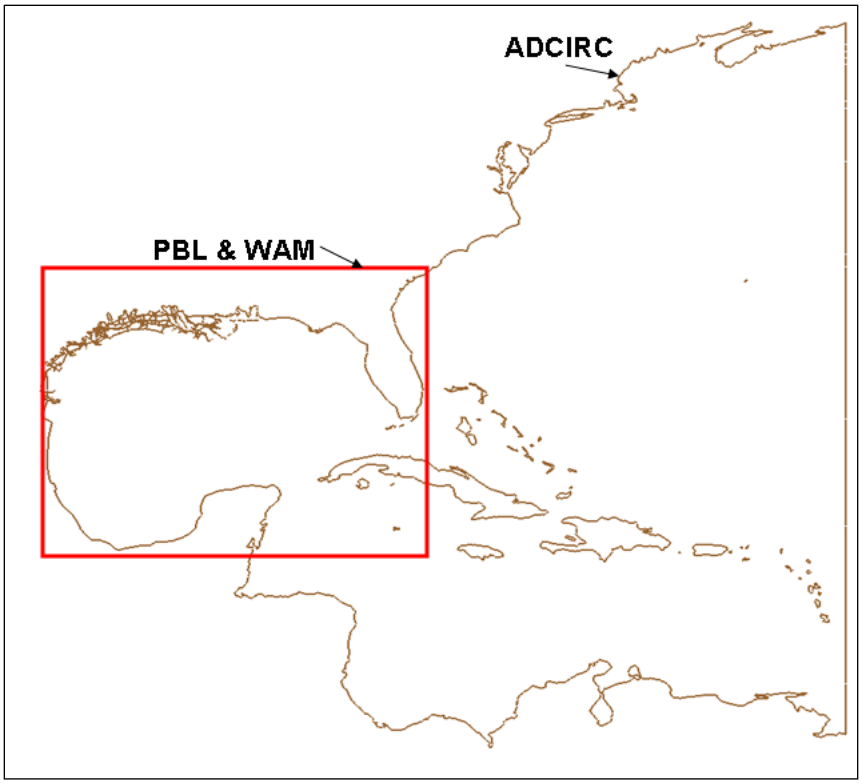

Figure 4-4. ADCIRC (brown), TC96 PBL (red), and WAM (red) model domains.

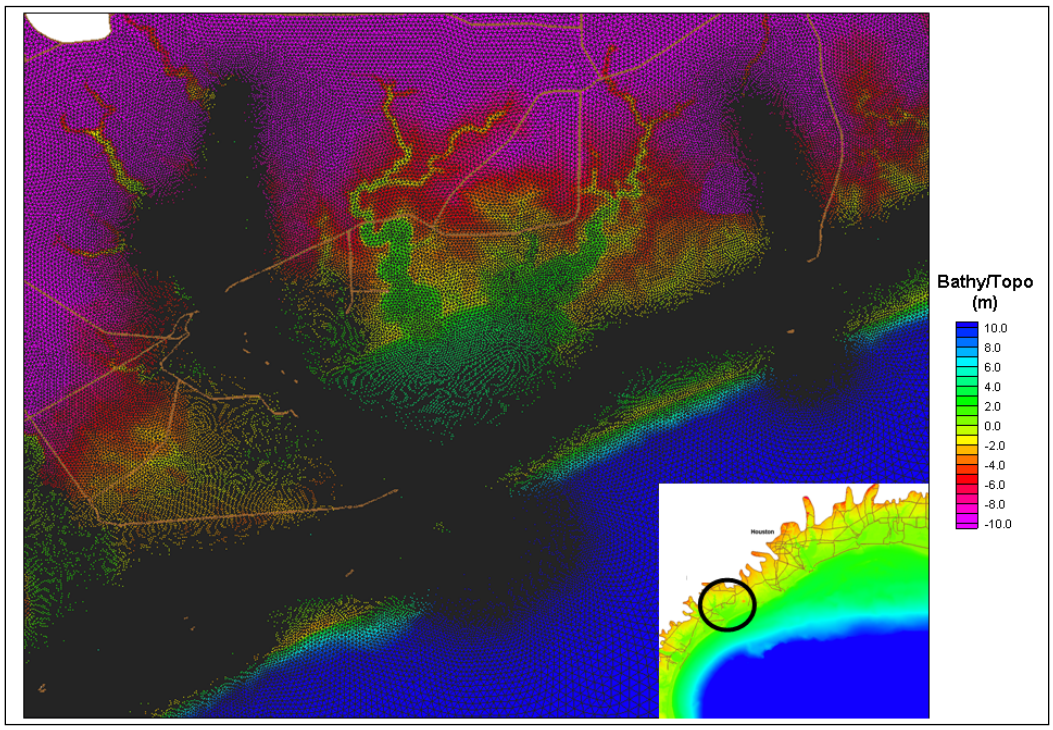

Figure 4-5. ADCIRC mesh in project area, colors represent bathymetry and topography and black lines are mesh elements.

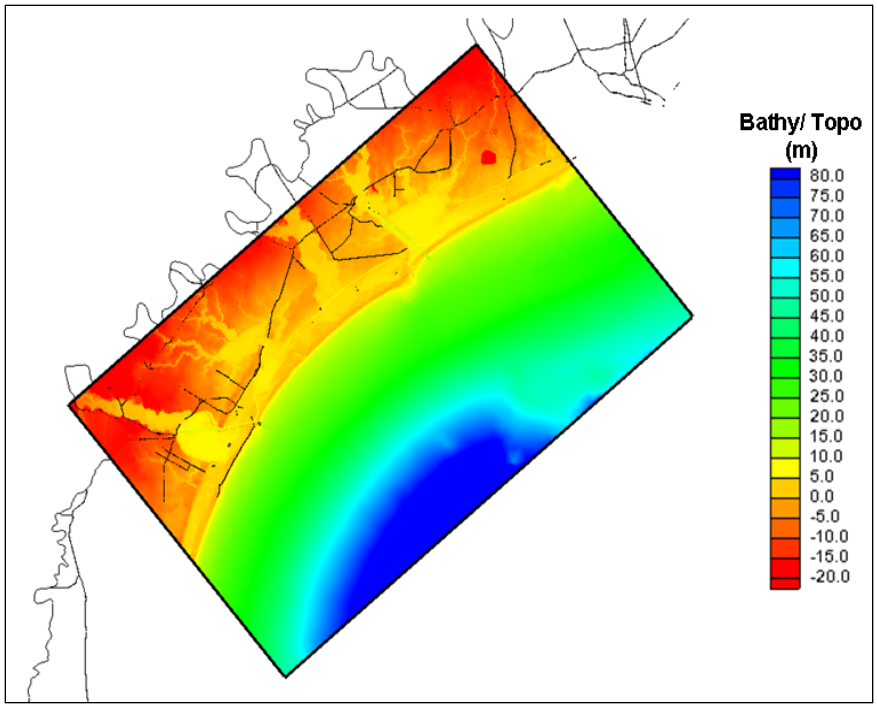

Figure 4-6. STWAVE grid.

Accurate modeling of wave and storm surge levels requires accurate wind and pressure field input. For historical storms, best wind products are developed by expert meteorologists using data assimilation techniques. For synthetic storms, the TC96 PBL model is applied to construct snapshots of wind and atmospheric pressure fields every 15 minutes for driving the surge and wave models. Storms are defined by a track and time-varying wind field parameters. For each storm, a unique set of input conditions is defined. The data file includes the track position in space and time, the forward speed and direction, central pressure, pressure scale radius (which is related to the radius to maximum winds), a rotation angle, and a pressure profile peakedness parameter termed the Holland B factor (Holland, 1980). The wind and pressure field is generated and positioned on a fixed longitude/latitude grid system covering the Gulf of Mexico. Based on the location of the storm center, these snapshots describe the temporal and spatial evolution of a hurricane. The final wind and pressure fields resulting from TC96 are targeted on a grid domain. The temporal variation in these fields is typically set to 1800 s, (30-min average wind). All wind-fields are marine-exposure (no effective roughness variations for land/sea changes), and generated at a 10 m elevation. The effect of ground cover on winds as the hurricane makes landfall is accounted for within the ADCIRC storm surge model. In addition, ADCIRC applies a wind drag coefficient based on Garratt (1977), which has a cap of 0.0035. Example output from the TC96 for storm 027 from the storm suite is given in Figures 4-7 to 4-9. Figure 4-7 represents the spatial variation of the maximum wind speed, and Figure 4-8 is the minimum overall pressure distribution. The wind field product (Figure 4-7) reflects the storm's path and displays the spatial coverage of high winds, an indication of the breadth in the hurricane core. Figure 4-7 also shows the decay in the wind speed magnitude as it makes landfall. As this hypothetical storm approaches the coastline, the wind speed decreases from approximately 61 m/s at its maximum to around 48 m/s at landfall, indicative of the pressure field filling. The minimum pressure distribution (Figure 4-8) clearly shows the storm track position, the radius to maximum winds, and where the filling of the pressure field occurs. An example plot of the wind speed and wind direction vectors is shown in Figure 4-9. The wind

direction vectors point in the direction the winds are blowing. The wind speed contouring shows near continuous lines from the land to sea, indicative of generating an exclusive set of marine exposure wind fields. For this storm, the wind speed maximum is found in the right front quadrant of the storm.

The WAM offshore wave simulations supply the two-dimensional wave spectra in the coastal area to be used as input boundary conditions to the nearshore wave modeling effort supported by STWAVE. The WAM directional wave spectra are output every 15-minutes at discrete frequency and direction bands at specified save locations for the boundary conditions. Example output from WAM is given in Figure 4-10. Figure 4-10 is a plot of the maximum total significant wave height field for storm 27 from the storm suite. The envelope of high waves coincides with that of the wind core (see Figure 4-7). The maximum overall significant wave height (H_{mo}) for this simulation is approximately 67.2 ft offshore. In the coastal area closer to shore, the H_{mo} results diminish to less than 26.2 ft.

The numerical model STWAVE simulates nearshore wave transformation and generation. Example output generated from the STWAVE model results are provided in Figure 4-11. Figure 4-11 shows the maximum significant wave height in the vicinity of Matagorda. Wave period and wave direction are also calculated by STWAVE. The significant wave heights, periods, and directions in representative sections can be selected as boundary conditions for calculating wave runup and overtopping, wave forcing on structures, or for other design purposes.

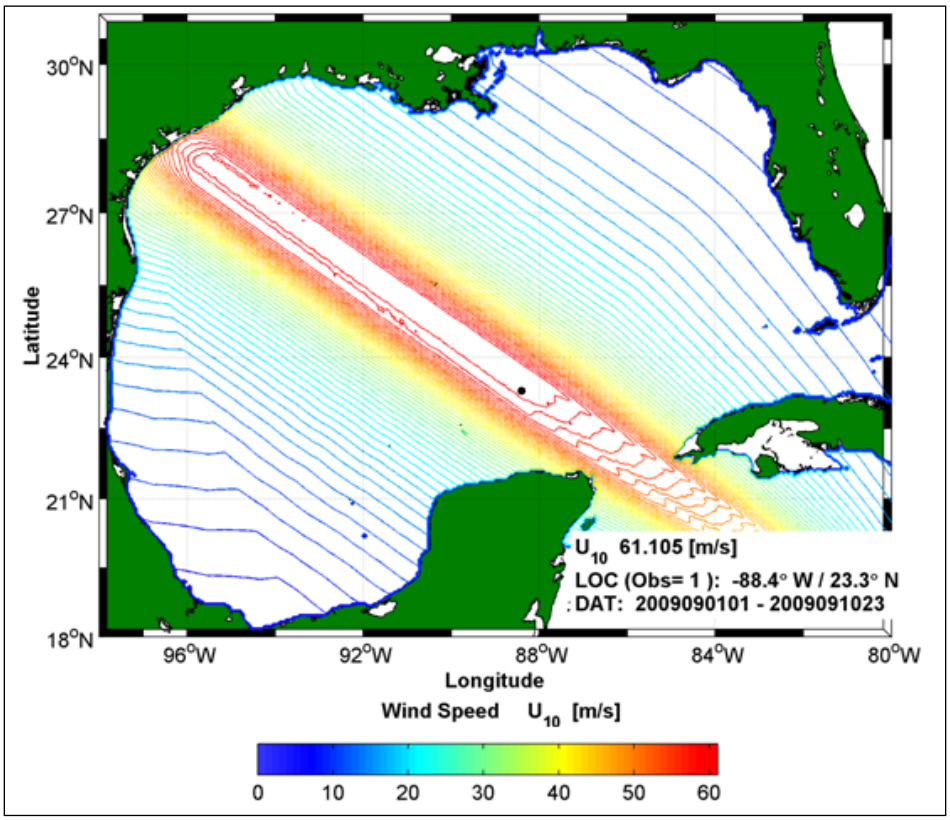

Figure 4-7. Example of maximum wind speed contours generated by TC96 (Storm 027).

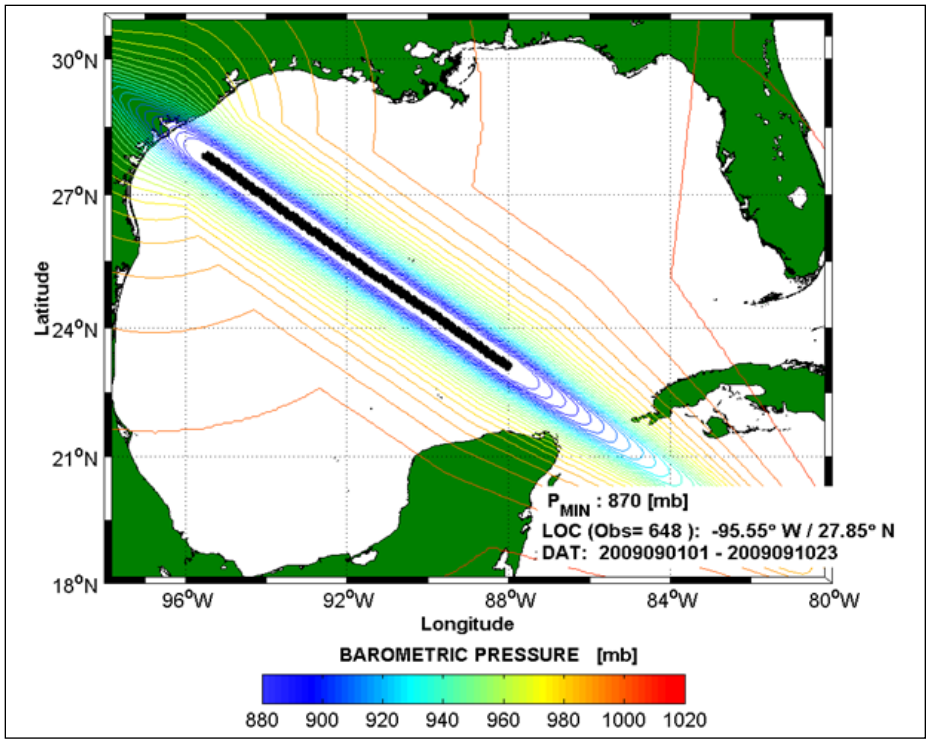

Figure 4-8. Example of minimum pressure field contours generated by TC96 (Storm 027).

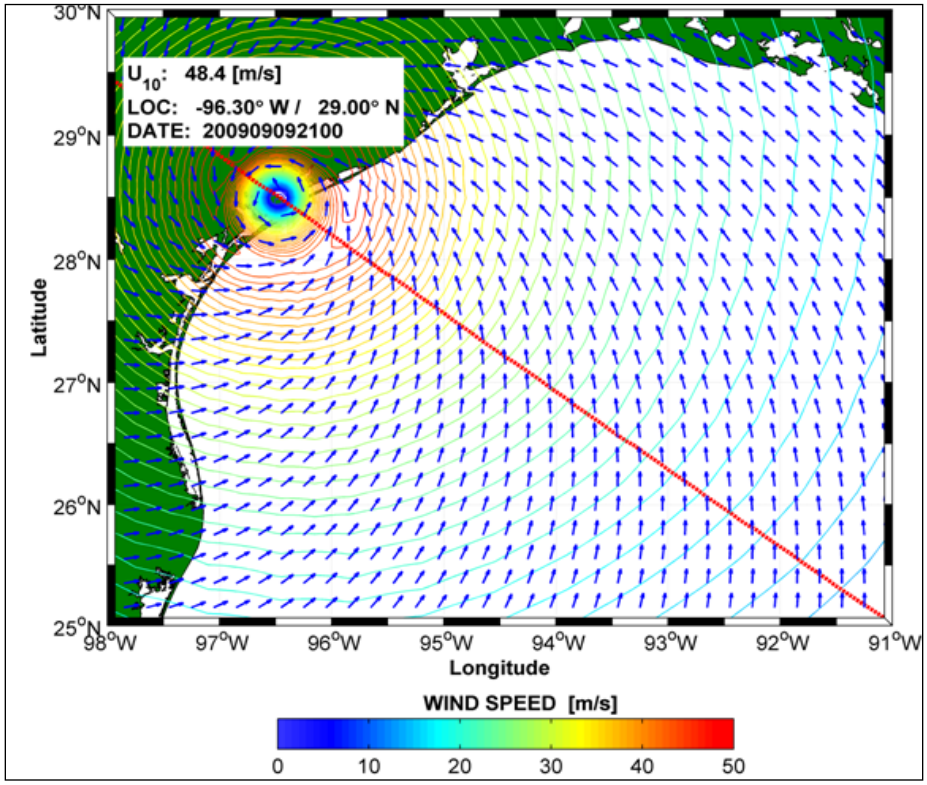

Figure 4-9. Example snapshot of the wind speed (color contoured) and wind direction at the landfall output from TC96 (Storm 027).

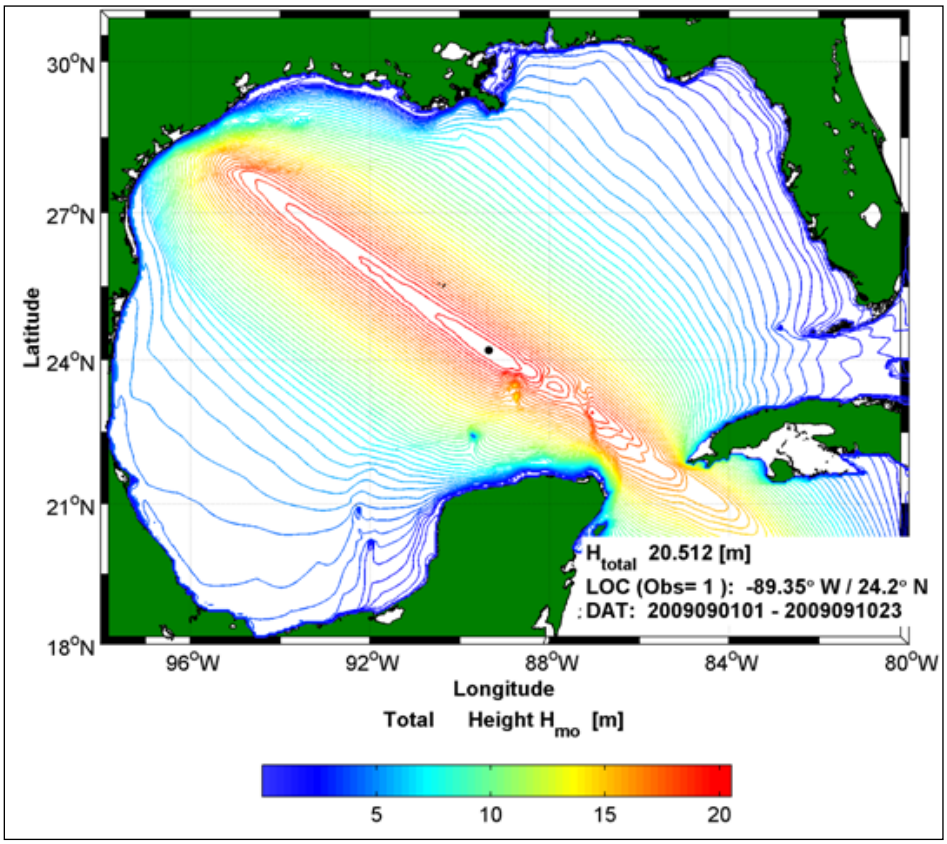

Figure 4-10. Example of maximum overall total significant wave height contours generated by WAM (Storm 027).

ADCIRC estimates the water level across the entire grid at each time step. A time history of water levels can be saved at any grid location over the duration of a storm. To provide peak water levels, the entire spatial domain is examined during every model time step to determine if water levels exceeded the previous time step's maximum water level at each point in the domain. The result of this analysis is a maximum envelope of water level for a given simulation and an example of this output generated from ADCIRC is provided in Figure 4-12. Figure 4-12 is the envelope of maximum water level in the Matagorda, Texas area for storm 27 from the storm suite (Table 4-1). The hydrographs and peak water levels obtained from ADCIRC can be used to estimate flood risk and for flood damage reduction planning and design purposes.

Table 4-2 shows the surge levels at the site of interest for these test runs, represented as a black dot in Figure 4-12, along with all of the other parameters listed in Table 4-1. The surges at this point vary by only 2.1 ft (28.8 to 30.9 ft) over the parameter variations executed. The site elevation is approximately 28 ft. The dashes in Table 4-2 indicate that the site of interest was not inundated during the simulation. In an attempt to emphasize the natural organization inherent in the surge results, Figure 4-13 shows the pairs of surge levels for 880 mb and 870 mb simulations plotted against the pressure differential, with all the other parameters held constant. As can be seen here, the surges for the larger pressure differentials are always slightly higher than the surges for the smaller pressure differentials. It is also evident that the slope of the increase is somewhat larger for Track 1 storms (shown in black) compared to Track 2 storms (shown in red), with surge levels in the Track 1 storms increasing about 0.8 ft per 10

mb increase in the pressure differential an surge levels in the Track 2 storms increasing about 0.5 ft per 10 mb increase in the pressure differential.

What is not immediately obvious in Figure 4-13 is that the increase in storm surge levels is actually considerably less than expected based on pressure differential scaling. In such scaling, we would expect the surge levels to increase linearly with pressure differential (Irish and Resio, 2010) which, for these simulations, should increase surge levels by about 7.6%. Instead, the increases are only about 2.3% to 3.0% for Track 1 storms and by about 1.5% to 1.7% for Track 2 storms. Three factors play major roles in this nonlinear behavior in surge levels. First, although the planetary boundary layer model used for these simulations has been shown to produce a relatively linear relationship between the pressure differential and velocity squared over a wide range of pressure differentials and storm sizes, this linearity does not extend to very large pressure differentials in large storms (see Figure 4-14). Second, the ADCIRC model applies a wind drag coefficient formulation based on Garratt (1977) that caps the coefficient at 0.0035 at wind speeds greater than 40 m/sec. Third, the extent of flooding increases both along the coast and across the coast for large storms, which diminishes the effect of a specified increase in the pressure differential in very intense storms relative to the effect of the same increase in pressure differential in less intense storms.

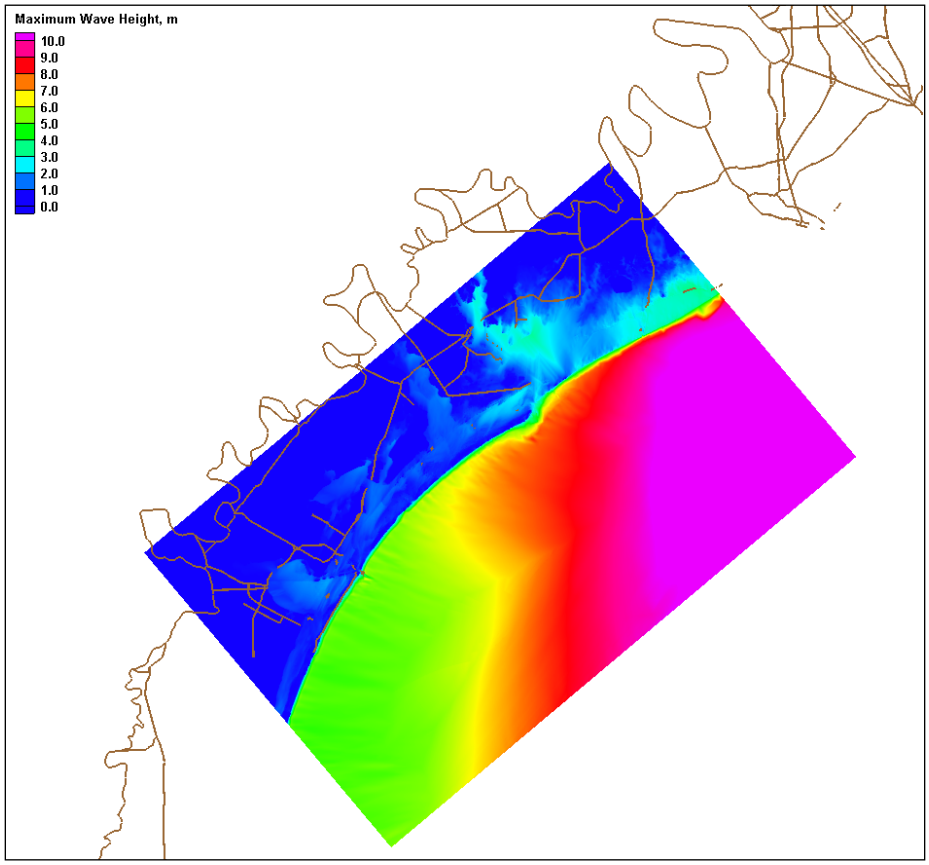

Figure 4-11. Example of maximum significant wave height generated by STWAVE (Storm 027).

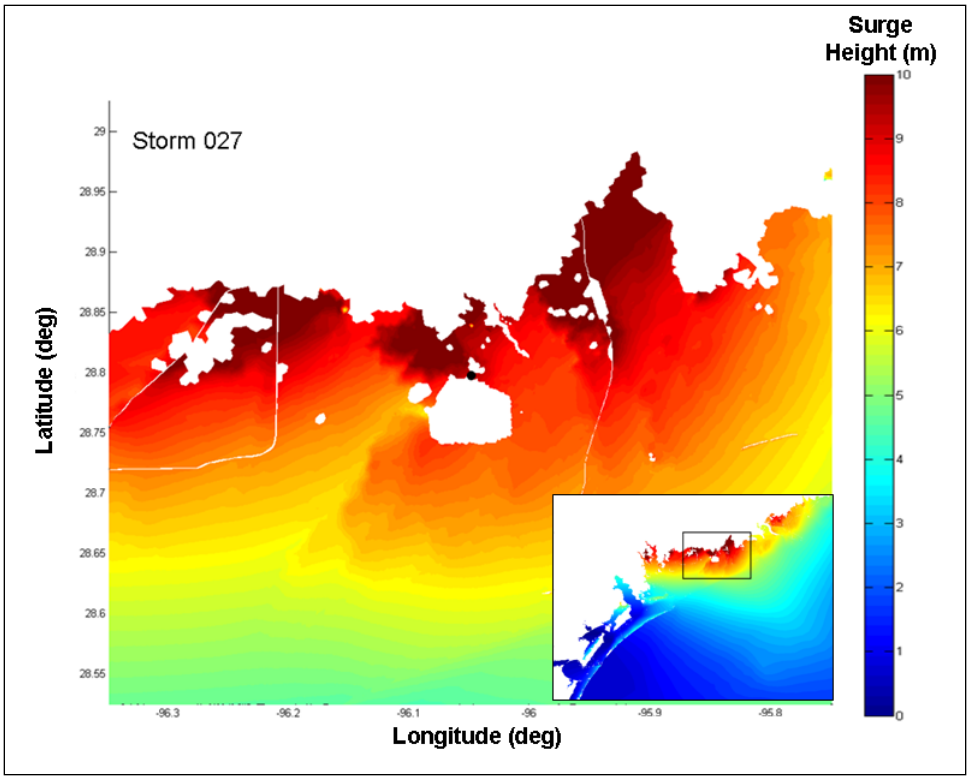

Figure 4-12. Example of envelope of maximum water level generated by ADCIRC.

Table 4-2. Surges produced by Matagorda Bay storms.

	Surge ft	Depth at Site, ft	Wind m/sec	Pres mb	W-Indf m/sec	P-Indf mb	Rp nm	Holland B	Vf kt
025	30.11	2.11	59.6	880	46.5	904	30-42	1.35-0.9	5.5
026	28.82	0.82	58	880	42.4	918.6	45-63	1.35-0.9	5.5
027	30.89	2.89	61.1	870	48.4	893.8	30-42	1.35-0.9	5.5
028	29.71	1.71	59.4	870	44.4	908.6	45-63	1.35-0.9	5.5
029	29.51	1.51	61.4	880	47.5	905.8	30-42	1.35-0.9	11
030	---	0	59.2	880	44.5	918.6	45-63	1.35-0.9	11
031	30.14	2.14	62.8	870	49.3	895.8	30-42	1.35-0.9	11
032	29.19	1.19	60.6	870	46.4	908.6	45-63	1.35-0.9	11
033	---	0	64.3	880	54.6	901.9	30-42	1.35-0.9	22
034	---	0	61.8	880	50.9	912.3	45-63	1.35-0.9	22
035	---	0	65.6	870	55.9	891.9	30-42	1.35-0.9	22
036	---	0	63	870	52.7	902.3	45-63	1.35-0.9	22
037	29.91	1.91	62.3	880	50	902.8	30-42	1.35-0.9	11
038	29.19	1.19	60	880	44.4	919.6	45-63	1.35-0.9	11
039	30.37	2.37	63.7	870	51.9	892.8	30-42	1.35-0.9	11
040	29.68	1.68	61.4	870	46.3	909.8	45-63	1.35-0.9	11
041	---	0	65.1	880	55.1	902.8	30-42	1.35-0.9	22
042	---	0	62.2	880	48.8	919.6	45-63	1.35-0.9	22
043	29.51	1.51	66.4	870	56.5	892.8	30-42	1.35-0.9	22
044	---	0	63.5	870	50.5	909.6	45-63	1.35-0.9	22

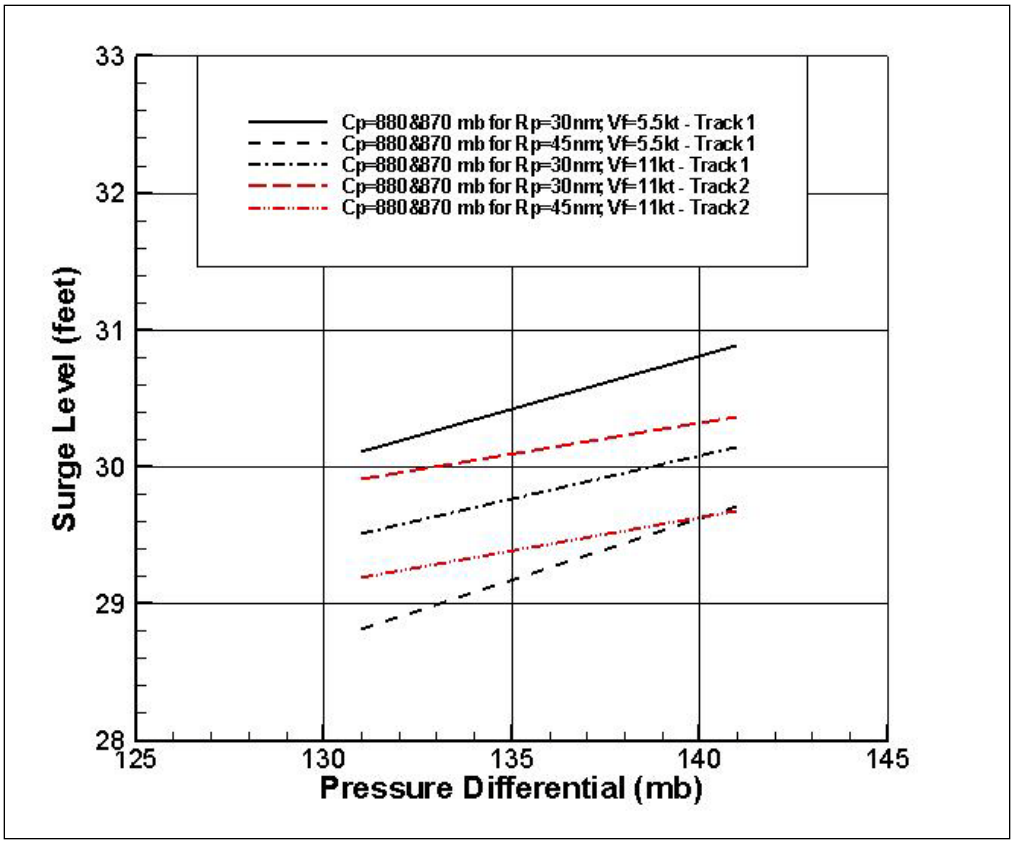

Figure 4-13. Lines drawn between pairs of ADCIRC simulations with different central pressures for various combinations of fixed storm track, storm size, and forward speed.

Figure 4-14 shows the relationship obtained from simulations with the planetary boundary layer model used here. The results indicate that up to a pressure differential of about 100 mb, the relationship is very linear; however, for larger pressure differentials, at least for the size of storm (30 and 45 nm in the offshore area) simulated here, the rate of increase of maximum wind speed squared with an increase in pressure differential diminishes. This explains part of the reason why the surge levels exhibit a reduced surge response relative to the expected pressure differential relationship; however, if we use the maximum wind speed squared scaling for surge levels, we still estimate that the increase in surge level of the 870 mb storms over the 880 mb storms would be about 5% for the Track 1 storms and 4.5% for the Track 2 storm. This is still larger than calculated with the model runs as the wind drag coefficient cutoff further reduces the surge response resulting in the nonlinear response. Recent analyses on drag coefficients have been made from GPS sonde wind speed profiles (Powell *et al.* 2003, and Powell 2006) and indicate that not only a drag cutoff is supported by data but that reduced drag coefficients may be appropriate for very high wind speeds in tropical cyclones. The Garratt formulation in ADCIRC applies a wind drag coefficient cutoff at wind speeds of approximately 40 m/sec and above, while the new GPS sonde data suggests that the drag coefficient should be reduced at these speeds. Reducing the drag coefficient for wind speeds greater than 40 m/sec would increase the nonlinear response of surge to increases in storm intensity. Therefore, the application of Garratt is conservative.

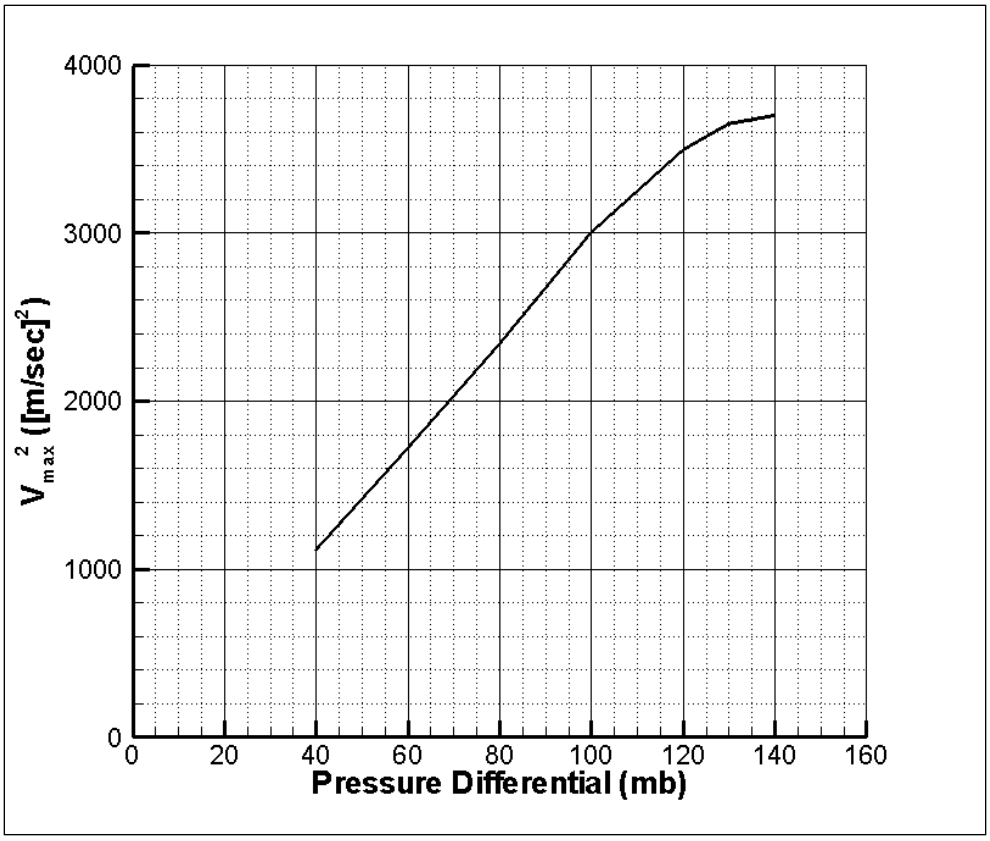

Figure 4-14. Relationship between maximum velocity squared and pressure differential for TC96 PBL model.

4.2 Estimate of Limiting Values for Very-Low Probability Surge Levels

Estimates of what might be the worst possible surge levels (the Probable Maximum Storm Surge, PMSS) at the site of interest can now be made. These estimates will be examined from both a probabilistic and a deterministic perspective. Similar to the approach used in recent risk assessments for flooding in the New Orleans area and elsewhere around the U.S. (IPET 2009; Niedoroda *et al.*, 2010), the basic framework for the probabilistic assessment will be based on the joint probability of the primary parameters shown to influence surge levels in coastal areas. In this context, the Cumulative Distribution Function (CDF) for surge levels can be written as:

$$F(\eta) = \int\ldots\int p(\Delta p, R_p, v_f, \theta_l, x_0) p(\varepsilon \mid \eta) \times H[\eta - \Psi(\Delta p, R_p, v_f, \theta_f, x_0 \mid \langle B \rangle, \left\langle \frac{\partial \Delta p}{\partial s} \right\rangle, \left\langle \frac{\partial R_p}{\partial s} \right\rangle, \left\langle \frac{\partial \langle B \rangle}{\partial s} \right\rangle) + \varepsilon] d\Delta p dR_p dv_f d\theta_f dx_0 d\varepsilon \quad \text{Equation 4-1}$$

where the terms inside the brackets denote averaging across the entire ensemble of storms for the quantities within them, i.e.

$\langle B \rangle$ denotes the average Holland B value for storms in the Gulf of Mexico;

$\left\langle \frac{\partial \Delta p}{\partial s} \right\rangle$ denotes the average nearshore change in the pressure differential with *s*;

$\left\langle \frac{\partial R_p}{\partial s} \right\rangle$ denotes the average nearshore change in the storm size with *s*;

$\left\langle \frac{\partial B}{\partial s} \right\rangle$ denotes the average nearshore change in the Holland B parameter with *s*; where

s is the spatial coordinate along the storm direction of travel.

There are two terms in Equation 4-1 which are represented probabilistically, the joint probability of all of the storm parameters, $p(\Delta p, R_p, v_f, \theta_f, x_0)$, and the conditional probability of the error in our representation of a storm, $p(\varepsilon|\eta)$. Each of these must be quantified to obtain a realistic estimate of the exceedance probability of the events modeled.

$$p(\Delta p, R_p, v_f, \theta_f, x_0) = \Lambda_1 \cdot \Lambda_2 \cdot \Lambda_3 \cdot \Lambda_4 \cdot \Lambda_5 \qquad \text{Equation 4-2}$$

where

$$\Lambda_1 = p(\Delta p \mid x_0) = \frac{\partial F[a_0(x_0), a_1(x_0)]}{\partial \Delta p} = \frac{\partial}{\partial \Delta p}\left\{ \exp\left\{ -\exp-\left[\frac{\Delta p - a_0(x_0)}{a_1(x_0)} \right] \right\} \right\} \text{ (Gumbel Distribution)}$$

$$\Lambda_2 = p(R_{\max} \mid \Delta p) = \frac{1}{\sigma(\Delta p)\sqrt{2\pi}} e^{-\frac{(\bar{R}_{\max}(\Delta p) - R_{\max})^2}{2\sigma^2(\Delta p)}}$$

$$\Lambda_3 = p(v_f \mid \theta_f) = \frac{1}{\sigma\sqrt{2\pi}} e^{-\frac{(\bar{v}_f(\theta_f) - v_f)^2}{2\sigma^2}}$$

$$\Lambda_4 = p(\theta_f \mid x_0) = \frac{1}{\sigma(x)\sqrt{2\pi}} e^{-\frac{(\bar{\theta}_f(x) - \theta_f)^2}{2\sigma^2(x)}}$$

$$\Lambda_5 = \Phi(x_0)$$

From the IPET (2009), the coefficients for the linear regression for the conditional storm size mean are obtained from:

$$\bar{R}_{\max} = 14. + 0.3 * (110. - \Delta p) \qquad \text{Equation 4-3}$$

with units for R_{max} in nm and units for Δp in mb implied. The standard deviation in this equation was estimated to be $\sigma(\Delta p) = 0.44\bar{R}_{\max}(\Delta p)$. To ensure some level of conservatism in the application of Equation 4-3, it is modified to the form:

$$\begin{aligned} \bar{R}_{\max} &= 14.0 + 0.3 * (110. - \Delta p) && \text{for } \Delta p \le 110 \\ &= 14.0 && \text{for } \Delta p > 110 \end{aligned} \qquad \text{Equation 4-4}$$

which implies a lower limit of 6.16 nm for $\sigma(\Delta p)$.

Neglecting uncertainty (error) in the estimation of storm surge, the probability of exeedance for a combination of storm intensity and storm size can be estimated as:

$$p(\Delta p, R_{\max}) = p(R_{\max} \mid \Delta p)p(\Delta p) \qquad \text{Equation 4-5}$$

Analyses also documented in IPET (2009) show that the coefficients for the Gumbel Distribution in the vicinity of Matagorda Bay are a_0=62.67 and a_1=7.69. Using these coefficients for a Gumbel distribution and a normal distribution for the size distribution from Equation 4-4, the exceedance probabilities for any combination of pressure differential and storm size used in our simulations can be estimated. The smaller of the two storm sizes simulated was 30 nm in the offshore area, the value of the standardized variate, defined as $\hat{x}=\left[\frac{R_{\max}-\bar{R}_{\max}(\Delta p)}{\sigma(\Delta p)}\right]$, for this size and a standard deviation of 6.16 nm is $\frac{30-14}{6.16}=2.597$, while the value of the standardized variate for the larger storm is $\frac{45-14}{6.16}=5.032$. The likelihood of a storm as large as, or larger than, a given storms is:

$$F(\hat{x}) = 1 - \frac{1}{\sqrt{2\pi}}\int_{-\infty}^{\hat{x}} e^{-\frac{\hat{x}^2}{2}} d\hat{x} \qquad \text{Equation 4-6}$$

where $\hat{x}$ is the standardized storm size variate for that storm. For the smaller storm, this yields a value of 3.82 x 10^{-3}; and for the larger storm, this yields a value of 9.94 x 10^{-8}. For the Gumbel coefficients determined for this site, the probability of exceedance for a 880 mb hurricane is estimated to be 1.38 x 10^{-4}; and for a 870 hurricane, it is estimated to be 1.38 x 10^{-5}. The estimated probability for the hurricane landfall from the IPET study is specifically for the annual probability of such a landfall occurring within an alongshore "window" of 1-degree longitude at a latitude of 29.5 degrees, or approximately 52.2 nm.

Table 4-3 contains the exceedance probabilities for the 4 combinations of size and pressure differential used in our simulations, based only on size and intensity. Recalling that we have also restricted the storm approach direction by specifying the track heading at landfall and the landfall location is actually more restricted than a storm simply occurring anywhere within a 52.2 nm window centered on the simulated track, it is likely that the actual probabilities are reduced by about another order of magnitude or so over the values listed in Table 4-3. However, an exact estimate of such long return period events is not really the focus of this discussion. Instead, these probabilities have been quantified only to show that the events being simulated are indeed very extreme event storms and cover the range well beyond the 10^{-6} annual frequency level sometimes used in discussions of risk of damage to critical nuclear facility infrastructure (NRC, 1986).

Table 4-3. Annual probabilities of a storm with a combination of size and intensity equal to or greater than the storms simulated in this study.

	Δp=133 mb	**Δp=143 mb**
R_p= 30 nm	5.27 x 10^{-7}	5.27 x 10^{-8}
R_p= 45 nm	1.37 x 10^{-11}	1.37 x 10^{-12}

Up to this point, it has been shown that, neglecting uncertainty in our estimates, the probabilities are very small for the types of storms simulated here. If we were to treat the uncertainty in the pressure differential in terms of an extrapolation from the data from Equation 3-2, we would see that the estimated width of the confidence band would be about 50 mb for estimates in the neighborhood of the 10^{-6} annual frequency level. Thus, although we have shown that the events simulated are expected to be extremely rare, we still need to pursue a quasi-deterministic upper limit in the storm intensity to avoid having to perform simulations with 820 mb hurricanes.

The MPI of a hurricane has been postulated as an upper limit for extreme tropical cyclone intensities at least since the late 1970's (see for example: World Meteorological Organization, 1976 and Mooley, 1980). Before that time, theoreticians had recognized the existence of thermodynamic and dynamic constraints on the energy available for tropical cyclone intensification, even when unencumbered by proximity to land (see for example: Riehl, 1954; Miller, 1958; and Malkus and Riehl, 1960). More recently, Emanuel (1986, 1991) and Holland (1997) formulated theoretical models for estimating maximum tropical cyclone intensity. In an evaluation of the performance of these two MPI models, Tonkin *et al.* (2000) examined storms within 1) the Australian/southwest Pacific region, 2) the northwest Pacific region, and 3) the North Atlantic region. Since our primary interest is focused on the Gulf of Mexico, a subsection of the North Atlantic region, we will limit our discussion here to results for that region.

Figure 4-15 shows the geographic area encompassed within the "North Atlantic region" as defined by Tonkin *et al* (2000). Figure 2-4 presents the results from Tonkin *et al.*'s application of the Emanuel Model (black dots joined by a solid line), Holland's model (dashed line), and observed intensities (open triangles joined by a solid line). This application used a climatological mean Sea Surface Temperature (SST) defined over the period 1950 to 1979. Evans (1993) results indicated that there was little gain in predictive skill when actual monthly SST values are used in place of the climatological mean.

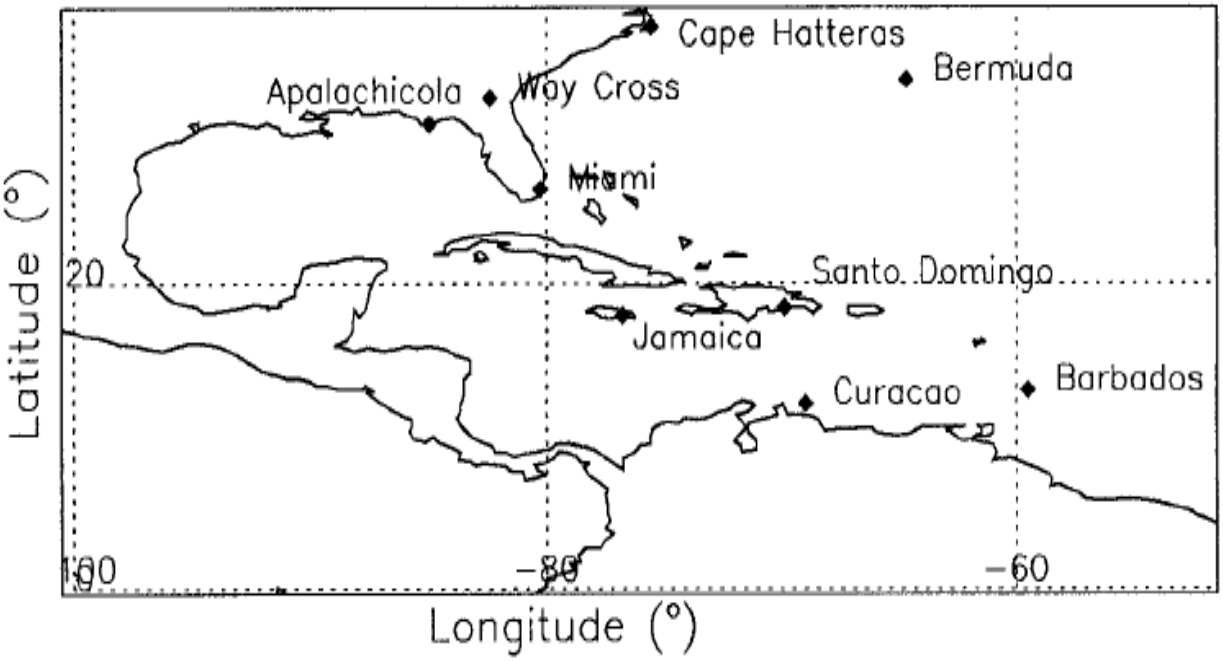

Figure 4-15. Geographic area used in Tonkin *et al.* (2000) study.

As can be seen in Figure 2-4 and as widely accepted from theoretical considerations, a strong relationship exists between climatological SST values and the lowest central pressures. We see that, in the range of SST values from 26° to 28° (C), the minimum central pressures of the Holland Model, the Emanuel model and the observed intensities are all in approximate agreement. Above 28° (C), the observations continue to show decreasing central pressures with increasing values of SST; whereas, the Emanuel and Holland models do not.

Figure 2-5, taken from Schade (2000), shows another approximation for the MPI. In this paper, Schade suggests that the effect of the SST field on tropical cyclone intensity is twofold. First, the large-scale ambient SST field "sets the stage for the tropical cyclone." Second, the intensity of a tropical cyclone is highly sensitive to the reduction of the SST in the interior region of the storm due to the response of the ocean to surface winds. Thus, whereas the concept of the MPI is well founded, many of its details are still under development. The 85% humidity line shown in Figure 2-5 will be taken as the upper limit here, since this is reasonably consistent with the upper limit of the data shown in Figure 2-4.

Figure 4-16 shows the average August to September SST for the Gulf of Mexico during the period 1940 to 2006. As can be seen here, the highest average values during this part of the year (the peak of hurricane season) have varied from as low as 28.17° C in 1984 to as high as 29.49° C in 1962. The dotted vertical line in Figure 2-5 shows this historical maximum plotted on top of Schade's results. The heavy solid line along the top of that figure denotes the MPI value without consideration of any negative feedback of the type discussed by Schade; thus, it is expected to represent a maximum possible threshold for the MPI. From Figures 2-4, 2-5, and 4-16, it can be argued that a value of 880 mb represents a very sensible (perhaps slightly conservative) value for the MPI in the Gulf of Mexico, without consideration of significant global warming effects on SST's that might drive them higher than the level of the 1960's.

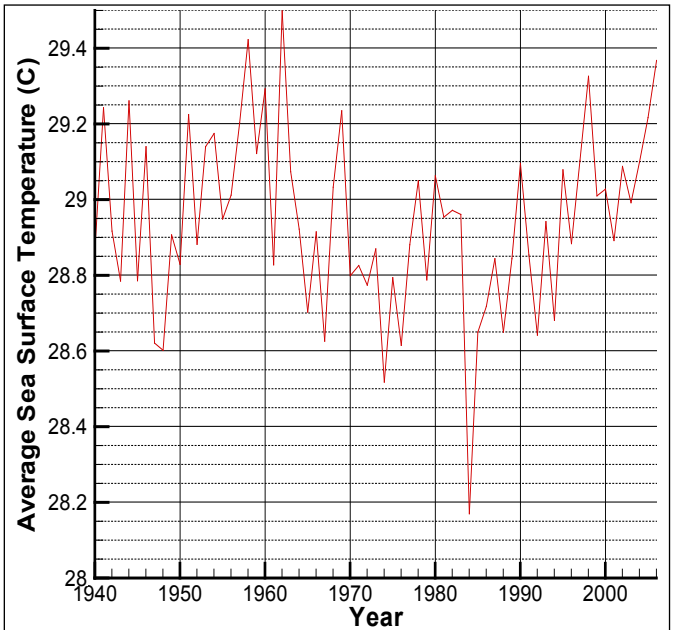

Figure 4-16. Variation of average August through October SST in Gulf of Mexico from 1940 through 2006 (from Extended Reconstructed Sea Surface online repository).

In a situation with perfect theories and models, the 880 mb value for central pressure could be applied to an exact model of bathymetry, wind, waves, and surges and obtain a deterministic limiting value for the PMSS; however, there are at least four sources of variability that should be considered in the application of the MPI to the estimation of the maximum surge:

1. Uncertainty in the MPI;
2. Uncertainty in storm surge prediction;
3. Potential climate variability over the projected design lifetime; and
4. Tide levels accompanying the maximum surge event.

Each of these sources of uncertainty listed can be further broken down into contributions from two basic types of uncertainty: 1) aleatory uncertainty, which is due to the lack of sample size in empirical data used and/or the existence of unresolved/unpredictable variations in system behavior, and 2) epistemic uncertainty, which is due to the lack of understanding of the physics of and/or relationships within the system.

4.2.1 Uncertainty in the MPI

To estimate the inherent uncertainty in our estimate of the MPI, it should be noted that the models used to obtain these estimates are highly parameterized and that the data supporting the postulated relationships contain considerable uncertainty, as seen in Figure 2-4. In addition, the existing MPI concept does not address the issue of storm size, so one is forced to assume that the MPI value is independent of storm size, which is probably not a very good assumption, but at least is expected to be conservative. The scatter of points around a linear regression line through the observed data (triangles) in Figure 2-4 has a standard deviation of about 4 mb. Since a direct estimate of the uncertainty in the MPI is not included within the modeled values, a slightly higher value, 5 mb, is taken as an indicator of the uncertainty in our estimate of the MPI.

4.2.2 Possible Errors in Storm Surge Prediction

Most comparisons of model predictions versus observed surge levels involve simulations which use “best winds” to drive the coupled wave-surge models (Bunya *et al.*, 2010). Studies of computer simulations with parametric winds are conducted less frequently; however, such studies are actually much more valuable in understanding and quantifying coastal flooding risks, since the risk estimates invariably must use wind-field representations with reduced dimensions to be able to characterize the multivariate statistical variations involved in the JPM approach. Figure 4-17 shows a comparison of surges predicted by the same coupled wave-surge model system as used here against measured high water marks (HWM). This figure and similar comparisons for Hurricane Rita indicate that the uncertainty in these predictions can be characterized by a standard deviation of about 1.5 ft. This value is somewhat an optimal value where considerable effort was spent in developing careful bathymetries and in local validations. A somewhat larger value of 2.0 ft is taken as representative of a more general estimate of the error in such model predictions.

4.2.3 Potential Climate Variations Over the Design Lifetime

There are many site specific patterns of coastal evolution expected along US coastlines in the coming years. The effects of climate variability, sea level rise, and subsidence will all play important roles in this evolution. Natural features of the coastal landscape and the vegetation types covering landscape features affect surge propagation in coastal areas (Wamsley *et al*.

2010). However, these effects have not been well quantified to date and there is a large degree of uncertainty associated with these changes. The general approach recommended for NRC consideration is to separate the sea level change issue from the climate effects on storm patterns and intensities, since local subsidence can be such a major component of the former. Subsidence and other forms of coastal landscape evolution can be incorporated into the model grids if these are expected to contribute significantly to future storm surge levels, such as in deltaic areas. However, for most applications, assuming that an estimate for relative mean sea level can be obtained for a site of interest, a simple approximation can be made to just add the sea level rise linearly to the surge level. Since we are using an MPI approach and not variations in storm frequency and intensity here, we can concentrate on the potential impact of climate variability on SST's, which would, in turn, affect the MPI value.

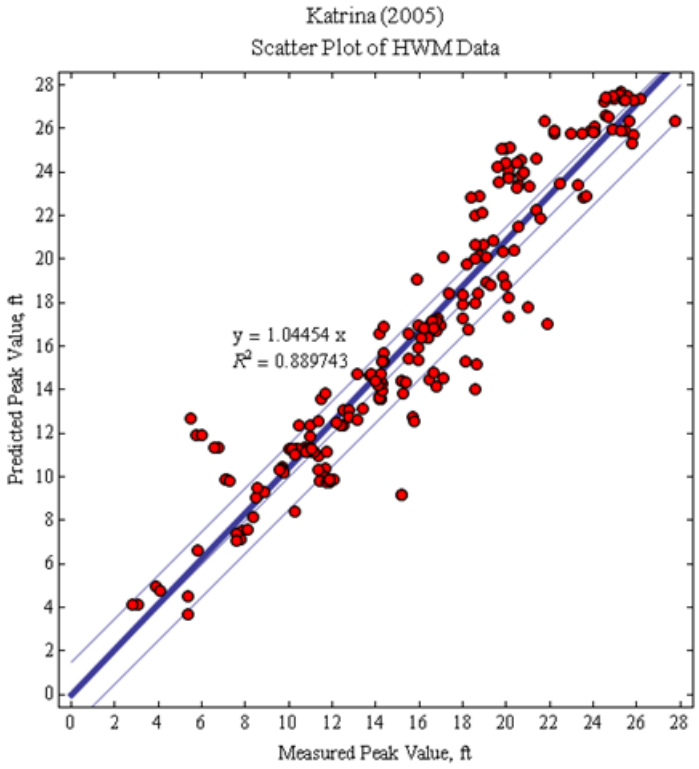

Figure 4-17. Comparison of observed USACE HWMs for Hurricane Katrina and the simulation using the PBL wind fields at the recorded USACE HWMs. Thin blue lines display a 1:1 correlation as well as 1.5 ft standard deviation on each side.

4.2.4 Tide levels accompanying the maximum surge event

Since tide levels are driven by astronomical forcing, rather than meteorological forcing, they are generally considered to be independent of hurricane surge levels. To account for this possibility, a tidal adjustment (η_{tide}) equal to the difference between mean higher high water and mean tide level should be added in the final computation of the PMSS. The difference between mean higher high water and mean tide level can be taken as a simple estimate of the additional sea level rise associated with a storm occurring at high tide versus a storm occurring at mid-tide

(the water level used in the numerical simulations. For Matagorda, this value is approximately 0.4 ft. The tide contribution can be much larger at other locations.

4.2.5 Impact of Uncertainties on the Estimated Upper Limit Surge

So how would all of these uncertainties impact the estimated upper limit surge level? First, the case in which the SST values are not affected significantly by climate variability is examined. The probability density function for the maximum surge, including uncertainty, can be expressed as:

$$F(\eta_*) = \int_{-\infty}^{\infty}\int_{-\infty}^{\infty} p(\eta_* \mid \Delta p = MPI, \varepsilon_1, \varepsilon_2)p(\varepsilon_1)p(\varepsilon_2)H(\eta_{MPI} + \varepsilon_1 + \varepsilon_2 - \eta_*)d\varepsilon_1 d\varepsilon_2 \qquad \text{Equation 4-7}$$

where

ε_1 is the uncertainty term related to errors in the estimation of the MPI
ε_2 is the uncertainty term related to surge modeling errors; and
η_{MPI} is the estimated maximum surge for the MPI given the storm set modeled.

Errors for both the estimation in the MPI and the model error follow a Gaussian distribution (Resio *et al*. 2008) and therefore Equation 4-7 can be approximated in a fashion similar to that of Equation 4-6. Since there are two different variances involved in these errors, they are summed before being applied in estimating the likelihood of exceedance, i.e., the standardized variate used in Equation 4-6 is:

$$\hat{x} = \left[\frac{\eta_{MPI} - \varepsilon_{tot}}{(\sigma_1^2 + \sigma_2^2)^{1/2}}\right] \qquad \text{Equation 4-8}$$

where the subscript "tot" refers to a term with the two sources of uncertainty summed. In this form the variances must be converted to the same physical units as the surge values.

In Equation 4-8, the first term is related to estimates of the MPI. Contributions to this include the uncertainty in the parameterized, quasi-empirical equations used for estimating the MPI. Here the 5 mb value noted previously is taken as a very rough estimate of the error in the MPI due to potential errors in the parametric model used in predicting the MPI. A simple linear form such as $\sigma_\eta = \sigma_{\Delta p}\frac{\partial \eta}{\partial \Delta p}$ for this should suffice to convert the standard deviation in the estimate of the MPI (5 mb) to an estimate for the expected standard deviation in the surge height due to uncertainty in the pressure differential of the MPI. Based on the slopes of the lines in Figure 4-13, we can estimate $\frac{\partial \eta}{\partial \Delta p}$ to be about 0.8 ft per 10 mb; since the rms for the pressure differential ($\sigma_{\Delta p}$) is 5, we obtain a final estimate of approximately 0.4 ft for σ_1.

From the information in Figure 4-17, one might estimate that the rms error in model estimates for surges is in the neighborhood of 1.5 ft; however, the case of the Katrina comparison is quite special, with considerable work done to ensure relatively good results in these comparisons. It is not at all clear that a truly "blind" set of predictions for a very low probability storm would have an rms error that is this small. As noted previously, the error in predictions of these very large storms in such a situation is assumed to be one-third larger, about 2.0 ft. This is an area where additional work is needed to provide a more defensible value; however, based on comparisons

for other storms (such as Hurricanes Rita, Gustav, and Ike), the value of 2 ft is reasonable. It is interesting to note that the expected effect of errors due to surge modeling uncertainties is considerably larger than the effect of uncertainties in the MPI. This is primarily due to the low slope of the $\frac{\partial \eta}{\partial \Delta p}$ term required to relate variations in the MPI to variations in surge for these very large storms. Thus, the sum of the two variances is $\sigma_{tot}^2 = \sigma_1^2 + \sigma_2^2 = (0.4)^2 + (2.0)^2 = 4.16$ where σ_1^2 is the variance associate with MPI uncertainty and σ_2^2 is the variance associated with the model prediction uncertainty. The combined total standard deviation is, $\sigma_{tot} = \sqrt{\sigma_1^2 + \sigma_2^2} = \sqrt{(0.4)^2 + (2.0)^2} = 2.04$, which is less than a 2% increase over the standard deviation based on the modeling error alone.

The problem with an unbounded error, such as might be associated with the upper limit of a Gaussian probability function, is that there is not a definitive estimate of the PMSS at a site, since there is no absolute upper bound to this error distribution. Since we do not have sufficient data to dispute this statement, it is difficult to rely on empirical data to establish an upper bound for errors. For example, in Figure 4-17, some of the data points show that predicted and observed values differ by as much as 8 ft, which is more than would be expected for the estimated standard deviation and the number of samples. Therefore, rather than attempting to determine an absolute upper bound, it seems advantageous to make use of the fact that our events are already characterized as having extremely low probabilities. To allow the uncertainty in the modeling to enter into our estimate of the maximum surge, without dominating the estimate, we will make use of a 1% threshold of exceedance estimate for our PMSS (equivalent to a "2.34-sigma" level). This decreases the overall probability of the expected occurrence of this event (as shown in Table 4-3) by about two additional orders of magnitude, but at least allows the model uncertainty to be considered.

The effect of climate variability on storm surges over the design lifetime of a structure is the final factor considered here. As noted previously, the evolution of coastal landscapes and the estimation of sea level rise are both very site specific and should be considered independently of the generic surge estimation methodology being described in this report. There have been many papers which have addressed possible impacts of climate on the frequency and intensity of hurricanes (tropical cyclones). A very good review of this topic can be found in Knutson *et al*. (2010). However, since only the MPI characteristic of storms is being treated, rather than an entire distribution of multiple storm characteristics, the investigation is restricted to only the impact of climate variability on the MPI. In this context, interest is focused on the likelihood of different SST's and the impact on the expected MPI.

The actual pattern of summertime SST's in the Gulf of Mexico (shown in Figure 4-16) resembles more of a cyclical pattern than a secular trend. For this reason, it is difficult to use existing data to project linearly into the future. Given the lack of projected SST changes specific to the Gulf of Mexico, a 1.0^o C increase in SST was used to represent a reasonably conservative estimate for the potential increase in this parameter over a 100-year facility design life. The 1.0^o C is based on the measured increase in mean SST in the Northern Atlantic over the last 100 years (Rayner *et al.* 2003). From Figure 2-5, such an increase can lead to about a 14 mb increase in the MPI value. This, in turn, increases the associated surge by about 1.2 ft.

4.2.6 Putting All Factors into a Single Estimate for the Matagorda Bay Site

The deterministic estimate of the PMSS at the Matagorda Bay site can be taken as the largest surge produced by an MPI storm (880 mb) in our storm suite. From Table 4-2 we see that this value is 30.1 ft. If we were absolutely certain that this was the correct value for MPI that was possible within our study area over the design lifetime of our structure and if we knew that our models (including all bathymetric information) were absolutely accurate, this would be a reasonable estimate of the PMSS at this site. Since none of these assumptions are justified, we should add some additional margins to account for our uncertainty. As previously computed, the estimate of the root-mean-square error in our estimates of surge levels due to potential inaccuracies in our MPI value and in current state-of-the-art modeling methods (σ_{tot}) is 2.04 ft. Allowing for a $2\sigma_{tot}$ margin in our surge estimates will decrease the expected annual frequency of an event by about 2 orders of magnitude, which combined with the estimated probability from Table 4-3 shows that the estimated annual probability would be 5.27×10^{-9}. Adding the $2\sigma_{tot}$ "uncertainty margin" to the deterministic estimate gives us an estimate of 34.2 ft for our estimated value of the PMSS, neglecting climate variability. If we add the potential impact of a 1.0^{o} C increase in SST on the MPI, this would add another 1.2 ft to the estimated PMSS, yielding a final value of 35.8 ft. Or, in a simple equation form, we have:

$$\text{PMSS} = \text{PMSS}_{\text{deterministic}} + \text{Uncertainty}_{\text{MPI+Models}} + \text{Uncertainty}_{\text{Climate}} + \text{Tidal Effects}$$

For our site (feet): Equation 4-9

35.8 = 30.1 + 4.1 + 1.2 + 0.4

4.3 Analyses of Surges at Two Sites in Florida

Following the computer runs and analyses for Matagorda Bay, an additional set of surge simulations and analyses were conducted for the Levy County and Turkey Point nuclear sites in Florida to investigate how well the methodology developed for Matagorda Bay would work elsewhere. Figures 4-18 and 4-19 show the model domains for these simulations. Figures 4-20 and 4-21 show the bathymetric/topographic information used for these model runs, with the specific point saved for subsequent analyses shown on each figure. All site and flood elevations are reported relative to the NAVD88 datum. It should be noted that the surge simulated for Levy County did not inundate the proposed site. Therefore, in order to demonstrate the method, the estimated surge near the Crystal River Energy Complex is reported for Levy County.

For the Levy County site, based on historical storm tracks, tracks similar to that in Figure 4-22 are able to develop and maintain very high intensity and size, due to the geometric constraints of the surrounding land areas. Strong storms must be imbedded within the westerlies to make landfall in the Tampa area. Examples of recent storms in the Gulf of Mexico of this class are Opal in 1995 and Wilma in 2005. The tracks in Figure 4-22 were selected to approach at an angle that maximizes storm surge. The same storm transformation algorithms used for the Matagorda Bay site to decay storm intensity, increase its size, and diminish its Holland *B* value during hurricane approach to land were used here. Table 4-4 provides relevant information on the set of storms simulated for this site.

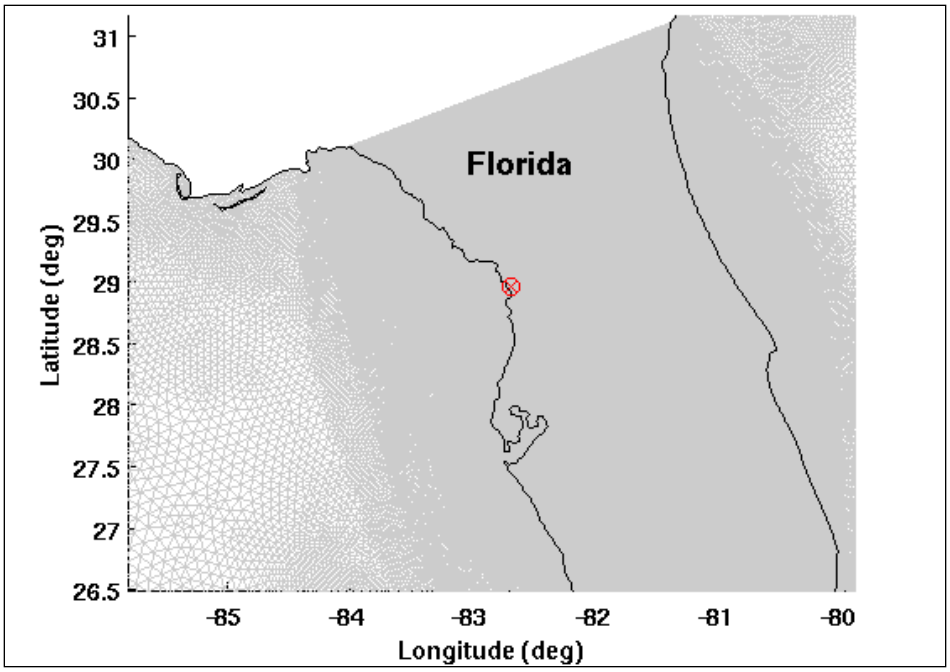

Figure 4-18. ADCIRC mesh near the project area, marked with a red circle and x, for the Levy County site in Florida.

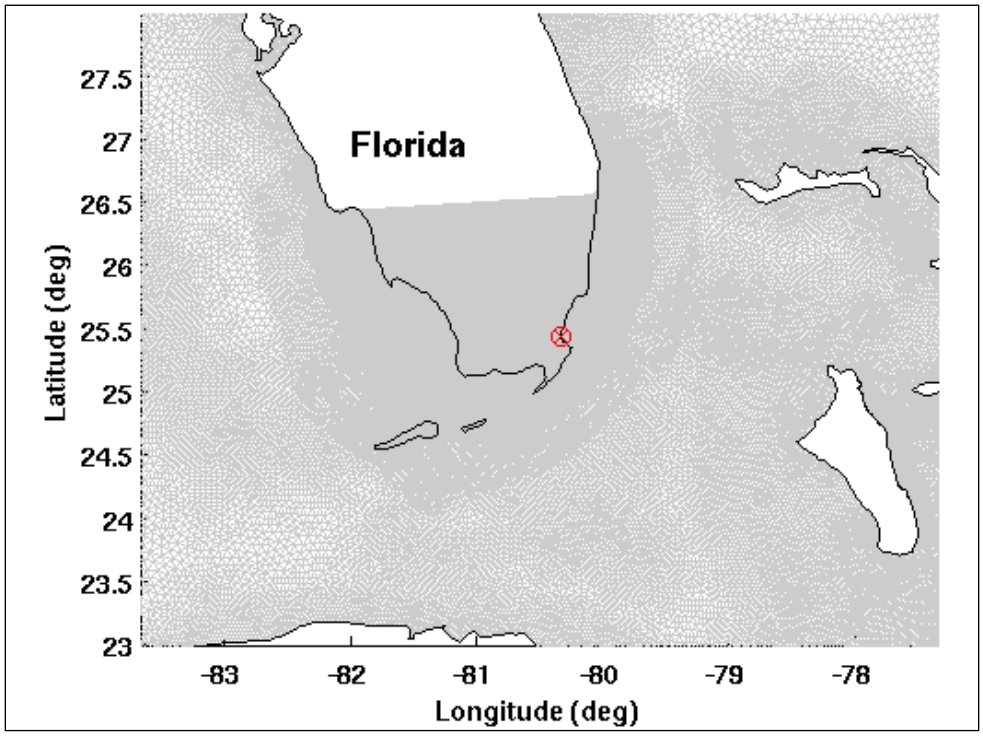

Figure 4-19. ADCIRC mesh near the project area, marked with a red circle and x, for the Turkey Point site in Florida.

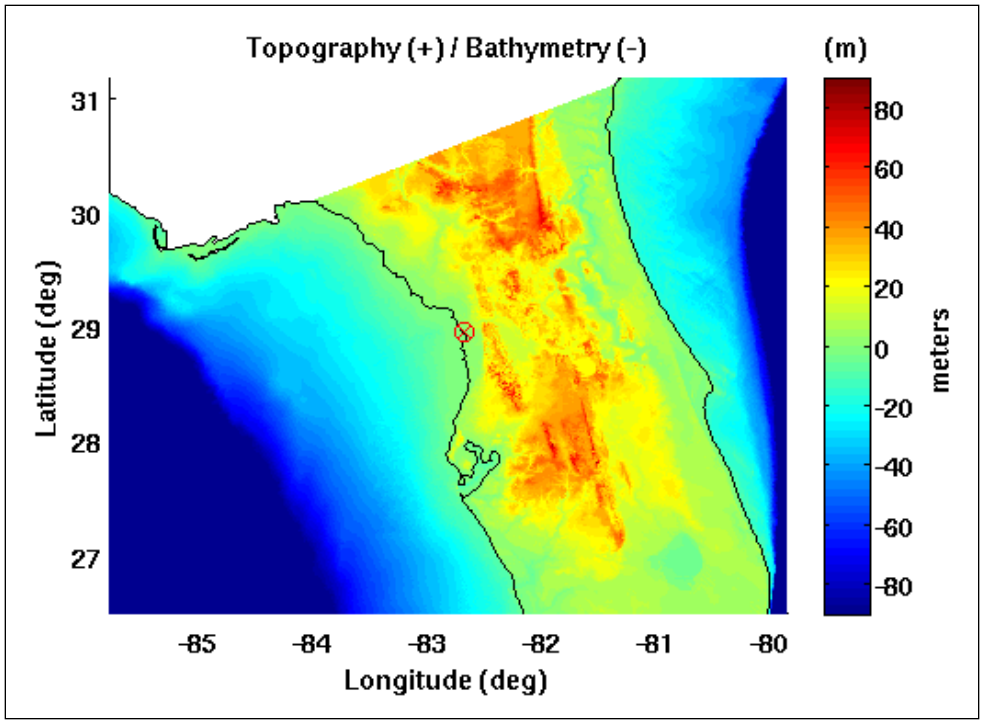

Figure 4-20. ADCIRC topography and bathymetry contours near the project area, marked with a red circle and x, for the Levy County site in Florida.

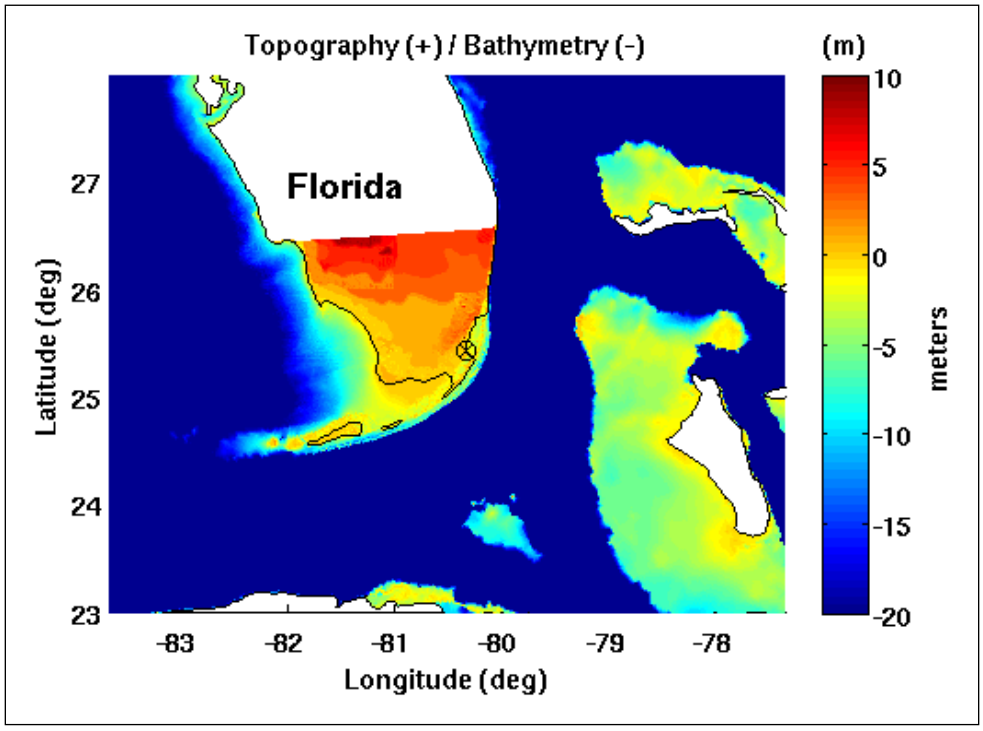

Figure 4-21. ADCIRC topography and bathymetry contours near the project area, marked with a black circle and x, for the Turkey Point site in Florida.

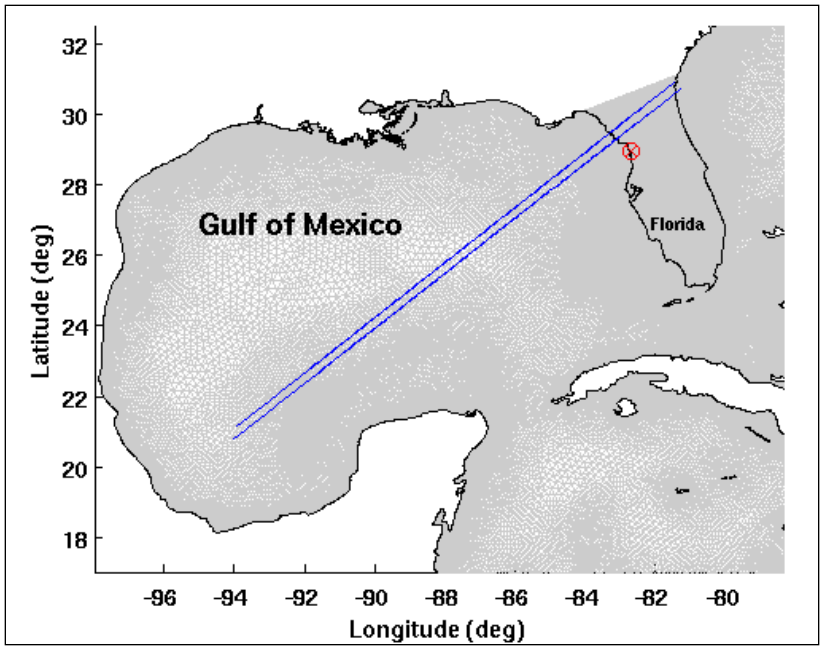

Figure 4-22. Storm tracks, blue lines, for the Levy County site, shown with a red circle and x, in Florida.

Table 4-4. Storm parameters and surge for Levy County site.

Storm	Surge	Wind	Pres	W-Indf	P-Indf	Rp	Holland B	Vf
	ft	m/sec	mb	m/sec	mb	nm		kt
1	29.89	59.48	880	45.25	910	30-39	1-1.35	5.5
2	31.86	60.98	870	47.19	900	30-39	1-1.35	5.5
3	29.33	60.87	880	47.47	910	30-39	1-1.35	11
4	30.97	62.29	870	49.36	900	30-39	1-1.35	11
5	26.41	64.08	880	52.99	910	30-39	1-1.35	22
6	27.82	65.39	870	54.46	900	30-39	1-1.35	22
7	30.51	57.66	880	44.23	910	45-58.5	1-1.35	5.5
8	32.41	59.05	870	46.14	900	45-58.5	1-1.35	5.5
9	30.68	58.74	880	46.13	910	45-58.5	1-1.35	11
10	32.35	60.12	870	47.97	900	45-58.5	1-1.35	11
11	29.76	61.63	880	50.10	910	45-58.5	1-1.35	22
12	31.14	62.91	870	51.82	900	45-58.5	1-1.35	22
13	10.93	39.81	960	21.96	990	45-58.5	1-1.35	5.5
14	18.04	48.40	930	32.29	960	45-58.5	1-1.35	5.5
15	25.26	54.76	900	39.98	930	45-58.5	1-1.35	5.5

At the Turkey Point site, two critical tracks appeared feasible (Figure 4-23) and both were included in the simulations conducted. Since our basis for the storm transformation during approach to land is based on Gulf of Mexico data, this transformation was not included in the storms affecting the Turkey Point site. Table 4-5 provides relevant information on the set of storms simulated for this site.

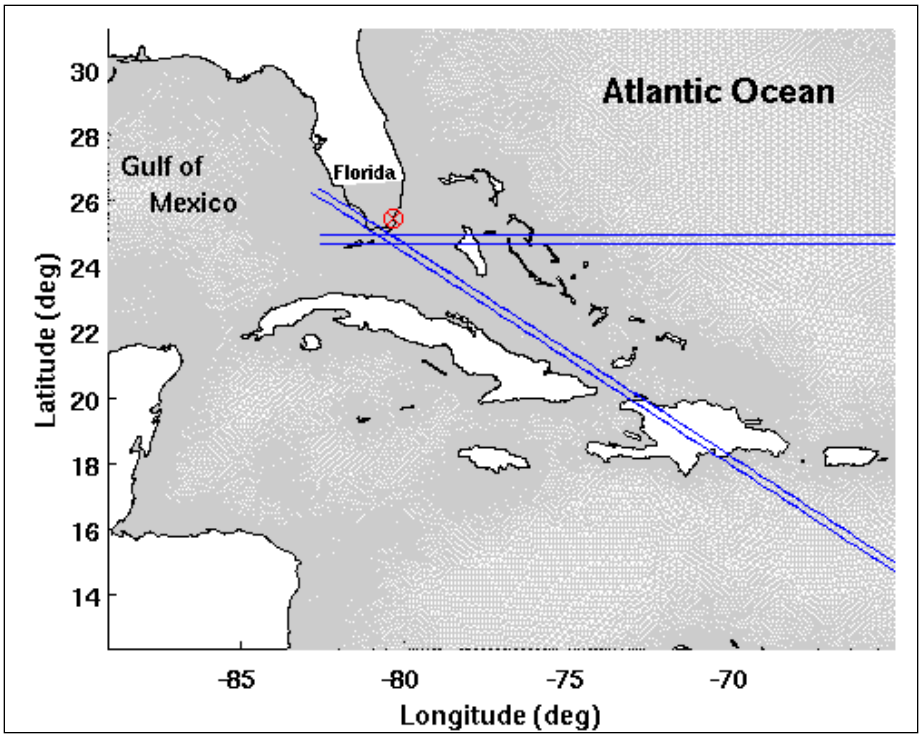

Figure 4-23. Storm tracks, blue lines, for the Turkey Point site, shown with a red circle and x, in Florida.

Following the methodology developed for Matagorda Bay, we obtain the following estimates of the PMSS for the two sites in Florida, assuming that the MPI value is still in the neighborhood of 880 mb:

Levy County (ft)

$PMSS = PMSS_{deterministic} + Uncertainty_{MPI+Models} + Uncertainty_{Climate} + Tidal\ Effects$

$37.7 = 30.7 + 4.1 + 1.2 + 1.7$ Equation 4-10

Turkey Point (ft)

$PMSS = PMSS_{deterministic} + Uncertainty_{MPI+Models} + Uncertainty_{Climate} + Tidal\ Effects$

$26.1 = 19.7 + 4.1 + 1.2 + 1.1$ Equation 4-11

At first glance, these values seem rather high for the site being investigated. Since the predictive models have been shown to be reasonably accurate, even for surges of the magnitudes generated here, there is no obvious reason to suspect that these surge levels are biased high due to the modeling system used. However, the storms simulated in this "upper-limit" analysis are certainly large intense storms, which have not yet been encountered in the areas of interest. Because of this, it is important to evaluate the likelihood of the storms used here are much less frequent than the value used for other safety considerations (an annual frequency of 10^{-6}). This will be done in Section 4.4.

Table 4-5. Storm parameters and surge for Turkey Point site.

Storm	Surge	Wind	Pres	W-Indf	P-Indf	Rp	Holland B	Vf
	ft	m/sec	mb	m/sec	mb	nm		kt
1	16.11	59.66	880	59.41	880	30	1.35	5.5
2	16.60	61.15	870	60.87	870	30	1.35	5.5
3	14.67	61.15	880	61.00	880	30	1.35	11
4	15.55	62.57	870	62.42	870	30	1.35	11
5	12.89	63.92	880	63.92	880	30	1.35	22
6	13.39	65.22	870	65.22	870	30	1.35	22
7	15.09	57.60	880	57.57	880	45	1.35	5.5
8	15.52	59.03	870	59.01	870	45	1.35	5.5
9	14.73	58.97	880	58.97	880	45	1.35	11
10	15.16	60.37	870	60.37	870	45	1.35	11
11	12.93	61.11	880	61.00	880	45	1.35	22
12	13.71	62.46	870	62.36	870	45	1.35	22
13	19.72	60.18	880	59.18	880	30	1.35	5.5
14	20.37	61.65	870	60.64	870	30	1.35	5.5
15	18.14	62.76	880	60.85	880	30	1.35	11
16	18.80	64.15	870	62.28	870	30	1.35	11
17	15.62	64.97	880	63.78	880	30	1.35	22
18	16.11	66.29	870	65.10	870	30	1.35	22
19	18.90	58.45	880	57.65	880	45	1.35	5.5
20	19.52	59.87	870	59.06	870	45	1.35	5.5
21	18.31	60.31	880	58.84	880	45	1.35	11
22	18.90	61.64	870	60.24	870	45	1.35	11
23	16.34	62.28	880	61.49	880	45	1.35	22
24	16.90	63.56	870	62.77	870	45	1.35	22
25	11.98	41.58	960	40.29	960	30	1.35	5.5
26	15.58	50.73	930	49.45	930	30	1.35	5.5
27	18.27	56.95	900	55.96	900	30	1.35	5.5

4.4 Analysis of 10^{-6} Storms at Two Florida Sites

Although uncertainty is often noted as a potential problem for very low probability events, the quantification of the effects of uncertainty on the risk has been an evasive problem. A very relevant point for licensing nuclear power plants in coastal areas is whether or not the storms defined by the upper limit analysis developed in this report are much less likely to occur than the accepted standard for safety at these plants, an annual frequency of 10^{-6}. To begin, historical data is analyzed to estimate the central pressure associated with an annual frequency of 10^{-6}. The conditional probability of storm size, with its dependence on storm intensity, is assumed to be the same as that used in the Gulf of Mexico study (IPET 2009). This assumption is much less conservative than assuming that the conditional storm size distribution is independent of storm intensity; since it predicts that large intense storms are much rarer than large moderate intensity and weak storms. Under this assumption, the approximate probability of the smaller of the two storms (an R_{max} of 30 nm) is on the order of 0.01. Thus, when this probability for the storm size is combined with the 0.0001 probability for storm intensity, a 10^{-6} value for the overall hazard probability is obtained.

4.4.1 Levy County Site

A careful analysis of hurricane data for the west coast of Florida, as expected, shows that most storms move east to west through this area. However, these storms usually have passed over land in getting into the Gulf of Mexico and do not produce large storm surges along the west coast of the state. In order to focus our analysis on storms of the type that produce significant surges along the west coast of Florida, the storm sample is stratified to include only storms with a general west to east motion in a latitude-longitude box with boundaries at 81^{o} W and 85^{o} W longitude and 25^{o} N and 30^{o} N latitude, and will further limit the storms to those with central pressures which are less than 990 mb in this box. Using the most recent reanalysis data available from NCDC (HURDAT)[1], we find that most storms before about 1940 did not report central pressures; consequently, we shall limit our data set for analysis to the interval 1940 to 2009 (70 years).

Table 4-6 shows a list of the selected storms, their central pressures and the years in which they occurred. Table 4-7 gives the results for a Generalized Extreme Value (GEV) analysis in terms of the expected central pressure associated with selected return periods (taken here as just 1 over the annual frequency) and the standard deviation as a measure of the confidence band of this estimate. It should be noted that the difference in the length of coast considered to be a "direct hit" in terms of the surge levels produced must be accounted for and the length of coast considered in the analysis upon which Table 4-7 is based. In a similar fashion to our probabilistic interpretation at the Matagorda Bay site, it is assumed that a direct hit occurs when the storm makes landfall within a ±1 R_{max} distance along the coast, centered on the location of the maximum surge at the site of interest. Since we used an approximate along-coast distance of 240 nm, this introduces another factor of 4 into the estimated return periods shown in Table 4-7. Thus, a 10,000-year value would become the 40,000-year value with this adjustment and the 884 mb estimate for the 10,000-year central pressure would become a 903 mb estimate for the 10,000-year central pressure within this reduced coastal domain.

Table 4-6. Storms included in analysis of extremes for Levy County site.

Year	Name	Minimum Central Pressure (mb)
1944	Not Named	968
1946	Not Named	979
1947	Not Named	989
1948	Not Named	963
1948	Not Named	975
1950	Easy	958
1953	No Named	985
1964	Isbell	964
1968	Gladys	965
1982	Alberto	985
1998	Mitch	987
1999	Irene	986
2000	Gordon	981
2001	Gabrielle	983
2004	Charley	947
2005	Wilma	950

[1] Available at http://www.nhc.noaa.gov/pastall.shtml

Table 4-7. Analysis of central pressures of hurricanes for selected return periods at the Levy County site: Results are for a storm striking anywhere along a 240 nm stretch of coast.

Return Period	Central Pressure (mb)	Standard Deviation
20	962	5.8
100	950	9.1
200	941	11.5
500	921	17.0
1000	912	19.4
5000	892	24.9
10000	884	27.3

Typically, the estimates in a table such as Table 4-7 would be used deterministically, and the size of the confidence bands would only be noted as a separate piece of information. With this deterministic interpretation, the estimate of the 1-in-10,000 central pressure is about 23 mb higher than the MPI value and the surges associated with Storm 15 (a 900-mb storm) would represent a better estimate of the risk-based surge levels. However, the implication of this is that uncertainty has no impact on our risk estimates, which runs counter to intuition.

The traditional form of an extremal distribution can be written in terms of a deterministic estimate given by the best-fit GEV Distribution. In the case of the west Florida hurricanes, the best-fit distribution was very close to a simple Gumbel distribution, so the Gumbel distribution is used here. From the analysis the following estimate of the Cumulative Distribution Function (CDF) from Table 4-7 is obtained, with X in this case denoting the value of the pressure differential, related to the central pressure by the relationship X=1013-c_p:

$$a)\ F'(X) = \exp\left\{-\exp\left[-\left(\frac{x-a_0}{a_1}\right)\right]\right\}$$

where

a_0 = 31.7 and a_1 = 12.34

$F'(X)$ is the best fit to the data not adjusted to an annual basis

and the Poisson-Gumbel Distribution for return period is: Equation 4-12

$$b)\ T_r = \frac{1}{\lambda[1-F'(X)]}$$

where

λ is the annual frequency (= 16/280) and

T_r is the return period in years; which yields for the annualized CDF, $F(\eta)$:

$$c)\ F(X) = 1 - \frac{1}{\lambda T_r}.$$

It should be noted that the annual frequency factor is simply the number of storms which occurred divided by four times the number of years where the additional factor of four in the denominator comes from the spatial adjustment mentioned previously.

If no uncertainty existed in our estimate of the CDF for pressure deviations, the encounter risk of a particular pressure deviation could be taken directly from Equation 4-12c; however, the risk of encountering a particular magnitude of pressure differential (X), for a fixed expected value of annual frequency should be understood to be non-zero for other values than the single deterministically estimated value; and the effect of possible values deviating from the

deterministic estimate should be considered when forming a "risk-based" estimate of the exposure to a particular extreme value. A more realistic treatment of the risk associated with the return periods in Table 4-7 can be obtained by quantifying the effects related to their probabilistic variation around the deterministic value. The estimated standard deviation, typically used to construct control curves around the deterministic estimate, provides a good means of quantifying the spread of the probabilities around the deterministic estimate; and in this context, the probability of a pressure differential can be written in terms of an integral in two dimensions with a delta function to reduce it back to a single dimension:

$$p(X) = \int_0^{\infty} \int_{-\infty}^{\infty} p[\hat{X}(T_r) + \varepsilon \mid \hat{X}] p(\hat{X}) p(\varepsilon) \delta(\hat{X} + \varepsilon - X) d\varepsilon d\hat{X}(T_r)$$

Equation 4-13

where

$\hat{X}(T_r)$ denotes the deterministic estimate of X for a given return period and

ε denotes the deviation from the the deterministic surge estimate.

In Equation 4-13, the estimate for $p(\varepsilon)$ is taken as a Gaussian distribution with the mean value at $\hat{\eta}$ and the standard deviation taken from Equation 3-2. However, as seen in Table 4-7, the uncertainty in the estimated pressure deviation increases with return period, i.e.:

$$p(\varepsilon \mid \hat{X}) = \frac{1}{\sigma(\hat{X})\sqrt{2\pi}} e^{-\frac{1}{2}\left(\frac{\varepsilon}{\sigma}\right)^2}$$

Equation 4-14

where

$\sigma(\hat{\eta})$ is the standard deviation of the estimate at a given value of $\hat{\eta}$.

The deviation has a mean value of zero, so no mean value is shown inside the exponential function in Equation 4-14.

To integrate Equation 4-13, the range of the deviations was limited to less than or equal to ±5 standard deviations (with an appropriate normalization coefficient included in the integral to ensure that no probability was inadvertently omitted from the total integral) and the relationship between the standard deviation and the deterministic estimate of the pressure differential was fitted empirically,

$$\sigma(X(T_r)) = \sigma(X(T_{20})) + \frac{\sigma(T_{10000}) - \sigma(T_{20})}{\ln(10000) - \ln(20)} \left[\ln(T_r) - \ln(T_{20})\right]$$

Equation 4-15

where the number subscripts on the return periods denote specific return periods in years. This provides a good fit to the data for the entire range of values between return periods of 20 years to 10,000 years.

Since the question at hand relates to the return period of the MPI value compared to the 10,000-year minimum central pressure, results are first converted to a return period representation before they are presented, using standard forms for this conversion,

$$T_r(X) = \frac{1}{1 - F(X)}$$

Equation 4-16a

with

$$F(X) = \int_{0}^{\infty} \int_{-\infty}^{\infty} p[\hat{X}(T_r) + \varepsilon \,|\, \hat{X}] p(\hat{X}) p(\varepsilon) H(\hat{X} + \varepsilon - X) d\varepsilon d\hat{X}(T_r) \qquad \text{Equation 4-16b}$$

where

$H(\bullet)$ is the Heaviside Function, equal to 1 if $\bullet \geq 0$ and equal to 0 if $\bullet < 0$.

Figure 4-24 shows the results of this integration for three cases compared to the original deterministic estimate. Case 1 is the deterministic solution for the return period based on the best-fit Gumbel Distribution. Case 2 is a test of the numerical algorithm generated by representing the probability of the deviations as a delta function (i.e. all of the probability exactly on the deterministic line), which was computed as a test case for the integration algorithm. As expected, this case exhibited no significant deviations from Case 1, so the Case 1 and Case 2 lines are identical. Case 3 shows the results using standard deviations equal to the estimated standard deviations divided by two; and Case 4 shows the results for the standard deviations as fit to the data in Table 4-7. These results show that the very low probability tail of the distribution is markedly affected by standard deviations comparable to those obtained in the fit to the Florida west coast data on central pressures. The results shown in Figure 4-24 show that the 1 in 10,000 (10^{-5}) frequency central pressure, based solely on a statistical analysis, is approximately 887 mb. This value is slightly higher than the MPI value of 880 mb and would likely produce surges in the range of 28.9 to 29.2 ft for a storm with a radius to maximum winds equal to 45 nm and in the range of 28.2 to 28.5 ft for a storm with a radius to maximum winds equal to 30 nm. It should be noted that the estimate for the 10^{-6} annual probability surge level considered only some of the possible storm combinations. A larger suite of storms (i.e. a larger subset from an extended joint probability method) would have to be considered in order to establish a better estimate of the 10^{-6} annual probability surge level.

4.4.2 Turkey Point Site

In this Section, a similar procedure to that developed in the previous Section is followed. In this case, east-to-west moving storms within a latitude-longitude box with boundaries at 77.4° W and 80.4° W longitude and 23.5° N and 27.5° N latitude are considered, and, similar to the Levy County site, the storms are further limited to those with central pressures which are less than 990 mb in this box. For the same reasons as noted for the Levy County site, the period of record is chosen to be 1940 to 2009 (70 year).

Table 4-8 gives a list of the selected storms, their central pressures and the years in which they occurred. Table 4-9 gives the results for a GEV analysis in terms of the expected central pressure associated with selected return periods (again taken here as just 1 over the annual frequency) and the standard deviation for the confidence band of this estimate. Similar to the case of Levy County, if we assume that the “direct hit” zone is approximately 60 nm wide, an additional factor of four is introduced into the estimates in Table 4-9 to account for the longer length of coast (240 nm versus 60 nm) included in the sample of extremes used in Table 4-9 compared to the “direct hit” length. A note should be given here that, unlike the Levy County site, the data for Turkey Point did exhibit considerable curvature away from a Gumbel Distribution; however, the analyses was kept consistent and proceeded with usage of the best-fit Gumbel distribution to estimate the effects of uncertainty.

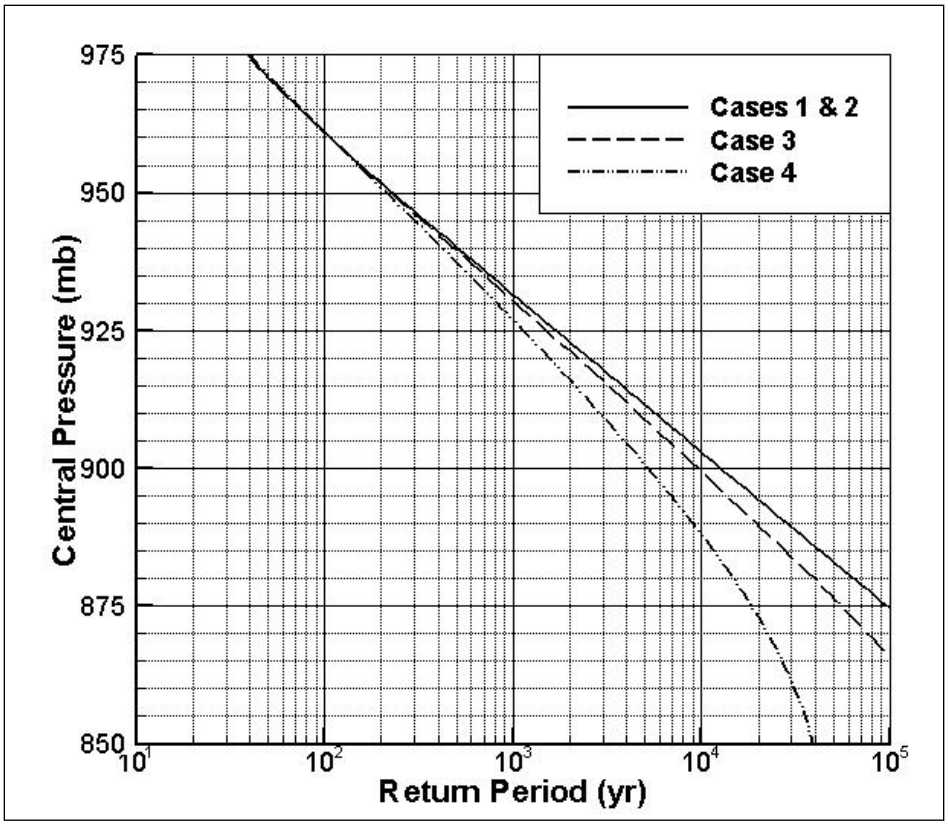

Figure 4-24. Comparison of "risk-based" return periods for central pressures without uncertainty considered (Cases 1 and 2) and with uncertainty considered (Cases 3 and 4) for the Levy County site using data from 1940-2009. Case 4 represents the actual estimate for the Levy County site.

Table 4-8. Storms included in analysis of extremes for Turkey Point site.

Year	Name	Minimum Central Pressure (mb)
1947	Not Named	947
1949	Not Named	954
1960	Donna	932
1964	Cleo	968
1965	Betsy	952
1966	Inez	985
1979	David	972
1992	Andrew	930
1995	Erin	980
2004	Frances	958
2004	Jeanne	951
2005	Katrina	983
2005	Rita	985

Table 4-9: Analysis of central pressures of hurricanes for selected return periods at the Turkey Site: Results are for a storm striking anywhere along a 240 nm stretch of coast.

Return Period	Central Pressure (mb)	Standard Deviation
20	950	5.8
100	931	9.1
200	918	11.5
500	889	17.0
1000	877	19.4
5000	848	24.9
10000	835	27.3

Figure 4-25 shows a comparison of the same types of cases analyzed for the Levy County site. In this case, the uncertainty is substantially larger; and even by the 5,000 year return period, the effect of uncertainty is to lower the central pressure by about 25 mb. The data indicate that the hurricane population coming into the Turkey Point area is, in general, more intense than hurricane population coming into the west Florida area; therefore the statistically derived central pressure is considerable lower than the MPI in the Turkey Point area.

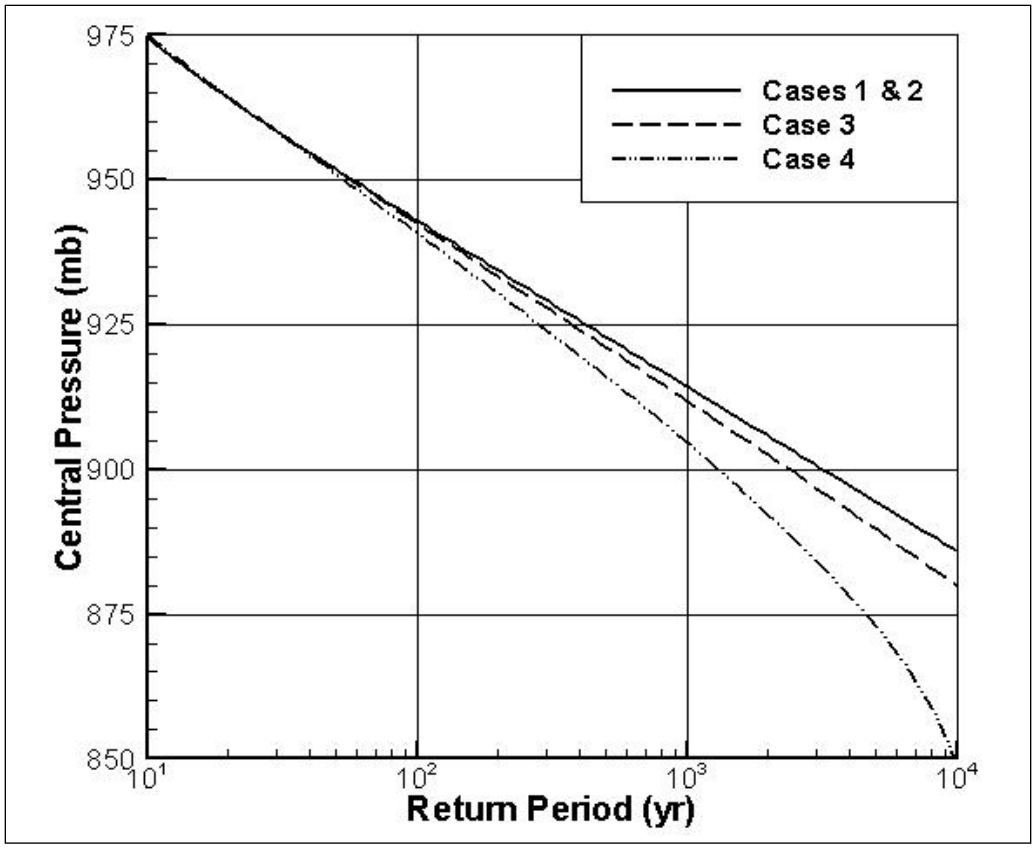

Figure 4-25. Comparison of "risk-based" return periods for central pressures without uncertainty considered (Cases 1 and 2) and with uncertainty considered (Cases 3 and 4) for the Turkey Point site using data from 1940-2009. Case 4 represents the actual estimate for the Turkey Point site.

4.5 Summary

An example of how a combined deterministic-probabilistic approach can be applied to estimate the PMSS (including a first approximation for effects of uncertainty) at three sites (Matagorda Bay, Texas; Levy County, Florida; and Turkey Point, Florida) has been presented. Guidance on quantifying the uncertainty in climatological parameters and within a state-of-the-art system is also provided. The uncertainty has traditionally been neglected in past upper-limit estimates of surge levels; but the magnitudes of these terms are not negligible. The values of the uncertainty terms developed here can serve as reasonable first estimates for the entire Gulf of Mexico, since the MPI values and the modeling uncertainty factors are similar throughout this region. The recommended estimate for uncertainty due to the estimation of the MPI and the models is 4.1 ft and the uncertainty due to climate parameters is estimated at 1.2 ft.

The possibility that the upper limit storms are much larger than the 10^{-6} annual probability used for safety standards at nuclear power plants is also examined at the two Florida sites. As part of this effort, the importance of quantifying the impact of uncertainty on estimated surges for a fixed frequency level was stressed and a method to accomplish this was developed. In the applications here, the estimated central pressures for the 10^{-4} annual probability were shown to be about 15 mb lower when the effects of uncertainty were included. In the two Florida cases examined here, the PMSS value for Levy County exceeded the 10^{-6} annual probability surge. Furthermore, at Turkey Point, the annual probability associated with the PMSS was smaller than 10^{-6}.

5.0 SCREENING METHOD

Appendix C of Regulatory Guide 1.59 contains maps and tables of estimated surges for the U.S. Gulf and Atlantic coasts that nuclear power plant applicants can use to determine if flooding might be severe enough near their prospective site to warrant more detailed definitions of design-basis floods. The USACE was tasked by the NRC Office of Nuclear Regulatory Research to develop an updated screening approach that includes data collected and analysis methods developed since the publication of Regulatory Guide 1.59. The screening method recommended for NRC consideration should include criteria for proceeding or not proceeding to more detailed definitions of design-basis floods and explicitly consider local conditions and bathymetry that may affect flood level estimates.

This Section documents a proposed screening approach to determine if a prospective site is at risk of flooding from coastal storms. It begins with a description of surge propagation with an emphasis on the importance of the local surrounding coastal landscape and the strength and duration of the relevant storm forcing. These complexities drive the development of a recommended approach that computes a critical storm surge flood elevation map that is compared to a controlling site elevation and provides criteria for proceeding to more detailed estimation of design-basis floods. The methodology incorporates an open-coast surge calculation, wind wave effects, tide, and uncertainty to estimate a conservative elevation threshold that provides the criteria. The recommended method for developing the critical flood elevation is demonstrated for sites at Matagorda, TX; Biloxi, MS; Levy County, FL; and Turkey Point, FL. The comparison of the computed critical flood elevation to a controlling topographic elevation for screening a prospective nuclear power plant site is demonstrated at Matagorda.

5.1 Processes That Affect Storm Surge

As hurricanes and extra-tropical storms approach the coast, four storm-related phenomena can occur to modify local water levels: setup due to wind, low barometric pressure, set up due to wave forcing, and rainfall. Storm winds force water towards the coast and typically create the greatest change in local water elevation. Low barometric pressure provides a secondary effect, creating a bulge in the water surface around the center of the storm. Wave forcing creates a local setup on the coast. Rapid storm rainfall can also increase the local water elevation. Additional factors not related to the storm itself are the astronomical tide and river flows at the time the storm reaches the coast. The spatial scales of the relevant forcing processes, such as the wind and wave fields can range from meters in complex shallow areas to hundreds of kilometers in large deep basins.

Storm surges are greatly influenced by the geometry of the basin and continental shelf leading up to the coastal floodplain. A mildly sloping continental shelf, such as in the Gulf of Mexico, results in a higher storm surge as compared to a coast with a steeper bathymetry. The Atlantic and Gulf of Mexico basin geometries are very complex in both the “cross-shelf” and “along-shelf” directions. These coasts are characterized by natural features such as bays, inlets, barrier islands, and wetlands. Natural feature details at a finer scale, such as coastal streams, distributaries in wetlands, and the vegetation types covering landscape features, also affect surge propagation in coastal areas. Man-made features, including extensive levee, rail and road systems, navigation channels, canals, and culverts must also be resolved.

The complexities of modeling surge propagation and the interaction of coastal storms with natural coastal features are discussed by Westerink *et al.* (2008), Resio and Westerink (2008),

and Wamsley *et al.* (2010). Model accuracy requires 1) the application of a model with sufficient spatial resolution to represent important bathymetric/topographic features accurately and 2) that all terms contributing to the surge are represented in the proper physical context. Processes that affect storm surge inundation include atmospheric pressure, winds, air-sea momentum transfer, waves, river flows, tides, and friction due to land cover. Numerical models exist that can properly define the physical system and include an appropriate non-linear coupling of the relevant processes. A coupled surge-wave model must be applied and the computational domain must be sufficiently large to negate the need for empirical factors along an offshore grid boundary. Therefore, there is no "short cut" to estimating coastal surges that considers all the local conditions for critical applications such as determining flood risk at specific prospective nuclear power plant sites. Such an application requires not only resolution of the ocean basin, but also detailed representation of the coastal floodplain to be incorporated into modeling system meshes or grids. These highly detailed meshes are expensive to construct and result in computational run time requirements that are considerably higher than for simpler models. In addition, the coastal flood plain is constantly changing due to both human development and natural processes which necessitates frequent updating of the meshes.

5.2 Requirements for a Screening Approach

The preceding discussion emphasizes that there is not a simple method to properly estimate coastal surges for prospective nuclear power plant sites that considers all the local conditions. Any prospective nuclear site that is vulnerable to coastal storm surge flooding should be required to have a detailed analysis performed. Therefore, the purpose of the screening approach should be to identify a critical elevation that defines whether or not a prospective site is at risk for coastal surge flooding. The determination of the critical elevation should be relatively simple to apply, consistently determined across the coast, and incorporate an appropriate level of conservatism.

The critical flood elevation should be determined with an appropriate modeling system. However, available surge model systems and their application can vary widely. For example, each model may apply different formulations of the wind or bottom drag law that can result in extremely different surge estimates for the same storm, particularly for large storms. The quality of surge estimates is also dependent on the model domains and how boundary conditions are applied. Therefore, each screening application should be carefully reviewed to ensure that an appropriate determination is made with respect to the coastal surge flood risk at any given site.

A coupled system of wind, wave, and coastal circulation models has been developed and implemented for regions in both the Gulf of Mexico and the Atlantic, as described in Section 4. The system combines the TC96 PBL model (Thompson and Cardone 1996), the WAM offshore (Komen et al 1994) and STWAVE nearshore (Smith et al 2001, Smith 2007) wave models, and the ADCIRC (Westerink *et al.* 2008; Bunya *et al.* 2010) basin-to-channel scale unstructured grid circulation model. The model includes the nonlinear coupling of multiple processes (e.g. riverine flow, tide, wind, waves) that contribute to storm surge. The domains are large enough to capture the required basin-to-basin and basin-to-shelf physics. The modeling system can be run at very high-resolution, accurately representing the physical system with resolution on the order of 10 m. The system has undergone extensive validation with Gulf of Mexico storms including hurricanes Betsy, Andrew, Ivan, Katrina, and Rita. Based on these extensive validation efforts, the details of the models and error associated with surge simulations with this system are relatively well known compared to other modeling frameworks. The ADCIRC

modeling framework is therefore recommended for generation of the open coast surge estimate for screening purposes.

The open coast surge estimate for screening purposes will need to be generated with meshes that do not have detailed representations of the coastal flood plain due to the expense in developing these grids. Since a detailed analysis is not part of the screening flood elevation estimation, an appropriate level of conservatism should be incorporated into the flood estimates. The screening method includes mechanisms to ensure that a reasonable, but conservative, estimate of a critical flood elevation is made, as discussed in the following section.

5.3 Screening Method

The coupled system of wind, wave, and coastal circulation models previously discussed is appropriate for a detailed coastal surge analysis. The model includes the nonlinear coupling of multiple processes and can be run at very high resolution, accurately representing the physical system with resolution on the order of 10 m. This allows fine details of the coastal flood plain to be resolved that are important to accurately estimate surge levels a specific sites. Unfortunately, this high level of detail is expensive to develop in computational meshes and requires extensive computer resources to calculate. The coupling of the wave models also adds complexity and requires significant resources to compute. However, estimates of open-coast Probable Maximum Storm Surge (PMSS) appropriate for screening can be predicted by applying the wind and surge models without resolving the coastal flood plain landward of the coastline. The wave setup can then be added separately by applying a factor discussed by Resio and Westerink (2008) that represents the ratio of the transfer rate from the wave field to the direct wind momentum transfer rate. Tidal effects and predicted sea level rise can also be incorporated. Finally, uncertainty must also be considered in the determination of the final critical flood elevation.

5.3.1 Open Coast PMSS Estimation

Because a conservative estimate of the PMSS is desired, a storm with an extreme upper limit for surge potential must be simulated[2]. This conservative PMSS for screening purposes will be referred to as the SPMSS (Screening PMSS). If the peak surge level at a point only depended on a single scalar variable, such as wind speed, the maximum value of that variable could clearly be associated with the maximum surge value. However, hurricane surge response at a specific site depends on several storm factors and not just a single, scalar variable (i.e. wind speed). Several recent studies (IPET 2009; Resio *et al.*, 2008; Irish *et al.*, 2008; Irish and Resio, 2010) have shown that the maximum surge can be estimated as a function of several storm parameters:

$$\eta_{\max} = \Phi_1(\Delta p)\Phi_2(R_{\max})\Phi_3(x - x_0)\Phi_4(v_f)\Phi_5(\theta_f) \qquad \text{Equation 5-1}$$

where the multiplicative functions Φ_i depend on the specific bathymetric/topographic setting at the specific point being investigated, Δp is the peripheral pressure minus the central pressure (storm intensity), R_{max} is the distance from the eye to the maximum winds (storm size), x-x_0 denotes the alongshore position of the point of interest relative to the landfall position, v_f is the forward velocity of the storm, and θ_f is the angle of storm heading.

[2] Section 3 provides a detailed discussion on deriving very low probability surge levels. Key concepts are reviewed here.

The screening storm must consider reasonable parameter values that maximize surge potential. As discussed in Section 4, the surge functions associated with each of these parameters have asymptotic limits or natural limiting behavior. Irish and Resio (2010) noted that when the storm size becomes as large as the region of primary surge generation, additional increases in storm size do not produce substantial increases in storm surge. Analysis by Irish and Resio (2010) found that increases in offshore storm size above approximately 45 nm in the Gulf of Mexico resulted in negligible increases of storm surge. Therefore, for the Gulf of Mexico shelf, a reasonable upper limit on storm size for screening purposes is 45 nm. Changes in the forward velocity of a storm results in two physical mechanisms that have opposite effects on surge levels. Wind speeds inside a hurricane increase with increasing forward velocity of a storm due to the contribution of background winds, resulting in a potential increase in surge. Conversely, as the storm speeds up, the time winds blow over the surge generation area is decreased, resulting in a potential decrease in surge. For open coast simulations not allowing for inundation, such as those proposed for the screening method, the importance of the time scales for which winds blow over the surge generation area is reduced relative to the increases in wind speed. Therefore, a fast moving storm generates greater surges at the coast for these simulations and a forward velocity of 22 kt is proposed for screening.

The primary driver of surge potential is storm intensity. The surge function associated with storm intensity does not have a clear upper limit. However, the MPI of a hurricane has been postulated as an upper limit for extreme tropical cyclone intensities at least since the late 1970's (see for example: World Meteorological Organization, 1976 and Mooley, 1980). Emanuel (1986, 1987, 1991) and Holland (1997) formulated theoretical models for estimating maximum tropical cyclone intensity. Tonkin *et al.* (2000) evaluated the performance of these two MPI models in the North Atlantic region. Figure 2-4 presents the results from Tonkin *et al.*'s application of the Emanuel Model, Holland's model, and observed intensities. As can be seen in Figure 2-4 and as widely accepted from theoretical considerations, a strong relationship exists between climatological SST values and the lowest central pressures. In the range of SST values from 26^{o} to 28^{o} (C), the minimum central pressures of the Holland Model, the Emanuel model and the observed intensities are all in approximate agreement. Above 28^{o} (C), the observations and Holland model continue to show decreasing central pressures with increasing values of SST; whereas, the Emanuel model does not. Figure 2-5, taken from Schade (2000), shows another approximation for the MPI. Schade (2000) suggests that the effect of the SST field on tropical cyclone intensity is twofold: 1) the large-scale ambient SST field "sets the stage for the tropical cyclone"; and 2) the intensity of a tropical cyclone is highly sensitive to the reduction of the SST in the interior region of the storm due to the response of the ocean to surface winds. Therefore, the concept of the MPI is well formed, but many of the details are still under investigation.

Figure 4-16 shows the average August to September SST for the Gulf of Mexico during the period 1940 to 2006. The highest average values during this part of the year (the peak of hurricane season) have varied from as low as 28.17^{o} C in 1984 to as high as 29.49^{o} C in 1962. The dotted vertical line in Figure 2-5 shows this historical maximum plotted on top of Schade (2000) results. The heavy solid line along the top of Figure 2-5 denotes the MPI value without consideration of any negative feedback of the type discussed by Schade; thus, it is expected to represent a maximum possible threshold for the MPI. Figures 2-4, 2-5, and 4-16 support a reasonable estimate of 880 mb for the MPI in the Gulf of Mexico, without consideration of significant global warming effects on SST's that might drive them higher than the level of the 1960's. However, considering that many of details of the MPI are still under development and the desire for a conservative estimate for screening purposes, an MPI of 870 mb is proposed.

The parameters for the screening storm are summarized in Table 5-1. This storm must be simulated on tracks that make landfall along the Gulf of Mexico and Atlantic coasts. For different stretches of coastline, as determined by the physical characteristics of the Gulf of Mexico and Western Atlantic basins, only certain types of tracks are physically realistic for major storms approaching the coast. For example, major storms approaching Matagorda, TX can form in the Bay of Campeche to the south or enter the Gulf of Mexico between Cuba and Yucatan. For Biloxi, MS, major storms enter the Gulf of Mexico between Florida and Cuba or between Cuba and the Yucatan. Figure 5-1 provides examples of the major storm tracks that make landfall in these two regions and at the Florida sites.

Table 5-1. Screening storm parameters.

Central Pressure (mb)	Radius to Maximum Winds (nm)	Forward Velocity (kt)
870	45	22

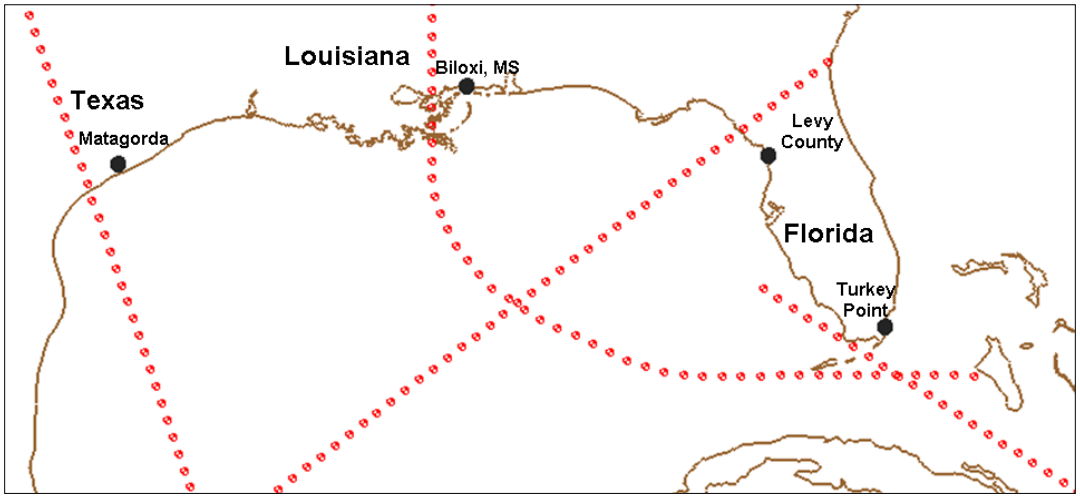

Figure 5-1. Location of Matagorda, TX, Biloxi, MS, Levy County, FL, and Turkey Point, FL, regions with storm tracks for screening storm.

Open coast surge estimation does not require simulation on a mesh that resolves the coastal flood plain and a simpler mesh can be applied. The USACE developed the East Coast 2001 Western North Atlantic (EC2001) mesh to compute a database of tidal constituents (Mukai *et al.* 2002). The EC2001 domain encompasses the Western North Atlantic Ocean, the Gulf of Mexico, and the Caribbean Sea (Figure 5-2) and can be applied to provide conservative estimates of open coast storm surge. The eastern open ocean boundary is along the 60-deg west meridian where the bathymetry is almost entirely in the deep ocean. The EC2001 has over 250,000 nodes and nearly 500,000 elements. Resolution varies from 25 km in the deep ocean to approximately 1 km along the land boundaries. The bathymetry in the mesh is defined from multiple databases, including ETOPO5 (National Geophysical Data Center, Nation Oceanic and Atmospheric Administration, Boulder, CO, 1988); the Digital Nautical Charts bathymetric database (U.S. Department of Defense, National Imagery Mapping Agency, Washington DC, 1999); and the NOS raw sounding bathymetric database (NOS Hydrographic Survey Digital Database). The coastline boundaries for EC2001 are from the Defense Mapping Agency's World Vector Shoreline database (Soluri and Woodson 1990). The final bathymetry

for EC2001 is shown in Figure 5-3. A complete description of the mesh and its development is provided by Mukai *et al.* (2002).

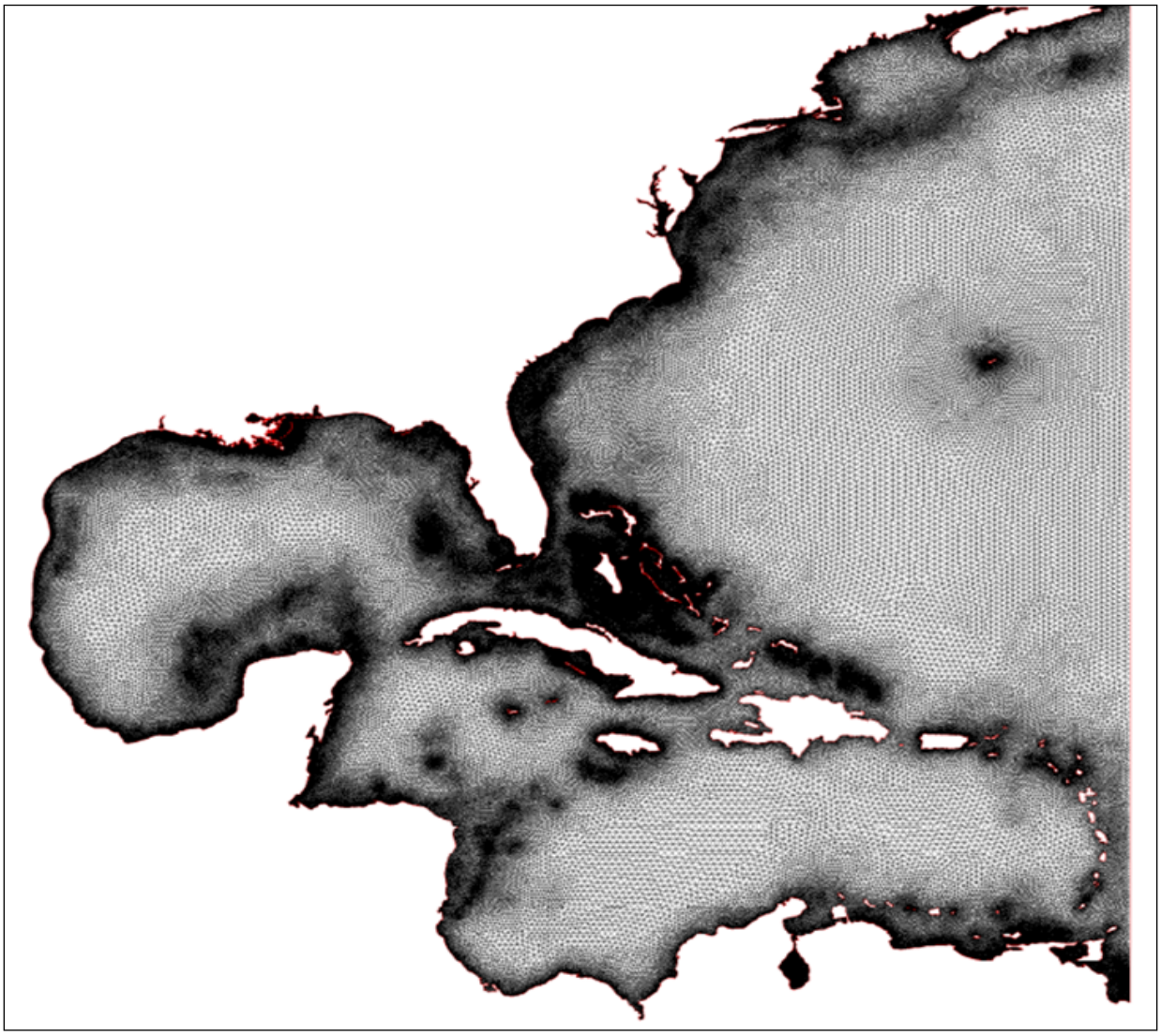

Figure 5-2. EC2001 finite element grid (from Mukai *et al.* 2002).

Hurricane simulations on the EC2001 mesh capture the required basin-to-basin and basin-to-shelf physics and include the nonlinear coupling of the relevant processes other than the transfer of momentum due to waves. The termination of the mesh at the shoreline precludes surge propagation inland and surge builds up at the coast, providing a generally conservative estimate of open coast surge elevations in the region of interest. To illustrate how surge estimates simulated on the EC2001 differ from those made on a mesh with a highly resolved coastal flood plain, results from simulations with the screening storm (Table 5-1) that makes landfall in the Matagorda, TX region (see Figure 5-1) are compared. The EC2001 and meshes in the Matagorda region are plotted in Figures 5-4 and 5-5.

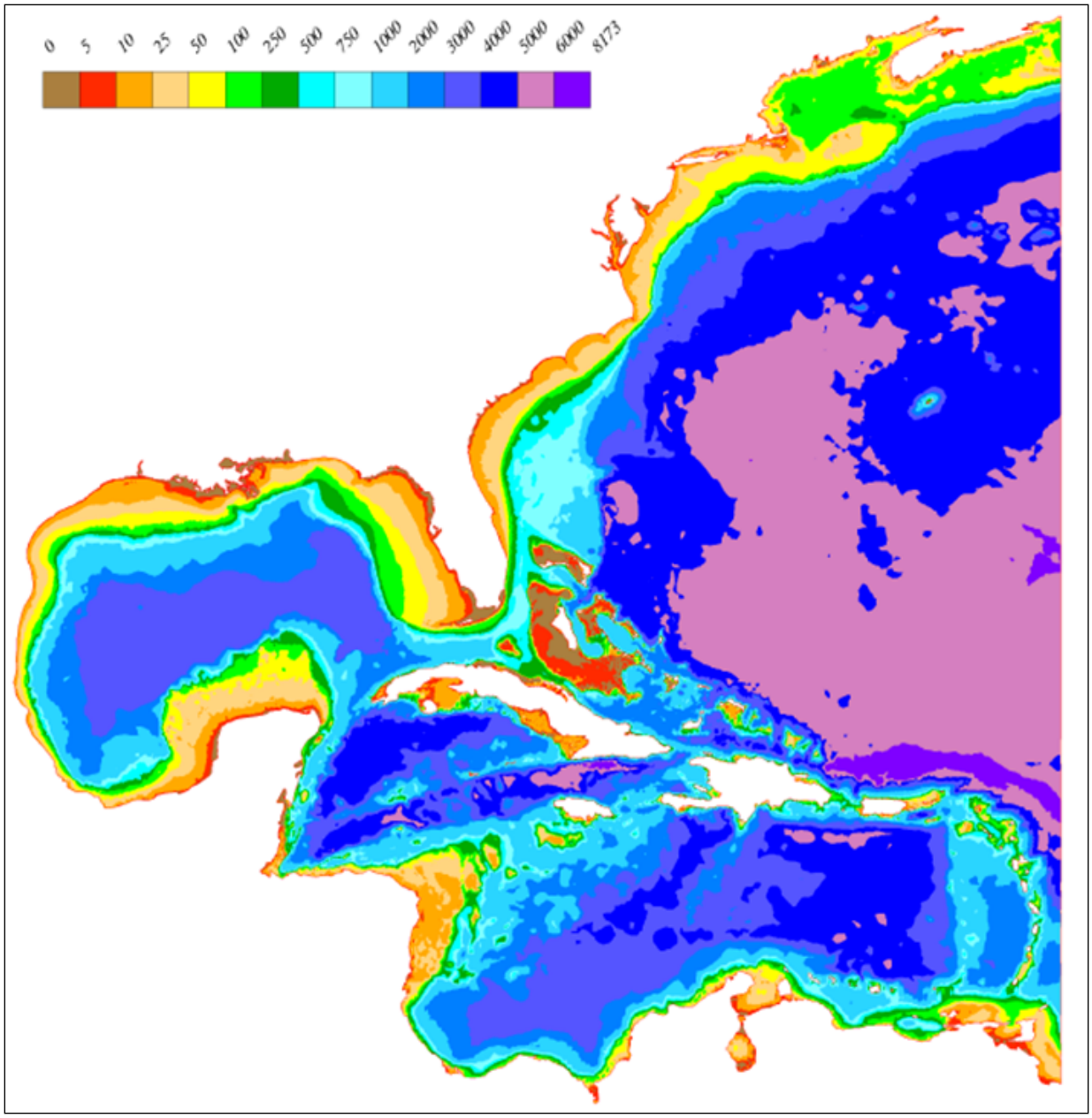

Figure 5-3. EC2001 composite bathymetry in meters relative to the geoid (from Mukai *et al.* 2002).

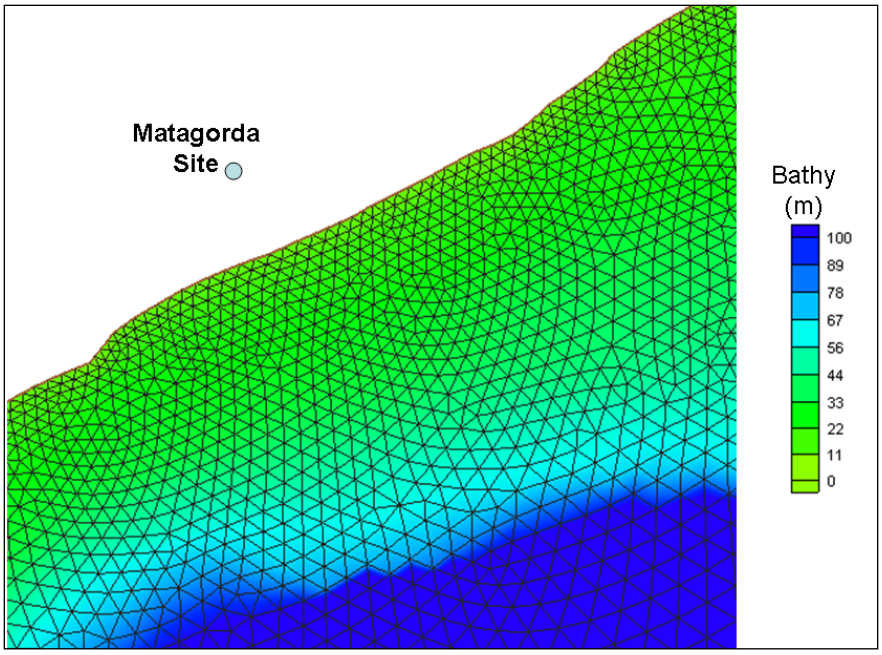

Figure 5-4. EC2001 mesh and bathymetry in the vicinity of Matagorda, TX.

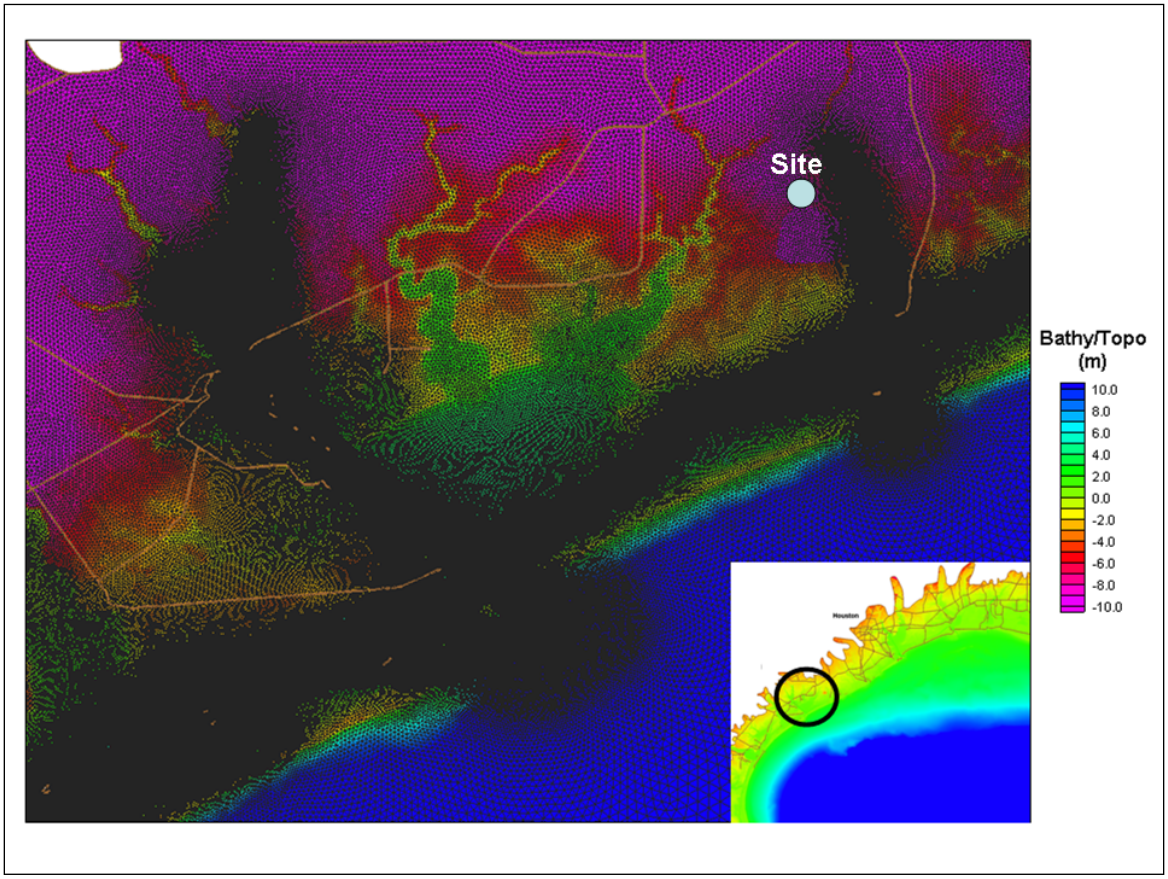

Figure 5-5. Detailed mesh and bathymetry/topography in the vicinity of Matagorda, TX.

The peak surge elevations for the screening storm making landfall in Matagorda with the EC2001 and detailed meshes are plotted in Figures 5-6 and 5-7, respectively. The peak surge at the coast is higher on the EC2001 mesh because the water is precluded from propagating inland. On the detailed mesh, as surge propagates inland, water elevation goes down with increasing distance in many areas but can also increase with topography. The peak surge elevations realized at inland locations are controlled by the surrounding coastal landscape and the strength and duration of the relevant forcing. The duration of the relevant forcing is primarily controlled by the forward velocity of the hurricane. Figure 5-8 is a plot of the peak surge elevations for a storm with the same parameters as the storm in Table 5-1, except that the forward velocity is 11 kt. The slower moving storm increases the duration hurricane winds propagate storm surge and results in greater peak surge elevations far inland, which can be seen by comparing Figures 5-7 and 5-8.

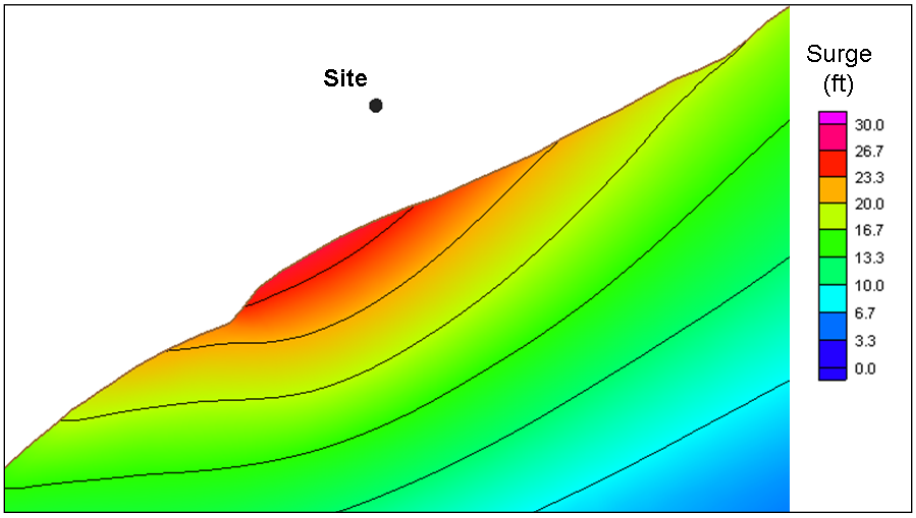

Figure 5-6. Matagorda peak surge elevations for screening storm on the EC2001 mesh.

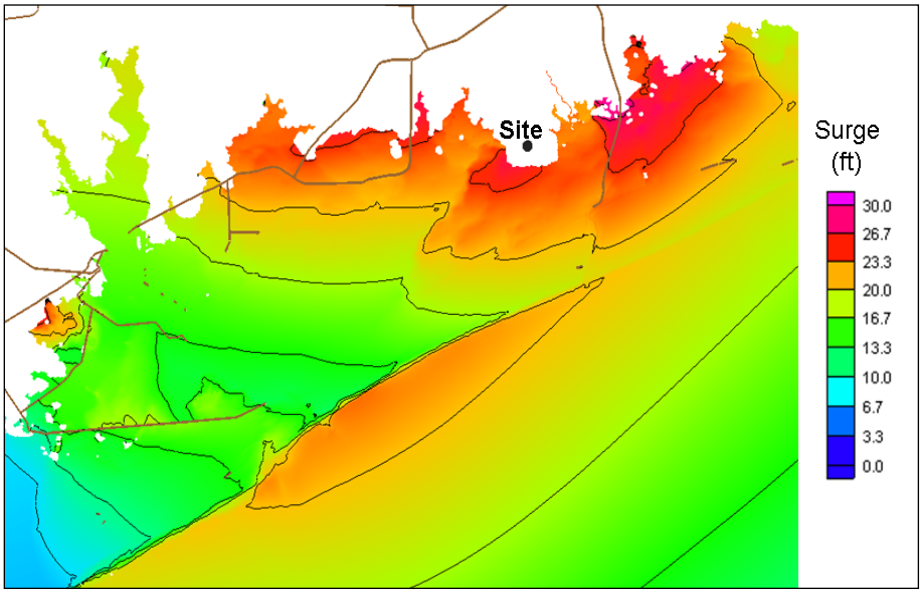

Figure 5-7. Matagorda peak surge elevations for screening storm on the detailed mesh.

A conservative surge estimate based on open coast surge must account for the variability associated with propagation inland. To understand how surges may vary spatially in both the cross shore and longshore directions, a suite of storms was simulated on a detailed mesh with tracks making landfall in the Matagorda, TX, Biloxi, MS, Levy County, FL and Turkey Point, FL regions. The suite of storms had pressure and size parameters consistent with those in Table 5-1. The suite included additional storms with slower forward velocities. In Figure 5-9, the peak surge elevations over all storms simulated are plotted versus the maximum surge on the EC2001 mesh at several locations across the coastal flood plain within 20 km of the maximum surge location at all four locations. The plot shows that the open coast surge estimate on the EC2001 is greater than most points in the region of interest. For Biloxi, the peak surge at all points across the region of interest simulated on the detailed mesh fall below the peak surge on the EC2001. However, at Matagorda, Turkey Point, and Levy County the controlling topography allows surge to propagate a longer distance inland, slow moving storms push water up the coastal flood plain and the peak water surface elevations at far inland points are greater than those at the coast. The maximum difference between the peak surge on the EC2001 mesh and the detailed mesh is approximately 5 ft (Figure 5-9), which provides a conservative estimate of the peak water level deviation due to variability of surge propagation inland (η_{dev}). This value will be considered a generally applicable correction factor for locations along the Gulf of Mexico to account for the variability associated with propagation inland and must be included in the final computation of the SPMSS. While the 5 ft correction factor is the maximum calculated for the various sites modeled and should provide a sufficient conservative estimate for the majority of the U.S. southern coast, this value may not be conservative for every coastal landscape and a greater value may be warranted in some circumstances.

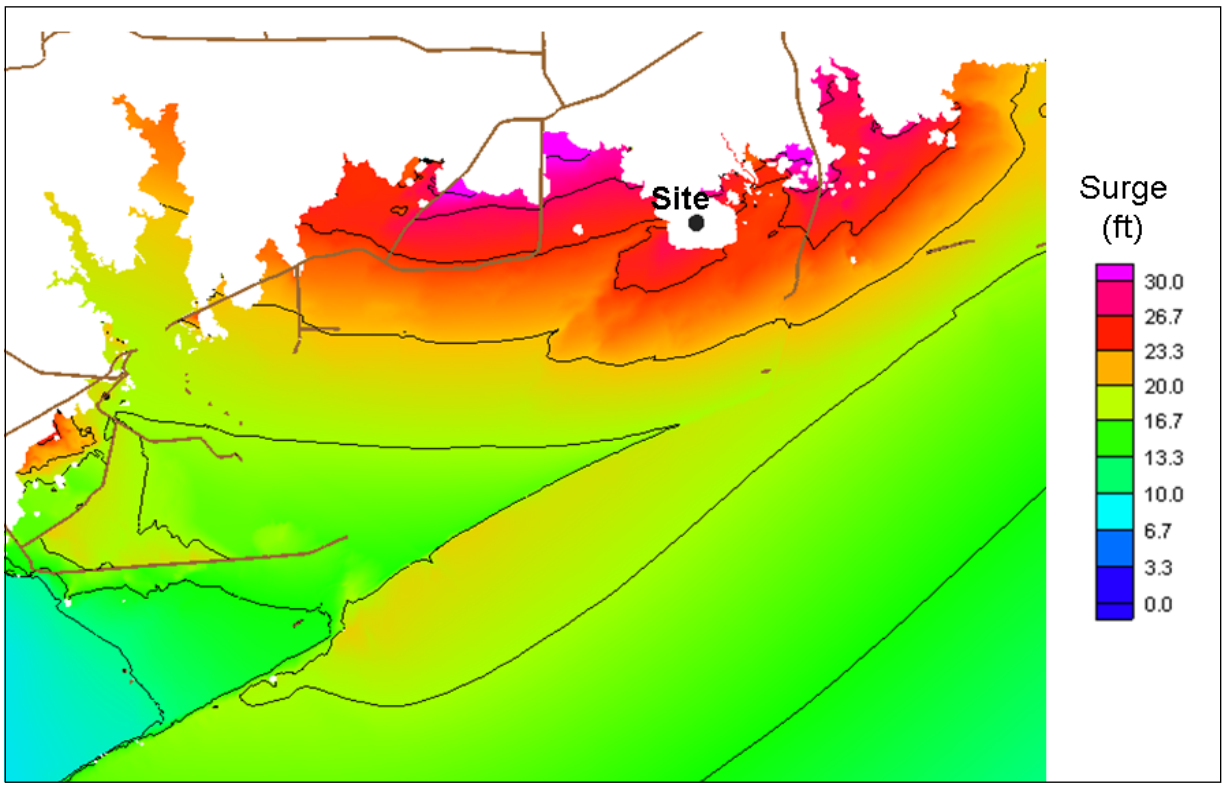

Figure 5-8. Peak surge elevations on the detailed mesh in the vicinity of Matagorda, TX for a storm with a central pressure of 870 mb, radius to maximum winds of 45 nm and a forward velocity of 11 kt.

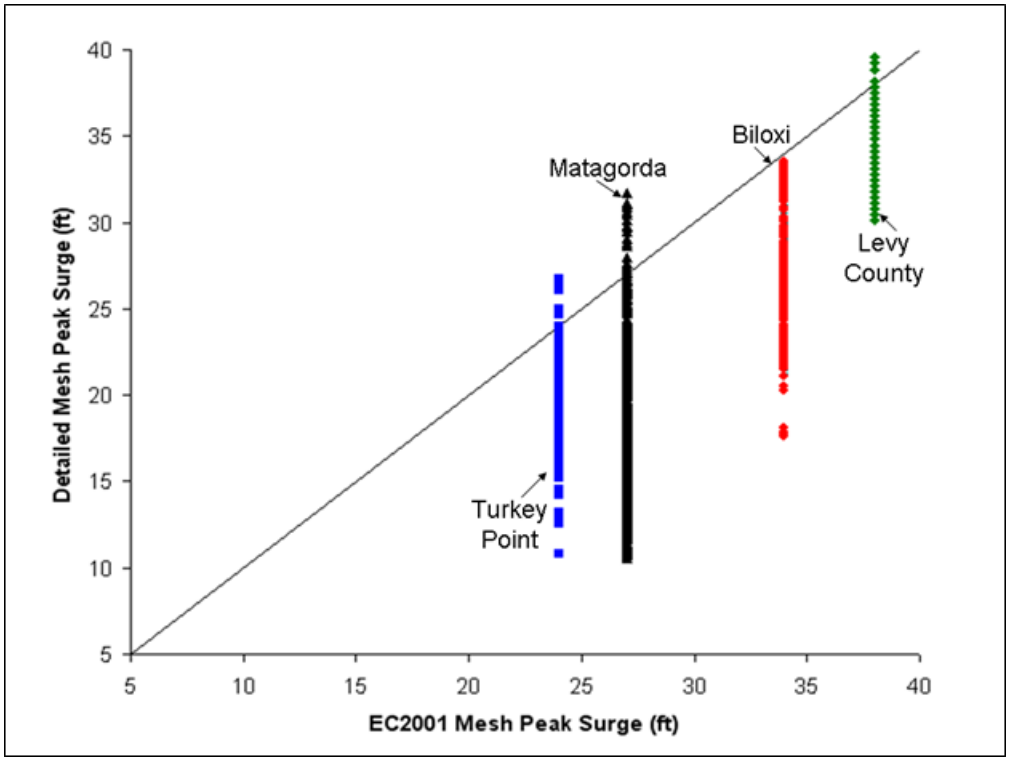

Figure 5-9. Peak surges on detailed mesh plotted versus the peak surge for the screening storm on the EC2001 mesh.

5.3.2 Tidal Effects

All simulations are run at mean tide level. A storm may, however, occur at high tide which would result in higher peak surge elevations. To account for this possibility, a tidal adjustment (η_{tide}) equal to the difference between mean higher high water and mean tide level should be added in the final computation of the SPMSS.

5.3.3 Wind Wave Effects

Wave setup that occurs due to the momentum transfers from waves must also be included in maximum surge elevations. The momentum source, termed a radiation stress, is produced by a divergence in the momentum flux within the wave field and is primarily related to wave breaking. The momentum loss rate from wave breaking is dependent on the slope and depth of the sea bottom, and varies considerably throughout a region of interest and from site to site. The introduction of this source can be accomplished by coupling wave and surge models as previously discussed and would be required for a detailed analysis. However, an estimate of the wave setup can be made based on estimates of the ratio of the transfer rate from the wave field to the direct wind momentum transfer rate (R) as discussed by Resio and Westerink (2008). The function that defines the variability of R is provided by considering the different wave breaking forms assumed in various wave models and theoretical approaches and simulated wave momentum loss rates. Figure 5-10, which is based on an approach introduced by Resio and Westerink (2008), shows the envelope of the resulting estimates of R on different bottom slopes.

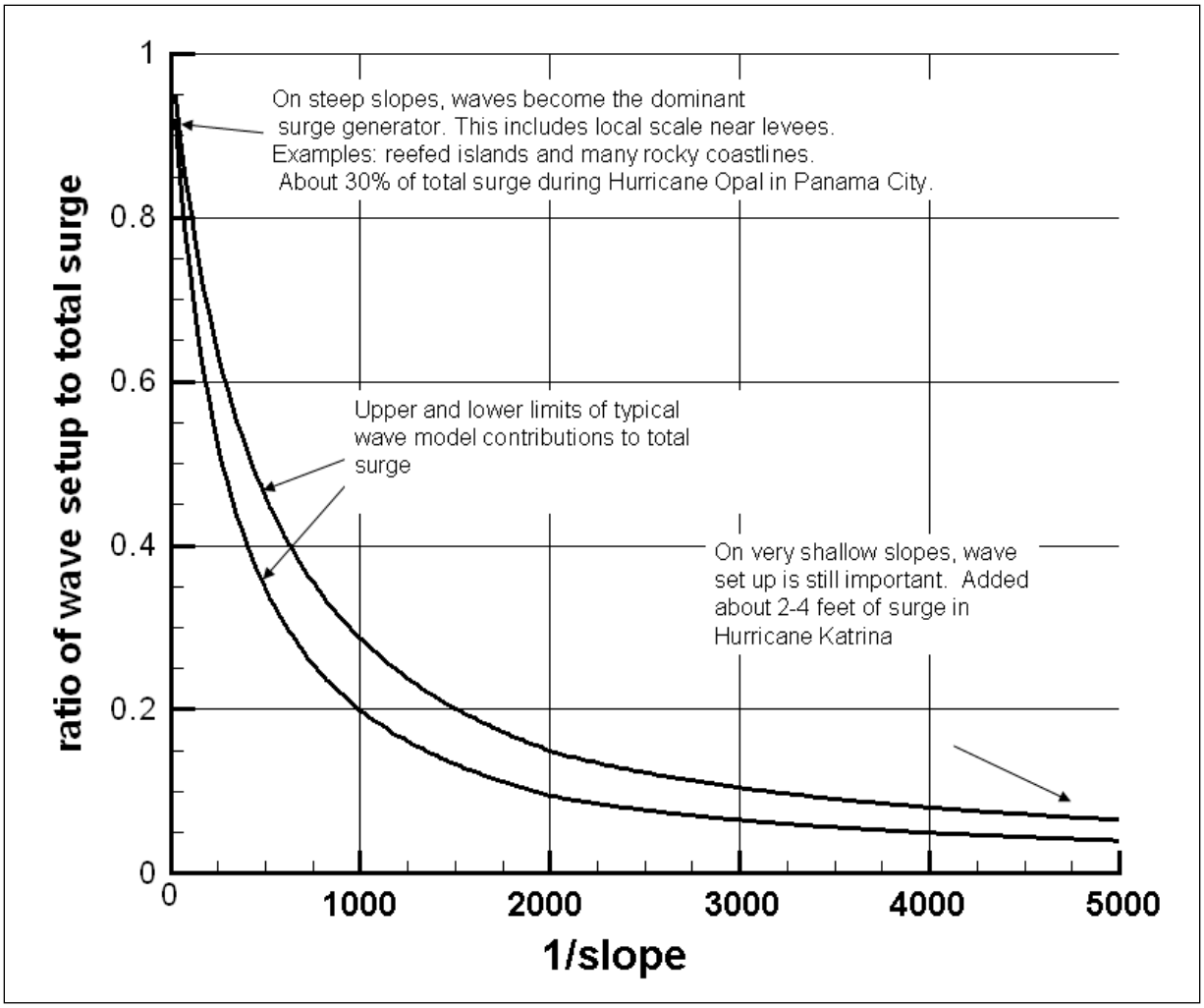

Figure 5-10. Approximate upper and lower limits of the ratio of the wave contribution to water levels at the coast (wave setup) to the total surge at the coast.

The relationship described by Figure 5-10 can be applied to estimate the wave setup along the coast for the SPMSS storm, assuming there is not significant offshore sheltering of waves. The only shoreline along the Gulf and Atlantic coasts subject to significant offshore wave sheltering is south Florida due to the presence of the Bahamas (see Figure 5-3). Application of Figure 5-10 in this area results in an overestimate of wave setup as documented in Table 5-2. Table 5-2 provides the wave setup estimated from Figure 5-10 and the maximum wave setup computed with a fully coupled, high resolution modeling system for the Matagorda, TX, Biloxi, MS, Levy County, FL, and Turkey Point, FL regions. The wave setup from screening purposes is determined by calculating the offshore slope at all four locations according to Irish and Resio (2010), obtaining the *R* value from Figure 5-10, and then solving for the wave setup based on *R* and the peak surge calculated at the coast on the EC2001 mesh. Wave setup can be estimated as:

$$\frac{R}{1-R} * \eta_{model} \qquad \text{Equation 5-2}$$

Table 5-2. Estimated wave setup

		Wave Setup (ft)	
	R **(from Figure 5-10)**	**Function(R, η_{model}) (Equation 5-2)**	**Coupled Numerical Model***
Matagorda	0.15	4.8	5.0
Biloxi	0.10	3.8	2.7
Levy County	0.05	2.0	1.6
Turkey Point	0.20	6.0	1.7
*Note: Maximum wave setup across entire area of interest			

The maximum wave setup calculated with a detailed coupled model system was determined by comparing coupled model system results with and without radiation stress forcing applied. As seen in Table 5-2, this approach provides a reasonable estimate of wave setup at all sites, except Turkey Point, where offshore waves are subject to sheltering by the Bahamas. The wave sheltering results in much lower setup than that predicted with equation 5-2 and the *R* value should be adjusted down for south Florida sites. Based on the analysis here, an *R* value of 0.1 for southeast Florida should provide a reasonable, yet conservative estimate of wave setup.

Flooding at a site can also occur as a result of wave runup and overtopping. A detailed analysis of wave runup would require the bathymetric/topographic profile at the site location and application of a Boussinesq wave model or an approach such as that described by Melby (2012). Any wave runup at a site would be dependent upon the design of the nuclear plant and it is therefore impractical to estimate at the time a screening analysis is performed. For screening purposes, it is therefore proposed to include a freeboard value. The appropriate value will vary depending on regional and local conditions and should be carefully considered. For example, in the case of a facility not on the open coast and where there is overland surge propagation, such as Matagorda TX, 3 ft can be considered a reasonable value based on engineering experience. For nuclear facility sites on the open coast, this value may need to be greater. The values used here are for illustration purposes and each application should be carefully reviewed to ensure a proper freeboard value is applied.

5.3.4 Uncertainty

Three sources of variability that should be considered for estimating the SPMSS: uncertainty in the MPI; uncertainty in storm surge prediction; and potential climate variability over the projected design lifetime. Because a conservative value of 870 mb for the MPI is being considered for the screening storm, the uncertainty in the MPI can be considered accounted for. However, the uncertainty in the storm surge prediction and potential climate variability must also be considered and added to the final SPMSS value.

The coupled modeling system being applied for the screening storm suite has been validated with multiple storms in the Gulf of Mexico. Based on these validations, uncertainty in the model predictions can be characterized by a standard deviation of about 1.5 ft (see Bunya *et al*. 2010). The uncertainty in model prediction should account for two times the standard deviation, giving an uncertainty in model predictions (U_{model}) of 3 ft.
Climate variability must also be considered both with respect to sea level change and climate effects on storm patterns and intensities. To account for sea level change, an estimate of the relative mean sea level for the project design life must be obtained. For screening purposes, the most conservative estimates for sea level rise (SLR) should be applied and based on the

best available information available at the site of interest. (Note that projected drops in sea level will not be considered for screening purposes.) This estimate can then be added directly to the SPMSS. Relative SLR can be extremely site specific and estimates should be carefully considered.

The climate impact on the MPI is determined by the impact of climate variability on SST's. The actual pattern of summertime SST's in the Gulf of Mexico (shown in Figure 4-16) resembles more of a cyclical pattern than a secular trend. For this reason, it is difficult to use existing data to project linearly into the future. Given the lack of projected SST changes specific to the Gulf of Mexico, a value based on the measured mean rise in SST in the northern Atlantic over the past 100 years of 1.0° C (Rayner *et al*. 2003) was assumed as the potential increase in this parameter over a 100-year design life. From Figure 2-5, a 14 mb increase in the MPI value can be estimated for a 1.0° C increase in SST. Based on analysis by Irish and Resio (2010), this will increase the associated surge by about 1.2 ft ($U_{climate}$).

5.3.5 Final SPMSS Estimate

All components of the critical flood elevation are described above and must be combined to provide a final estimate of the SPMSS. The contributions from the various components can be broken down as:

Surge predicted by model from wind and pressure forcing:	η_{model}
Wave setup:	$\frac{R}{1-R} * \eta_{model}$
Deviation due to variability of surge propagation inland	η_{dev}
Freeboard to account for wave runup:	F
Mean higher high water less mean tide level at site location:	η_{tide}
Uncertainty in model storm surge predictions:	U_{model}
Uncertainty in MPI due to climate variability:	$U_{climate}$
Estimate of sea level rise over project life	η_{RSLR}

Combining the above in equation form, the PMSS is defined as:

$$SPMSS = \eta_{model}\left(\frac{1}{1-R}\right) + \eta_{dev} + F + \eta_{tide} + U_{model} + U_{climate} + \eta_{RSLR} \qquad \text{Equation 5-3}$$

The modeled screening storm surge on the EC2001 mesh (η_{model}) is 27 ft for Matagorda, 34 ft for Biloxi, 38 ft for Levy County, and 24 ft for Turkey Point (see Figure 5-9). The deviation due to variability in surge propagation inland is 5 ft for all locations. The difference between mean higher high water and mean tide level (η_{tide}) is approximately 0.4 ft at Matagorda, 0.9 ft at Biloxi, 1.7 ft at Levy County, and 1.1 ft at Turkey Point. Table 5-2 provides the *R* values for all locations. For illustration purposes, a freeboard (*F*) of 3 ft will be used for the sites further inland (Matagorda and Levy County) and a 4 ft value will be used for the facilities near the open coast. However, in actual application a careful consideration should be made of local conditions in making this estimate. The uncertainties (U_{model} and $U_{climate}$) are the same for all sites and, as previously discussed, are equal to 3.0 ft and 1.2 ft, respectively. The computed estimate of

SPMSS must be combined with an estimate of relative sea level rise at a prospective site to give a final critical flood elevation. For illustration purposes, the η_{RSLR} estimate will be based on the high eustatic sea level rise function given in the Intergovernmental Panel on Climate Change 2007 report. For a 100-year project life, the η_{RSLR} is estimated to be approximately 3.8 ft. Therefore, the SPMSS is equal to:

$$SPMSS = (27)\left(\frac{1}{1-0.15}\right) + 5 + 3 + 0.4 + 3 + 1.2 + 3.8 = 48.2\,\text{ft} \quad \text{Matagorda} \quad \text{Equation 5-4}$$

$$SPMSS = (34)\left(\frac{1}{1-0.1}\right) + 5 + 4 + 0.9 + 3 + 1.2 + 3.8 = 55.7\,\text{ft} \quad \text{Biloxi} \quad \text{Equation 5-5}$$

$$SPMSS = (38)\left(\frac{1}{1-0.05}\right) + 5 + 3 + 1.7 + 3 + 1.2 + 3.8 = 57.7\,\text{ft} \quad \text{Levy Cty} \quad \text{Equation 5-6}$$

$$SPMSS = (24)\left(\frac{1}{1-0.1}\right) + 5 + 4 + 1.1 + 3 + 1.2 + 3.8 = 44.8\,\text{ft} \quad \text{Turkey Pt} \quad \text{Equation 5-7}$$

5.4 Screening Criteria

The computed critical flood elevation is compared to the controlling elevation for the prospective site. The controlling elevation is defined as the highest continuous topographic contour between the coast and the prospective site. If the controlling elevation is less than the critical flood elevation, a detailed surge and wave analysis must be performed. Conversely, if the controlling elevation is greater than the critical flood elevation, the site is considered not at risk for coastal storm surge flooding and no further analysis would be required.

To demonstrate how the proposed screening method would be applied in practice, a screening analysis for a prospective site at Matagorda, TX is presented. The SPMSS elevation at Matagorda is 48.2 ft. Figure 5-11 is a topographic map in the vicinity of the prospective site at Matagorda, TX. Inspection of Figure 5-11 identifies a controlling elevation of 27 ft. Because the controlling elevation is less than the critical flood elevation, a detailed surge and wave analysis is required at Matagorda, TX.

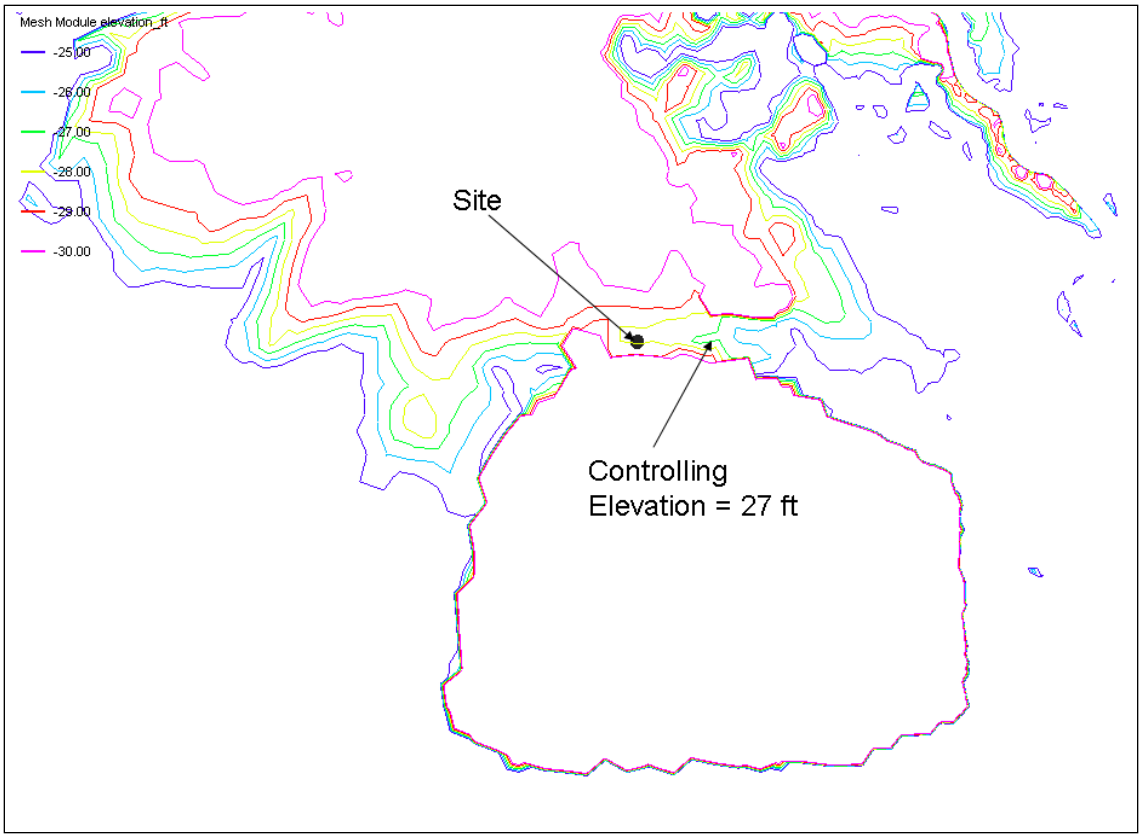

Figure 5-11. Topographic contours (elevations between 25 and 30 ft) in the vicinity of prospective site at Matagorda, TX.

5.5 Summary

This Section documents a screening methodology to determine inundation limits from maximum possible intensity storms. The methodology is efficient in that it makes use of a surge modeling system applied on a mesh that does not resolve the coastal floodplain. The SPMSS is computed through consideration of wind wave effects, tide, and uncertainty and adding these contributions to the surge estimate obtained from the numerical model. An estimate of relative sea level rise at a site is added to obtain the final SPMSS which provides a critical flood elevation that defines a line of safety beyond which critical infrastructure is safe from coastal storm surge. If a specific prospective site is being considered, the controlling elevation of the site, defined as the highest continuous topographic contour between the coast and the prospective site, is compared to the critical flood elevation. If the controlling elevation is less than the critical flood elevation, a detailed surge and wave analysis is required. If the controlling elevation is greater than the critical flood elevation, no further analysis is required.

The purpose here is to document the overall procedure and little attention is given to the details in estimating components of the SPMSS that are highly dependent on local conditions and/or may vary temporally as this is beyond the scope of this report. Specifically, it is recommended that NRC consider additional analysis be conducted to provide guidance in estimating appropriate values of $\eta_{dev,}$ F, and η_{RSLR}. For example, the $\eta_{dev,}$ applied in this Section's examples are based on a limited number of simulations. Additional simulations could be

conducted for various coastal landscape types to develop a range of η_{dev} values that is a function of coastal flood plain slope. Given the complexities in making these estimates and the fact that available surge model systems and their application can vary widely, each screening application should be carefully reviewed to ensure that an appropriate determination is made with respect to the coastal surge flood risk at any given site.

6.0 SUMMARY AND PMSS ESTIMATION PROCEDURES RECOMMENDED FOR NRC CONSIDERATION

Design criteria for nuclear power plants require, in part, that structures, systems, and components important to safety be designed to withstand the effects of natural phenomena, including floods, without loss of capability to perform their safety functions. The objective of this project is to provide the NRC with a technical basis for estimating probable maximum water levels due to the storm surge from extreme events along the southern coast of the U.S. for consideration in evaluating flood protection for nuclear power plants. Two fundamentally different methods for estimating design surge levels have been utilized in past studies. Deterministic methods typically use the estimated maximum surge value from either a single storm or a small set of storms as its design level and do not consider the probability of that surge level. Probabilistic methods consider surges from a range of events along with the probabilities of those events and attempt to develop a relationship between surge levels and return period. Both the deterministic-based and probability-based approaches to the estimation of very-low-probability hurricane surges have deficiencies and it is recommended to combine the two methods. The hybrid approach determines which factors affecting hurricane surges can be shown to have asymptotic upper limits and which factors should be treated within a context that allows for natural uncertainty in estimating an upper limit for surges at a specified site. The discussion in Section 3 supports the existence of an upper limit for hurricane generated surges in natural environments and a procedure is recommended for estimating maximum surge at a site of interest.

Section 4 provided an example of how a combined deterministic-probabilistic approach can be applied to estimate the PMSS (including a first approximation for effects of uncertainty). The consideration of uncertainty has traditionally been neglected in past upper-limit estimates of surge levels; but it has been demonstrated that the magnitudes of these terms are not negligible. The possibility that the upper limits of storm surge are much larger than the 10^{-6} annual probability used for safety standards at nuclear power plants was also examined. As part of this effort, the importance of quantifying the impact of uncertainty on estimated surges for a fixed frequency level was stressed; and a method to accomplish this was developed. In the applications here, the estimated central pressures for the 10^{-4} annual probability were shown to be about 15 mb lower when the effects of uncertainty were included. In the two Florida cases examined here, the PMSS value for Levy County exceeded the 10^{-6} annual probability surge and was smaller than the 10^{-6} annual probability surge for Turkey Point.

The final recommended procedure for estimates of the PMSS at sites within the Gulf of Mexico is summarized below:

1. Since it is obvious a limit to the influence of coastal hurricane surges exists, it is advantageous to consider a conservative screening filter to avoid requiring detailed computations in areas where they are clearly unnecessary. Section 5 establishes such a screening filter and develops a proposed approach for a simplified, conservative approximation to coast storm flood risk at prospective nuclear power plant sites which should be considered before detailed computations are performed. The methodology is efficient in that it makes use of a surge modeling system applied on a mesh that does not resolve the coastal floodplain. The SPMSS is computed through consideration of wind wave effects, tide, and uncertainty and adding these contributions to the surge estimate obtained from the numerical model. An estimate of relative sea level rise at a site is added to obtain the final SPMSS which provides a critical flood elevation that defines a line of safety beyond

which critical infrastructure is safe from coastal storm surge. If a specific prospective site is being considered, the controlling elevation of the site, defined as the highest continuous topographic contour between the coast and the prospective site, is compared to the critical flood elevation. If the controlling elevation is less than the critical flood elevation, a detailed surge and wave analysis is required. If the controlling elevation is greater than the critical flood elevation, no further analysis is required (i.e. it is not necessary to execute steps 2 to 6 below).

2. If a detailed analysis is required, a high resolution state-of-the-art coupled wave-surge model with accurate bathymetric-topographic data should be developed and the modeling system validated at the site of interest.

3. Develop a suite of synthetic storms. The storm suite should include a range of hurricane parameters and combinations of those parameters. For the southern U.S. coast, guidance for selecting the parameters to be simulated is:

    a. Central Pressure: Storms with an MPI of 880 mb (consistent with Schade (2000)) and a central pressure that is 10 mb lower than the MPI.
    b. Radius to Maximum Winds: Storms with an offshore R_{max} of 30 nm and 45 nm. These values are larger than any storms in the Gulf of Mexico with intensities greater than approximately 930 mb. In addition, as shown in Figure 3-5, on a 1 to 10,000 slope for an 880 mb storm, there is little or no variation of surge height with a change in storm size above an R_{max} of approximately 40 nm.
    c. Forward Speed: Three storm forward speeds should be simulated, a slow, medium, and fast, from approximately 5 to 22 knots. This range is based on the joint distribution storm speeds and central pressures in the Gulf of Mexico as shown in IPET (2009),
    d. Holland B: The Holland B should be set to 1.27 which is the mean value for the Gulf of Mexico (IPET 2009).
    e. Track: The track should be set to maximize storm surge potential. Irish et al. 2008 and Irish and Resio 2010 show that the peak is close to one Rmax from the landfall location. The position and orientation of the tracks should be based on an analysis of historical high surge potential storm tracks in the area of interest and have minimal land interference as they approach the coast.

    A typical storm suite is given in Table 4-1. The central pressure, radius to maximum winds, and Holland B all vary systematically during the storm's approach to land. Systematic variation in these parameters is identical to that used in the IPET (2009) and was also adopted for Gulf of Mexico FEMA and USACE studies. For details on the variation in these parameters see Appendix 8 of IPET (2009). It should be noted that these values are for the southern U.S. Gulf of Mexico coast only and are not applicable for other regions.

4. Applying the validated modeling system, simulate the surges that would be produced by these storms at the location of interest and determine the largest predicted surge. The modeling system can applied with the existing mean sea level as the initial water level condition or include an estimate of eustatic sea level rise over the project life and an adjustment to reflect high tide. If these adjustments are not made to the initial water level condition, they must be added later. In areas with a large tidal range and/or high rates of sea level rise are estimated, it is recommended that the high water level is included in the modeling system.

5. Estimate the uncertainty in the estimate and add to the maximum calculated surge. Guidance for estimating the uncertainty is provided in Section 4 and a 5.3 ft adjustment is recommended. If the tidal and sea level rise adjustments are not included in the simulated water level, they must also be added.

6. Consideration must also be given to flooding potential from wave runup. A detailed analysis of wave runup requires very high resolution bathymetric/topographic data at the site location and application of a Boussinesq wave model or an approach such as that described by Melby (2012). Wave runup at a site is dependent upon the design of the nuclear plant and its protection features and its calculation is beyond the scope of this report.

The recommended procedure provides a technical basis for improving guidance on characterizing very low probability hurricane surge events. Fundamental limitations in the existing guidance relate to the modeling of hurricane surge events and the estimation of extreme storm parameters. The Bathystrophic Storm Surge model is extremely limited by restrictions and simplifications made in order to make the problem computationally tractable given the computer resources available in the early to mid 1970's. The model assumptions and simplifications reduce the applicability and accuracy of the model. Existing guidance for determination of extreme storm parameters relies on NWS 23, which makes several assumptions in the PMH that are now known to be invalid.

The new approach addresses both of these fundamental limitations in addition to improving on the screening method and considering uncertainty that is inherent in the estimation of storm parameters and the associated surge levels. Specifically the improvement upon previous guidance includes:

- Application of new modeling technology: A modern coupled system of wind, wave, and coastal circulation models that properly defines the physical system and includes an appropriate non-linear coupling of the relevant processes is recommended. An example of such a system is the USACE hurricane modeling system which combines the TC96 PBL model for winds, the WAM offshore and STWAVE nearshore wave models, and the ADCIRC basin to channel scale unstructured grid circulation model. Any modeling system that is applied should be well validated at the site of interest.

- Updated characterization of the MPI storm: Based upon the best available data and theoretical concepts, the MPI storm is allowed to attain a somewhat lover central pressure than previously considered. The storm size is estimated as a condition probability function of storm intensity. In addition, storm parameters are allowed to vary as the storm approaches the coast.

- Consideration of uncertainty: Previous guidance did not consider uncertainty in upper-limit estimates of surge levels. However, as has been demonstrated, that the magnitude of uncertainty is not negligible and it is considered in the new methodology.

- New screening method: The previous screening method was based on a pre-computed map of probable maximum surge values that was based on the invalid assumptions in the PMH and results from the inadequate Bathystrophic Storm Surge model. The new method utilizes the updated characterization of the MPI and appropriate modeling technology.

7.0 REFERENCES

Bodine, B.R., 1971: Storm surge on the open coast: Fundamentals and simplified prediction. Technical Memorandum No. 35, U.S. Army Corps of Engineers, Coastal Engineering Research Center, Virginia.

Bunya, S., Westerink, J., Dietrich, J.C., Westerink, H.J., Westerink, L.G., Atkinson, J., Ebersole, B., Smith, J.M., Resio, D., Jensen, R., Cialone, M.A., Luettich, R. ,Dawson, C., Roberts, H.J., and Ratcliff, J. 20010. A High Resolution Coupled Riverine Flow, Tide, Wind, Wind Wave and Storm Surge Model for Southern Louisiana and Mississippi: Part I–Model Development and Validation. Monthly Weather Review, 138, 345-377.

Cardone, V.J., Greenwood, C.V., and Greenwood, J.A. 1992. Unified program for the specification of tropical cyclone boundary layer winds over surfaces of specified roughness. Contract Rep. CERC 92-1. U.S. Army Engineer Waterways Experiment Station, Vicksburg.

Chow, S.H. 1971. A study of wind field in the planetary boundary layer of a moving tropical cyclone. MSC Thesis, School of Engineering and Science, New York University, New York.

Emanuel, K.A., 1986: An air-sea interaction theory for tropical cyclones. Part I: Steady state maintenance. J. Atmos. Sci., 43, 585-604.

Emanuel, K. A., 1987: The dependence of hurricane intensity on climate. Nature, 326, 483–485.

Emanuel, K. A., 1991: A scheme for representing cumulus convection in large-scale models. J. Atmos. Sci., 48, 2313–2335.

Garratt, J.R. 1977. Review of drag coefficients over oceans and continents. Mon Weather Rev., 104, 418-442.

Graham, H.E. and D.E. Nunn, 1959. Meteorological considerations pertinent to the Standard Project Hurricane, Atlantic and Gulf coasts of the United States, National Hurr. Res. Proj. Rep. No. 33, Weather Bureau, U.S. Dept of Commerce, Wash., D.C. 76 p.

Gringorten, I.I. 1962: A simplified method of estimating extreme values from data samples, J. Appl. Meterol., 2, 82-89.

Gringorten, I.I. 1963: Extreme-Value Statistics in Meteorology – A Method of Application, Air Force Surveys in Geophys. No. 125, A.F. Cambridge Res. Cen., Bedford, MA.

Gumbel, E.J. 1959: Statistics of Extremes, Columbia Univ. Press, New York.

Holland, G., 1980. An analytic model of the wind and pressure profiles in hurricanes. Monthly Weather Review, 108, 1212-1218.

Interagency Performance Evaluation Task Force, 2007. Performance evaluation of the New Orleans and southeast Louisiana hurricane protection system, vol IV - The Storm. U.S. Army Corps of Engineers, Washington, DC. Available at: https://ipet.wes.army.mil/

Interagency Performance Evaluation Task Force, 2009. Performance evaluation of the New Orleans and southeast Louisiana hurricane protection system, vol VIII – Engineering and Operational Risk and Reliability Analysis. U.S. Army Corps of Engineers, Washington, DC. Available at: https://ipet.wes.army.mil/

Kennedy, A.B., Gravois, U., Zachry, B.C., Westerink, J.J., Hope, M.E., Dietrich, J.C., Powell, M.D., Cox, A.T., Luettich, R.A., Dean, R.G. 2011. Origin of the Hurricane Ike forerunner surge. Geophysical Research Letters, 38, L08608, doi:10.1029/2011GL047090.

Irish, J.L., Resio, D.T., and J.J. Ratcliff, 2008: The influence of storm size on hurricane surge, J. Phys. Oceanogr., 38 (9), 2003-2013.

Irish, J.L., D.T. Resio, and M.A. Cialone, 2009: A surge response function approach to coastal hazard assessment: Part 2, Quantification of spatial attributes of response functions, J. Natural Hazards, 51 (1), 183-205,doi:10.1007/s11069-9381-4.

Irish, J.L. and D.T. Resio, 2010: A hydrodynamics-based surge scale for hurricanes, Ocean Engr. 37, 69-81.

Knutson, T.R., McBride, J.L., Chan, J., Emanuel, K., Holland, G., Landsea, C., Held, I., Kossin, J.P., Srivastava, A.K. and S. Masato, 2010. Tropical cyclones and climate change, Nature GeoSci. Rev. Art., Feb. 2010, DOI:10.1038/NGE0779.

Komen, G.J., Cavaleri, L., Donelan, M., Hasselmann, K., Hasselmann, S., and Janssen, P.A., 1994. Dynamics and modelling of ocean waves. Cambridge University Press, Cambridge.

Luettich R.A., Westerink, J.J., and Scheffner, N.W. 1992. ADCIRC: an advanced three-dimensional circulation model for shelves, coasts, and estuaries. Report 1, theory and methodology of ADCIRC-2DDI and ADCIRC-3DL. Technical report DRP-92-6. U.S. Army Engineer Waterways Experiment Station,Vicksburg.

Luettich, R.A., and Westerink, J.J. 2004. Formulation and numerical implementation of the 2D/3D ADCIRC finite element model version 44, XX. Available at: http://adcirc.org/adcirc_theory_2004_12_08.pdf.

Melby, J.A. 2012. Wave runup prediction for flood hazard assessment. ERDC/CHL TR-12-x. U.S. Army Engineer Research and Development Center, Vicksburg, MS.

Mooley, 1980 D.A. Mooley, Severe cyclonic storms in the Bay of Bengal, 1877–1977, Mon. Weather Rev. 108 (1980), pp. 1647–1655.

Mukai, A.Y., J.J. Westerink, R.A. Luettich, and D. Mark. 2002. Eastcoast 2001, A tidal constituent database for Western North Atlantic, Gulf of Mexico, and Carribean Sea. ERDC/CHL TR-02-24, U.S. Army Corps of Engineers Engineer Research and Development Center, Vicksburg, MS.

Niedoroda, A.W., Resio, D.T., Toro, G.R., Divoky, D., Das, H.S., and C.W. Reed. 2010: Analysis of the coastal Mississippi storm surge hazard, Ocean Engr. 37, 82-90.

Nuclear Regulatory Commission, 1986. Safety Goals for the Operations of Nuclear

Power Plants; Policy Statement; Republication, 51 FR 28044 & 51 FR 30028, 10 CFR Part 50, published 8/21/1986.

Pararas-Carayannis, G., 1975: Verification study of a Bathystrophic storm surge model. Technical Memorandum No. 50, U.S. Army Corps of Engineers, Coastal Engineering Research Center, Virginia

Powell, M.D., Vickery, P.J., and Reinhold, T.A. 2003. Reduced drag coefficient for high wind speeds in tropical cyclones. Nature, 422, 279-283.

Powell, M.D. 2006. Drag coefficient distribution and wind speed dependence in tropical cyclones. Final report to the NOAA Joint Hurricane Testbed Program, 26pp.

Powell, M.D. and T.A. Reinhold. 2007: Tropical cyclone destructive potential by integrated kinetic energy. Bull. Am. Meteorol. Soc. 88, 513-526.

Rayner *et al.* 2003. Global analyses of sea surface temperature, sea ice, and night marine air temperature since the late nineteenth century. J. Geophys. Res. 108, 4407.

Resio, D.T., Irish, J.L., and M.A. Cialone, 2009: A surge response function approach to coastal hazard assessment: Part 1, Basic Concepts, J. Natural Hazards, 51(1), 163-182, doi:10.1007/s11069-009-9379-y.

Resio, D.T., and Westerink, J.J. 2008. Modeling the physics of storm surge. Physics Today, 61(9),33–38.

Schade, L.R., 2000. Tropical Cyclone Intensity and Sea Surface Temperature. J. Atmosph. Sci., 57, 3122-3130.

Schwerdt, R.W., Ho, F. P., Watkins, R.R., 1979. Meteorological Criteria for Standard Project Hurricane and Probable Maximum Hurricane Windfields, Gulf and East Coasts of the United States, NOAA Tech Rep NWS 23, National Weather Service, NOAA, Dept of Commerce, Silver Spring, MD, 317 p.

Smith, J.M., Sherlock, A.R., and Resio, D.T. 2001. STWAVE: steady-state spectral wave model user's manual for STWAVE, version 3.0. ERDC/CHL SR-01-1. U.S. Army Engineer Research and Development Center, Vicksburg.

Smith J. M., and Sherlock, A.R. 2007. Full-plane STWAVE with bottom friction: II. Model overview. System-wide water resources program technical note. U.S. Army Engineer Research and Development Center, Vicksburg.

Soluri, E. A., and Woodson, V. A. 1990. 1990 World vector shoreline, International Hydrographic Review, LXVII(1).

Thompson, E.F., and Cardone, V.J. 1996. Practical modeling of hurricane surface wind fields. Journal of Waterway, Port, Coastal, and Ocean Engineering, 122(4):195–205. doi:10.1061/(ASCE)0733-950X(1996)122:4(195).

Tonkin, H., Holland, G.J. Holbrook, N., and A. Henderson-Sellers. 2000: An Evaluation of Thermodynamic Estimates of climatological maximum potential tropical cyclone intensity,

Mon. Wea. Rev., 128, 746-762.

Toro, G., Resio, D.T., Divoky, D., Niedoroda, A.W., and C. Reed, 2009: Efficient joint probability methods for hurricane surge frequency analysis, Ocean Engr. 37, 125-134.

Wamsley, T.V., Cialone, M.A., Smith, J.M., Ebersole, B.A. 2009. Influence of landscape restoration and degradation on storm surge and waves in southern Louisiana. Journal of Natural Hazards. 51, 1, 207-224.

Wamsley, T.V., Cialone, M.A., Smith, J.M., Atkinson, J.H., and Rosati, J.D. 2010. The potential of wetlands in reducing storm surge. Ocean Engineering 37 (1) 59-68. DOI 10.1016/j.oceaneng.2009.07.018.

Westerink, J.J., Blain, C.A., Luettich, R.A., and Scheffner, N.W. 1994. ADCIRC: an advanced three-dimensional circulation model for shelves coasts and estuaries, report 2: users manual for ADCIRC-2DDI. Dredging research program technical report DRP-92-6. U.S. Army Engineer Waterways Experiment Station, Vicksburg, MS.

Westerink, J.J., Luettich, R.A., and Muccino, J.C. 1994. Modeling Tides in the Western North Atlantic Using Unstructured Graded Grids, Tellus, 46A, 178-199.

Westerink, J.J., Luettich, R.A., and Militello, A. 2001. Leaky Internal-Barrier Normal-Flow Boundaries in the ADCIRC Coastal Hydrodynamics Code, Coastal and Hydraulics Engineering Technical Note, U.S. Army Engineer Research and Development Center, Vicksburg, MS.

Westerink, J.J., Luettich, R.A., Feyen, J.C., Atkinson, J.H., Dawson, C., Roberts, H.J., Powell, M.D., Dunion, J.D., Kubatko, E.J., and Pourtaheri, H. 2008. A basin to channel scale unstructured grid hurricane storm surge model applied to southern Louisiana. Monthly Weather Review, 136(3):833–864. doi:10.1175/2007MWR1946.1

World Meteorological Organization. 1976. The quantitative evaluation of the risk of disaster from tropical cyclones. WMO/TD-No.455, Special Environmental Report.

NRC FORM 335
(9-2004)
NRCMD 3.7

U.S. NUCLEAR REGULATORY COMMISSION

BIBLIOGRAPHIC DATA SHEET

(See instructions on the reverse)

1. REPORT NUMBER
(Assigned by NRC, Add Vol., Supp., Rev., and Addendum Numbers, if any.)

NUREG/CR-7134

2. TITLE AND SUBTITLE

The Estimation of Very-Low Probability Hurricane Storm Surges for Design and Licensing of Nuclear Power Plants in Coastal Areas

3. DATE REPORT PUBLISHED

MONTH	YEAR
October	2012

4. FIN OR GRANT NUMBER

N6676

5. AUTHOR(S)

Donald T. Resio, Ty V. Wamsley, Mary A. Cialone, and T. Christopher Massey

6. TYPE OF REPORT

Technical

7. PERIOD COVERED *(Inclusive Dates)*

12/08-12/11

8. PERFORMING ORGANIZATION - NAME AND ADDRESS *(If NRC, provide Division, Office or Region, U.S. Nuclear Regulatory Commission, and mailing address; if contractor, provide name and mailing address.)*

U.S. Army Engineer Research and Development Center
Coastal and Hydraulics Laboratory
3909 Halls Ferry Road
Vicksburg, MS 39180

9. SPONSORING ORGANIZATION - NAME AND ADDRESS *(If NRC, type "Same as above"; if contractor, provide NRC Division, Office or Region, U.S. Nuclear Regulatory Commission, and mailing address.)*

Division of Risk Analysis
Office of Nuclear Regulatory Research
U.S. Nuclear Regulatory Commission
Washington, DC 20555-0001

10. SUPPLEMENTARY NOTES

11. ABSTRACT *(200 words or less)*

The objective of this project is to provide the NRC with a technical basis for estimating probable maximum water levels due to storm surge from extreme events along the southern coast of the U.S. A review of the existing guidance was conducted and limitations in the technical basis for estimating storm surge identified. Required updates based on the most recent data available and state-of-the-practice analysis methods, tools, and models are recommended. A deterministic-probabilistic approach for estimating very-low probability hurricane storm surges for design and licensing of nuclear power plants in coastal areas is developed. The proposed approach determines which factors affecting hurricane surges can be shown to have asymptotic upper limits and which factors should be treated within a context that allows for natural uncertainty in estimating an upper limit for surges at a specified site. The proposed approach is demonstrated through application at three nuclear plant sites. A screening method is also developed to determine if a prospective site is at risk of flooding from coastal storm surge. The proposed screening method includes criteria for proceeding or not proceeding to more detailed definitions of design-basis storm surges and explicitly considers local conditions and bathymetry that may affect water level estimates.

12. KEY WORDS/DESCRIPTORS *(List words or phrases that will assist researchers in locating the report.)*

Hurricane, storm surge, ADCIRC, deterministic, probabilistic

13. AVAILABILITY STATEMENT

unlimited

14. SECURITY CLASSIFICATION

(This Page)
unclassified

(This Report)
unclassified

15. NUMBER OF PAGES

16. PRICE

Federal Recycling Program

UNITED STATES
NUCLEAR REGULATORY COMMISSION
WASHINGTON, DC 20555-0001

OFFICIAL BUSINESS

NUREG/CR-7134

The Estimation of Very-Low Probability Hurricane Storm Surges for Design and Licensing of Nuclear Power Plants in Coastal Areas

October 2012